UTILIZATION OF WYOMING BOTTOM ASH IN ASPHALT MIXES

Khaled Ksaibati
Shiva Rama Krishna Sayiri

Department of Civil & Architectural Engineering
University of Wyoming

March 2006

Acknowledgement

This report has been prepared with funds provided by PacifiCorp and the U.S. Department of Transportation to the Mountain-Plains Consortium (MPC). The MPC member universities include North Dakota State University, Colorado State University, University of Wyoming, and Utah State University.

Disclaimer

Abstract

Coal ash is the portion of ash rejected by the stack and collected at the base as a waste product. Coal ash is comprised of bottom ash and fly ash. Fly ash accounts for 70 percent to 80 percent of total coal ash and the rest being bottom ash. Only 39 percent of bottom ash is utilized with the rest being disposed of in mined out areas of coal mine. This represents a significant volume of waste material. There would be considerable benefit to finding a use for this material. It is the intent of this project to look into the effect of pavement performance when bottom ashes from three power plant sources in Wyoming (Laramie River, Dave Johnston, and Jim Bridger) are added into asphalt mixes. The performance of these mixes was evaluated by conducting a laboratory evaluation and field evaluation. The laboratory evaluation consisted of preparing samples and then testing them for rutting, low temperature cracking and stripping. The field evaluation was done using experimental test sections in Gillette. Wyoming. These experimental test sections were tested with the Falling Weight Deflectometer (FWD). In addition the Pavement Condition Index (PCI) values were also determined for all of the sections. The statistical analyses showed that the field performance of all bottom ash mixes were comparable to the control mix, while the laboratory evaluation showed that all the ash mix performance exceeded control mix performance.

Table of Contents

List of Tables

List of Figures

1. INTRODUCTION

1.1 Background

Coal ash, a by-product of the thermal power plants, causes environmental pollution, but can also be used for gainful purposes. More than half of the electricity produced in the U.S is generated by coal-fired power plants by burning approximately 1,000 million tons of coal every year [DOE, 2003]. In this process, 96 million tons of coal ash is produced [ACAA, 2002]. This coal ash consists of fly ash and bottom ash. Fly ash, being very fine, is carried through the furnace with the exhaust gases and is collected by ash precipitators. Bottom ash is heavier and falls through the bottom of the furnace, where it is collected in a hopper. Fly ash accounts for 70 to 80% of the coal ash, the rest being bottom ash. In the year 2002, approximately 19.6 million tons of bottom ash were produced [ACAA]. Of this total, 39% was gainfully utilized, the rest being disposed of in landfills or used to fill the mined out areas of coal mines prior to their reclamation. Disposal of coal ash is expensive and costs approximately $3/ton to $40/ton, depending on haul costs [ACAA]. In view of the high cost of disposal and environmental pollution caused by its generation and disposal, the gainful utilization of as much coal ash as possible is of vital importance. The utilization of coal ash as a raw material in applications that are environmentally and technically safe, and commercially viable should lead to a reduction of the amount of these by-products that end up in landfills. One such application of this bottom ash is as an aggregate replacement in pavement materials, as it possesses some of the properties similar to aggregate.

The gainful utilization of coal ash may lead to lower costs of power generation, which can be passed on to the consumer. Other related uses of coal ash are as embankment fill, roadway fill, and base courses.

1.2 Problem Statement

As the consumption of coal by power plants increases, so does the production of coal ash. Coal ash, in addition to other components, contains high concentrations of trace elements and heavy metals, including Al, As, Cd, Cr, Cu, Hg, Ni, Pb, Se, Sr, V, and Zn. Thus, an effective waste disposal system has to be adopted that can efficiently handle large volumes of coal ash and prevent environmental degradation due to the release of these trace elements into natural systems. Disposal of coal ash is expensive and will be a burden on the power industry.

Wyoming power plants consume nearly 25 million tons of coal each year [DOE, 2003], and produce a substantial quantity of unused bottom ash. Major portions of this ash are disposed of in mines prior to their reclamation. The successful use of bottom ash in asphalt pavements in Wyoming would provide significant economic savings. Therefore, the intent of this research project is to determine the feasibility of using bottom ash produced by Wyoming power plants in asphalt mixes.

1.3 Research Objectives

The main objectives of this study are to:

1. Evaluate the moisture susceptibility of Hot Mix Asphalt (HMA) mixes prepared with and without bottom ash.
2. Evaluate the potential for rutting of Hot Mix Asphalt (HMA) mixes prepared with and without bottom ash.
3. Evaluate the low temperature performance of Hot Mix Asphalt (HMA) mixes prepared with and without bottom ash.
4. Evaluate the field performance of bottom ash asphalt mixes using an experimental pavement test section with and without bottom ash. The Pavement Condition Index (PCI) values and Falling Weight Deflectometer (FWD) deflections are utilized to evaluate pavement performance.

1.4 Report Organization

Chapter II of this report is a literature review of: bottom ash, its uses in asphalt mixes, common distresses in pavements, methods to evaluate distress, and methods to limit moisture susceptibility. Also described in Chapter II are methods to evaluate structural capacity of pavements. Chapter III contains the experimental design and explains the testing procedures used in this study. Chapter IV discusses the data collected from all the tests performed in this study. Chapter V describes the field test section in Gillette, Wyoming, and contains Falling Weight Deflectometer deflection data corrected for temperature, pavement layer moduli backcalculated from FWD deflections using EVERCALC5.0 software, and Pavement Condition Index data. Chapter VI describes the statistical analysis of the laboratory and field results. Chapter VII summarizes the conclusions and makes recommendations for further research.

2. LITERATURE REVIEW

2.1 Introduction

In the United States, there are approximately 6.4 million kilometers (4 million miles) of roads, out of which 3.7 million kilometers roads are surfaced with asphalt or concrete, the rest being gravel surfaced or unsurfaced. The asphalt roads make up to 55% of the total road lengths [Stephen, 1999]. It is clear from the above statistics that asphalt concrete mixes contribute significantly to the mobility of society. The increasing use of asphalt pavements in new roadway construction requires large amount of virgin materials. As America's natural resources are consumed in greater quantities, the need for quality, inexpensive alternative aggregates becomes obvious. Bottom ash, a waste material from coal-fired power plants could be a suitable replacement for a portion of aggregate commonly used in asphalt pavements. Large quantities of bottom ash are produced every year. Disposal of this ash is costly and poses a serious problem on the environment. Bottom ash, if used as an aggregate replacement, may provide substantial savings to utility companies and highway agencies, and thereby solve disposal problems to some extent.

The performance of pavement relies mostly on the selection of the appropriate aggregate. When considering an aggregate for potential use in asphalt mix, it is important to determine if it possesses the desired characteristics. The most common distresses found in asphalt pavements are rutting, low temperature cracking and stripping. In states like Wyoming, where there are extreme seasonal temperature variations, designing an asphalt mix that performs well in both summer and winter is challenging. These temperature variations lead to cracking in roadway surfaces. To overcome this problem, pavement engineers began specifying asphalt cements with lower viscosities to increase the flexibility of the pavements. Although this solved the cracking problem, decreasing the viscosities of the asphalt cements led to plastic flow and rutting in hot summer months.

Ruts are the depressions that occur in a pavements wheel path due to heavy wheel loads. The Georgia Loaded Wheel Tester (GLWT) is one of the most common types of laboratory equipment used to test for rutting.

Low temperature cracking is a serious problem occurring in certain parts of the northern United States, Alaska, Canada, and other locations that experience severe cold weather. Factors contributing to low temperatures are high elevations, distance from moderating oceans, and northern latitude. The lowest temperature recorded in Wyoming was -53^0 C [Erickson, 1997]. Due to these extremely frigid temperatures, cracking of asphalt pavements is a serious problem. Haas and Anderson presented three causes of low temperature cracking. “First, thermally induced stresses exceed the tensile strength of the pavement. This does not consider stresses caused by traffic. Next, subgrades can crack from freezing and shrinking of the subbase or base. Finally, freezing and shrinking of the subbase or base cause cracks to propagate through the pavement” [Haas and Anderson, 1969]. Many tests have been developed to evaluate thermal cracking in asphalt mixes. The Tensile Stress Restrained Specimen Tester (TSRST) has been found to have the greatest potential to evaluate temperature cracking susceptibility because it simulates field conditions, is easy to perform, and accommodates large stone mixes [Vinson, 1990].

“Moisture damage of asphalt pavement is a problem that more than half of the state highway agencies are experiencing” [Lottman, 1988]. This damage is commonly known as stripping. Stripping is the separation of asphalt coating from the aggregate. The most serious consequence of stripping is the loss of strength and integrity of the pavement. Stripping can take many surface forms during its progression. Some of these include rutting and cracking. Several testing methods have been developed and applied in

the past to evaluate and predict the moisture susceptibility of asphalt mixes [Ksaibati and Zeng, 2003]. The developed tests can be classified into two categories, qualitative tests and quantitative strength tests. The Boiling Water Test (ASTM D3625) and Static-Immersion Test (AASHTO T182) are qualitative tests, while the Lottman Test (NCHRP 246), Tunnicliff and Root Conditioning (NCHRP 274), Modified Lottman Test (AASHTO T 283), Texas Freeze-Thaw Pedestal Test, and Immersion-Compression Test (AASHTO T165) are quantitative strength tests [Khandal, 1992].

2.2 Bottom Ash

Bottom ash and fly ash are the two types of ashes produced by thermal power plants in the process of the generation of electricity. Bottom ash, being heavier, falls through the bottom of the furnace where it is collected in a hopper, whereas fly ash, being very fine, is carried through the furnace with the exhaust gases and is collected by ash precipitators [Huang, 1990]. Bottom ash can be of two forms, dry bottom ash and wet bottom ash, depending on the type of unit used. Most of the Wyoming bottom ash is considered as wet. The ingredients in bottom ash are the same as those in mud and silt that, when combined with organic matter, eventually become coal. Bottom ash is granular, with the same upper and lower particle size limits as concrete sand. Bottom ash is angular in shape and may range in color from medium brown, to gray, to almost black. Bottom ash consists of melted sand and lime, with smaller amounts of oxides containing aluminum, iron, magnesium, sulfur and trace materials.

The majority of unused coal ash is bottom ash. In year 2003, 19.6 million tons of bottom ash was produced and only 39% of it was utilized and the rest was disposed of in landfills or used as fill in mined out areas of coal mines prior to their reclamation. Research into the use of coal ash as a construction material has been largely focused on fly ash rather than bottom ash, because fly ash accounts for 70 to 80% of total coal ash and the rest is bottom ash. Recent studies have indicated that bottom ash may possess desirable engineering properties and will not degrade performance properties when used to replace a portion of the fine aggregate in the asphalt mix.

There are several potential highway related uses for bottom ash. Some of these include:
[http://www.tfhrc.gov/hnr20/recycle/waste/cbabs1.htm]

- Road traction agent
- Road surface material
- Hot mix asphalt additive
- Road base
- Sand-blasting grit
- Snow and ice control

Eleven states currently allow bottom ash to be used as a road traction agent. Sixteen additional states also specify the use of coal combustion by-products (CCBs) for a variety of highway uses [Evans, 1995]. Wyoming does not currently utilize CCBs as a highway material. However, CCBs are exempted from the Wyoming hazardous waste regulations and there are no specific regulations addressing their use. The main environmental concern involving the use of bottom ash as a highway material is air quality. According to the information given by the Wyoming Department of Environmental Quality, bottom ash generates one-half of the PM10 dust (particulate matter smaller than 10 microns in size) as compared to scoria, a commonly used aggregate in Wyoming.

Specific gravity is an indicator of the quality of material. The specific gravity of bottom ash depends on the mineralogical composition of the ash as well as the porosity of the particles. A dense dry bottom ash may have a bulk specific gravity as high as 2.6, while a poor ash, with a large percentage of both porous

and popcorn particles, may be as low as 1.6. The smaller the percentage of popcorn-sized particles, the higher the specific gravity.

Bottom ash contains iron pyrites, which need to be removed before it is used as an aggregate replacement material, as these pyrites degrade the pavement's strength. No more than 30% of bottom ash as aggregate replacement should be used, because mixes with 50% or more of bottom ash in asphalt pavements were found to show unacceptable stabilities [Anderson, Usmen and Lyle, 1973].

2.3 Moisture Susceptibility

Moisture-induced damage of hot-mix asphalt (HMA) pavement can drastically reduce a pavement's expected designed life. This phenomenon is referred to as stripping and results when moisture causes a loss of bond between the aggregate and the asphalt binder. To combat this stripping, proper mix design is essential. However, if a mix is properly designed but not compacted correctly, it may still be susceptible to moisture damage because of high air void content that permits water to enter the HMA pavement. Therefore, a HMA mix should be tested in a situation where moisture does infiltrate the air voids of the mixture. Many tests are performed at 7% air voids for this reason [Robert et al., 1996]. The final step in the Superior Performing Asphalt Pavement System (SUPERPAVE) is evaluation of moisture susceptibility of the HMA mix. AASHTO T-283 is used for this step and is discussed in detail in the next chapter. A mix with Tensile Strength Ratio (TSR) value less than 70% is considered moisture susceptible [Parker and Gharaybeh, 1987].

2.4 Stripping

Stripping is the physical separation of the asphalt cement and the aggregate caused by loss of adhesion between the asphalt cement and the aggregate when water infiltrates the pavement. This is because water competes for bonding sites on the aggregate surface [Plancher and Petersen, 1998]. HMA mix loses its substantial strength when the asphalt and aggregate bond is weakened. Stripping usually begins at the bottom of the HMA layer and then travels upward. The gradual loss of HMA strength, over a period of time, will not only cause rutting but also shoving in the wheel path.

Various modes of infiltration will allow water to reach the bottom of the asphalt layer. Commonly, asphalt can become saturated if water is allowed to stand on the pavement surface due to no drainage or inadequate drainage. The locally elevated water table or the nearby water bodies result in lateral flow of water from the phreatic surface into the asphalt pavement. This results in internal pore pressure and results in weakened bond. In many cases, stripping is difficult to identify because it takes years for the surface indicators to show up.

Usually, mix designs specify an air void content of 3 to 5%. When the air void content is below 5%, it has been found that the HMA mix is impervious to water. Restricting an air void content below 5% may not be achieved in the field due to improper compaction which results in high air void content. If the air voids are above 8%, water can easily seep into the material. Excessive dust coating on an aggregate may inhibit the asphalt coating process and provide channels through which water may penetrate.

Some factors which contribute to stripping are: inadequate drying of aggregate, use of open-graded asphalt friction course, use of friable and weak aggregate, overlays on deteriorated concrete pavements, waterproofing membranes and seal coats [Khandal, 1992]. Use of anti-stripping additives can sometimes decrease asphalt's susceptibility to stripping [Tunnicliff and Root, 1984].

2.5 Methods to Evaluate Moisture Susceptibility

The Boiling Water Test, Lottman Test, Tunnicliff and Root Conditioning, Immersion Compression Test, Modified Lottman Test, Static Immersion Test, Texas Freeze-Thaw Pedestal Test and Texas Boiling Water Test are some tests conducted for testing the moisture susceptibility of HMA mixes [Khandal, 1992]. Each is described in the following sections.

2.5.1 Boiling Water Test

This is a qualitative test used to test the moisture susceptibility of HMA mixes. In this test, loose HMA mix is added to boiling water for a period of 10 minutes. The percent total visible aggregate that retains its original asphalt coating is estimated as below or above 95%. The primary use of this test is for the preliminary investigation of asphalt mixes. Stripping of fine aggregate mixes is difficult to find using this test method.

2.5.2 Static-Immersion Test

This is also a qualitative test (AASHTO T – 182), in which the mix is immersed in distilled water, which is maintained at 77^0F (25^0C) for 16 to 18 hours. Then, the percentage of total visible area of the aggregate that retains the asphalt coating is estimated as above or below 95% by observing the sample through the water. This is a subjective method with high variability and does not involve any strength tests [Brown et al., 2001].

2.5.3 Texas Boiling Water Test

The Texas Boiling Water Test (TBWT) is a visual rating of the extent of stripping after the mixture is boiled. In this test, the asphalt is heated at 325^0F (103^0C) for 24 to 26 hours. One to three hundred grams of unwashed aggregate are heated at the same temperature for 1 to 1.5 hours. Then the aggregate and asphalt are mixed together and are allowed to cool for two hours. A 1,000 ml beaker is filled halfway with distilled water and boiled. The mixture is placed in the boiling water for 10 minutes. Asphalt cement that is floating is skimmed off the top of the water. The water is cooled to room temperature and then the water is poured off. The mixture is emptied onto a paper towel and then graded. Three people grade the mixture at the same time and again the next day when the mixture gets dry. A mixture that retains 65 to 75% asphalt is suitable for use in the field [Kennedy, Roberts and Lee, 1983].

2.5.4 Lottman Test

This is a laboratory quantitative strength test, and was developed by Lottman. This test is used to predict the moisture susceptibility of asphalt concrete mixes. This test is well-known and is described in the National Cooperative Highway Research Program (NCHRP) 192 [Khandal, 1992]. The laboratory procedure that was developed was field tested in NCHRP 246 [Khandal, 1992].

Nine specimens are used in this test. The specimens are compacted to field air void percentage. These nine samples are divided into three groups of three each. Group one is the control, which are not conditioned. Group two cores are vacuum saturated with water for 30 minutes at 660 mmHg. Group two reflects the field performance of the HMA mix for the first four years of life. The third group is also vacuum saturated, but then it is put through a freeze-thaw cycle. Group three cores are frozen at 0^0F (-18^0C) for 15 hours. Then they are thawed at 140^0F (60^0C) for 24 hours. Group three is designed to reflect the field performance from the fourth year to the 12th year [Lottman et al., 1988].

After the prescribed number of conditioning cycles, these cores are subjected to the Indirect Tensile Strength Test or the Resilient Modulus Test (M_R). The retained tensile strength (TSR) is equal to the indirect tensile strength of the conditioned samples divided by the indirect tensile strength of the unconditioned samples. A minimum TSR of 0.70 is recommended [Lottman et al., 1988].

2.5.5 Tunnicliff and Root Conditioning

Tunnicliff and Root developed this method. This test uses six samples compacted to 6 to 8% air void content. These samples are divided into two groups of three each. The first group is not conditioned. The second group is vacuum saturated at 20 inches Hg to get a saturation level between 55 and 80%. After saturation, the samples are soaked in a water bath at 140^0F for 24 hours. The indirect tensile strength is performed at 77^0F (25^0C) with a loading rate of 2 in/min. The minimum acceptable TSR is 0.7 to 0.8 [Tunnicliff and Root, 1984].

2.5.6 Modified Lottman Test

This method was proposed by Khandal and was adopted by AASHTO in 1985. This test is a combination of the Lottman Test and the Tunnicliff and Root Test. Six specimens are produced with air voids between 6 and 8%, because higher air voids accelerate moisture damage on the cores. These six specimens are divided into two groups of three each. The first group of samples is not conditioned. The second group is saturated between 55 and 80% with water and is placed in the freezer (0^0F or -18^0C) for 16 to 18 hours. The frozen cores are then placed in a water bath at 140^0F (60^0C) for 24 hours. After conditioning, the Resilient Modulus Test or Indirect Tensile Strength Test is performed. The Indirect Tensile Strength Test is performed at 77^0F (25^0C) with a loading rate of 2 in/min. The minimum acceptable TSR is 0.7 after one single cycle [Brown et al., 2001].

2.5.7 Immersion-Compression Test

This test utilizes six cores. Each core is four inches in diameter and four inches in height. The cores are compacted with a double plunger at 3,000 psi for two minutes to get an air void content of 6 percent. The six cores are split into two groups. The first group is not conditioned. The second group is conditioned in water bath at 120^0F (49^0C) for four days or at 140^0F (60^0C) for one day. After conditioning, the unconfined compressive strength of each core is found. A testing temperature of 77^0F (25^0C) and a loading rate of 0.2 in/min. are used. The retained compressive strength is calculated. A retained strength of 70% is specified by many agencies [Brown et al., 2001].

The Immersion-Compression Test has produced retained strengths close to 100% even when stripping is visually evident in the cores; this is due to pore water pressure [Brown et al., 2001]. Thus, this test is not sensitive enough to measure the moisture-induced damage [Brown et al., 2001].

2.5.8 Texas Freeze-Thaw Pedestal Test

This test is conducted on HMA mix with uniform aggregate sizes. Since uniform aggregate size is used, the effects of mechanical properties of the aggregate are minimized. To perform this test, the asphalt and the aggregate are mixed using the Texas Mixture Design Procedure. After initial mixing, the mixture is reheated and is mixed two times additionally.

A cylindrical mold is used to compact the specimen. The specimen has a height of 19.05 mm (0.75 in.) and 41.3 mm (1.6 in.) diameter. A constant load of 27.6 KN (6,200 lbs) is applied for 20 minutes. Then the specimen is cured at ambient temperature for three days. Thermal cycling is performed on the

specimen. The specimen is placed on a stress pedestal in a jar, and is covered with 12.7 mm (0.5 in.) of distilled water. It is cycled through -12^0C (-10^0F) for 12 hours then 12 hours at 49^0C (120^0F). The number of freeze thaw cycles required for the sample to break indicates moisture susceptibility of the HMA mix. Mixes that were susceptible to moisture-induced damage survived less than 10 cycles [Kennedy, Roberts and Lee, 1983]. Mixtures that were not susceptible to moisture-induced damage survived more than 20 cycles [Kennedy, Roberts and Lee, 1983].

2.6 Methods to Limit Moisture Susceptibility

When moisture infiltrates into an asphalt pavement, there will be a loss of bond between the asphalt binder and aggregate. When this happens, pavements will suffer accelerated damage leading to failure and reduced pavement life. If the asphalt pavements suffer from moisture damage, there will be reduced performance and increased maintenance cost. To overcome this problem, various liquid or solid anti-stripping additives have been developed, which can be used to promote adhesion between asphalt and aggregate. Anderson and Dukatz [1982] reviewed the effects of commercially available anti-stripping additives on the physical properties of asphalt cement. It was found, from their studies on the physical and compositional properties of asphalt cement with anti-stripping agents, that anti-stripping additives tend to soften the asphalt, reduce the temperature susceptibility, and improve the aging characteristics of asphalt cement.

Preheating of aggregate removes moisture from the aggregates. It is found that reclaimed asphalt pavement (RAP) or aggregates precoated with asphalt have shown better moisture resistance than virgin aggregates [Kennedy, Roberts and Lee, 1983].

2.6.1 Anti-Stripping Agents

It is necessary to add anti-stripping agents if the asphalt mix is susceptible to moisture-induced damage. Liquid anti-stripping agents and lime additives are among the most commonly used types of anti-stripping agents. However, if an additive is added when it is not needed, there may be some adverse effects. Adverse effects include increased mix cost and maintenance or rehabilitation cost [Tunnicliff and Root, 1984].

2.6.1.1 Liquid Anti-Stripping Agents

Liquid anti-stripping agents are surface-active agents, which reduce the surface tension and promote a higher degree of adhesion of asphalt to the aggregate surface. Liquid anti-stripping agents are compounds that contain amines [Khandal, 1992].

Heating the asphalt to liquid state and then mixing liquid anti-stripping agent would be the easiest and most cost-effective method, but this is not a very effective method because only a portion of the additive reaches the aggregate. A more efficient method of utilizing a liquid anti-stripping agent is by adding it to the aggregate prior to the addition of binder [Kennedy, Roberts and Lee, 1983].

2.6.1.2 Lime Additives

Lime additives are found to be one of the most accepted methods of minimizing the moisture susceptibility of a mix. One reason for this is that lime reacts with most silicate aggregates to form a calcium crust. This crust has a strong bond with the aggregate and has sufficient porosity to allow penetration of the asphalt cement to form another strong bond. Generally, 1 to 1.5% lime by dry weight of aggregate is added to mix. It is necessary to add more lime additive if the mix contains lots of fine aggregate. This is due to the increased surface area of the aggregate. Usually three forms of lime are used: hydrated lime ($Ca(OH)_2$), quick lime (CaO), and Dolomitic limes (both types S and N) [Roberts et al., 1996]. The problem with dry hydrated lime is that it is difficult to maintain its coating on the aggregate surface until the asphalt cement coats the aggregate. Dry hydrated lime is sometimes added to wet aggregate that contains 3 to 5% water content by weight of lime.

2.7 Methods to Evaluate Low Temperature Cracking

The Thermal Stress Restrained Specimen Test has been found to be one of the most effective methods to evaluate low temperature cracking, because it closely simulates the field conditions to which the asphalt pavement is subjected.

2.7.1 Thermal Stress Restrained Specimen Test

The Thermal Stress Restrained Specimen Test (TSRST) device contains systems for controlling load, temperature and for data acquisition. The testing procedure is described in AASHTO. This test method determines the tensile strength and temperature at fracture for asphalt pavements by restraining it from contracting. When the specimen is restrained from contracting, tensile stresses develop in the specimen. When these tensile stresses become equal to the tensile strength of the specimen, the specimen fractures in tension. The basic requirement for this test is that it maintains the test specimen at constant length during cooling. A schematic of TSRST apparatus and its components are shown in the Figure 2.1. The system consists of load frame, a step motor, screw jack, computer data acquisition and control system, low temperature cabinet, temperature controller, and specimen alignment stand. The step motor keeps the specimen at a constant length throughout the test by using linear variable differential transformers (LVDT's). TSRST device used at the University of Wyoming is shown in Figure 2.2.

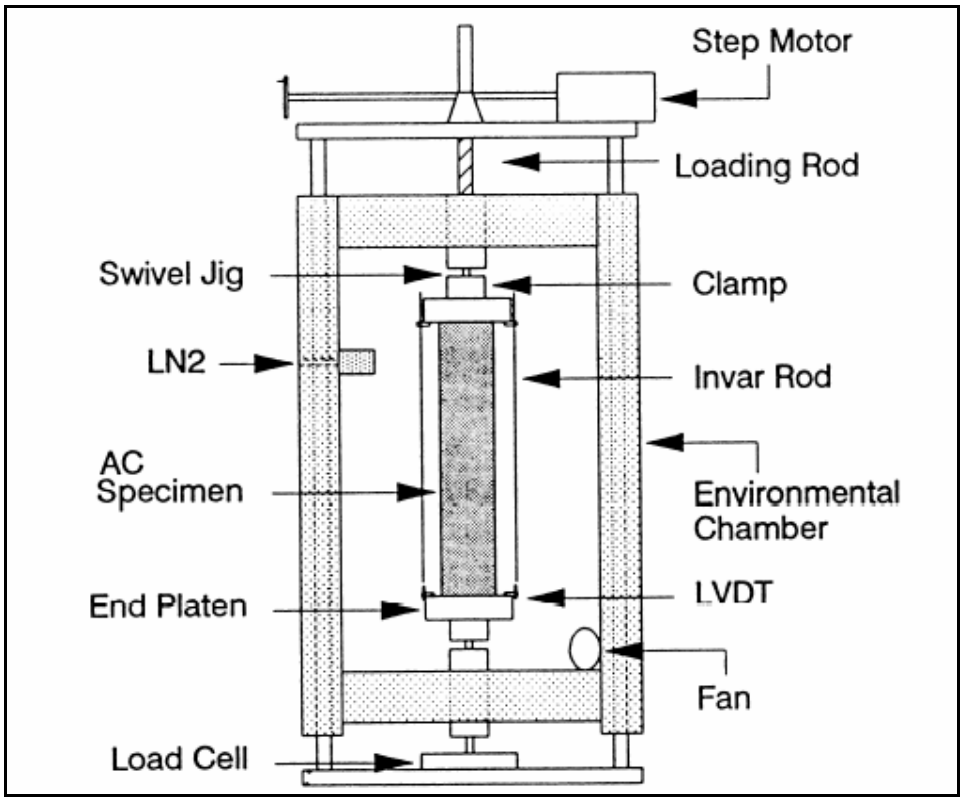

Figure 2.1 Tensile Stress Restrained Specimen Tester

Figure 2.2 Tensile Stress Restrained Specimen Tester

2.8 Methods to Evaluate Rutting

Ruts are the depressions caused in the pavement wheel paths due to the heavy traffic wheel loads. Figure 2.3 shows a picture of rutting in pavement due to heavy traffic wheel loading. Rutting starts from permanent deformation in any of the pavement layers or the subgrade. Lateral movement of consolidated layers because of heavy traffic loads causes rutting. Consolidation is the further compaction of asphalt layer after construction. This lateral movement of consolidated layers occurs due to inadequate compaction of HMA. Bituminous layers will get consolidated after construction but a problem arises when too much consolidation occurs. Under normal conditions, a four-inch layer compacted to 7 to 8% air voids during construction will get consolidated to 4 to 5% air voids in two to three summers and develop rut depths approximately 0.3cm (0.12in). Pavement with air voids greater than 8% are prone to rapid oxidation leading to cracking and raveling. Pavements with air voids less than 3% are susceptible to rutting. Therefore, HMA should be compacted to an air void level ranging from 3 to 8%, because repeated vehicular loadings will cause the HMA to eventually compact to air void of approximately 3 to 5%.

Figure 2.3 Rutting in Pavement

The past half-century has seen development of several rut testing devices. Some of them are obsolete but their concepts have been refined to simulate actual traffic characteristics. Currently, several testing devices are in use; each testing device has its own design and unique features that distinguish it from others. Some of them include French Rutting Tester, Hamburg Wheel Tracking Device, and Georgia Loaded-Wheel Tester. Each will be discussed in the following sections.

2.8.1 The French Rutting Tester

This device is considered as a “European Torture Test” because of the grueling conditions that it subjects to pavements. This tester is used in France to evaluate mixtures subjected to heavy traffic: mixtures that incorporate materials that tend to lead to rutting, such as some natural sands, and mixtures that have no performance history. This device tests rutting susceptibility of asphalt pavements using a reciprocating, pneumatic rubber tire pressurized to 0.6 $\pm$ 0.03 Mpa. The test specimens are slabs of dimensions 50 by 18 cm (19.7 by 7.1 in) and 2 to 10 cm (0.8 to 3.9 in) thick [Aschenbrener and Stuart, 1992]. One advantage of this test is that it can test two slabs simultaneously. The wheel load on both slabs must be equal to avoid asymmetric pressures on the tire assembly. Figure 2.4 shows a picture of a French Rutting Tester.

Figure 2.4 French Rutting Tester

Hydraulic jacks underneath the slabs push them upward to create the load. The standard load is 5,000 ± 50 N; the maximum load is 5,500 N. Pressure gauges on the control panel of the machine give the pressure in each jack. Each pressure gauge is calibrated in increments of 0.1 MPa using a load cell.

Initially, 1,000 cycles are applied at 15 to 25°C to densify the mixture and to provide a smoother surface. This requires approximately 15 minutes. The thickness of each slab is then calculated by averaging 15 thickness measurements taken at 15 standard positions using a gauge with a minimum accuracy of 0.1 mm. This thickness is considered the initial thickness of the slab. The slabs are then heated to the test temperature of 60 ± 2^0 C for 12 hours. A test temperature of 50 ± 2^0 C is sometimes used in France for base courses. The average rut depth in each slab is measured manually after 30, 100, 300, 1,000, and 3,000 cycles when testing 50-mm slabs, and at 300, 1,000, 3,000, 10,000, and 30,000 cycles when testing 100-mm slabs. The average percent rut depth based on the initial thickness of the slab is calculated. A pair of slabs can be tested in approximately 9 hours. The cost of the French Rutting Tester and LCPC plate compactor is around $185,000 [Aschenbrener and Stuart 1992].

2.8.2 The Hamburg Wheel Tracking Device

This device measures the rutting and moisture susceptibility of an asphalt paving mixture by rolling a steel wheel across the surface of an asphalt concrete slab that is immersed in hot water (generally held at 50ºC). This device was developed in the 1970s by Esso A.G. of Hamburg, Germany, based on a similar British device that had a rubber tire. This device was originally used by the city of Hamburg to measure rutting susceptibility. This test was performed for 9,540 wheel passes at either 40 or 50°C. Water is used to obtain the required test temperature instead of an environmental air chamber. When the number of cycles were increased to 19,000, it was found that some mixtures showed failure due to moisture damage. The specimens used in this test are 320 mm in length, 260 mm wide and thicknesses of 40, 80 or 120 mm. Thicknesses up to 150 mm can be tested in this device. The thickness of the specimen is a minimum of three times the nominal maximum aggregate size used in the mix.

Specimens are secured in reusable steel containers using plaster of Paris. Each specimen is placed into a container so that its surface is level with the top edge of the container. This allows the full range of the rut depth measurement system to be utilized. Containers are manufactured in heights of 40, 80, and 120 mm. Steel spacers can be placed under cores and pavement slabs if needed. The container with the specimen is then placed into the wheel-tracking device. The container rests on a steel plate; this provides

a rigid, load-bearing base for the specimen. The temperature of the water bath can be set from 25 to 70^0C. A commonly used test temperature in the Hamburg wheel tester is 50^0C. A water temperature of 50^0C is reached within 45 minutes. Specimens are conditioned at the test temperature for a minimum of 30 minutes. Heated coils in the water provide heat. The temperature of the water is then maintained by these heating coils and by introducing cold water. Figure 2.5 shows a picture of a Hamburger Wheel Tracking device.

Figure 2.5 Hamburger Wheel Tracking Device

This device tests two slabs simultaneously, using two reciprocating solid steel wheels. The wheel is loaded with 705 N (158 lbs). The machine is automated and records the deformations after each cycle. The inverse slope of the rut depth v. cycle curve is calculated simultaneously. Figure 2.6 shows an illustration of a typical rut depth v. cycle curve. The plot is straight, up to the stripping inflection point which is the point where stripping begins to occur on the sample. The straight segment of the plot is called creep slope, this is because of the plastic flow of the asphalt cement. The plot is straight past the stripping inflection point, except with a much higher slope. This segment of the plot is considered the stripping slope because all of the rutting is due to stripping instead of plastic flow. Rut depths less than 4mm (0.16 in) are considered to be acceptable in this test after 20,000 cycles. The approximate time taken to test a pair of slabs is 6six hours. The cost of the Hamburg Wheel Tracking Device is around $45,000 [Aschenbrener and Stuart, 1992].

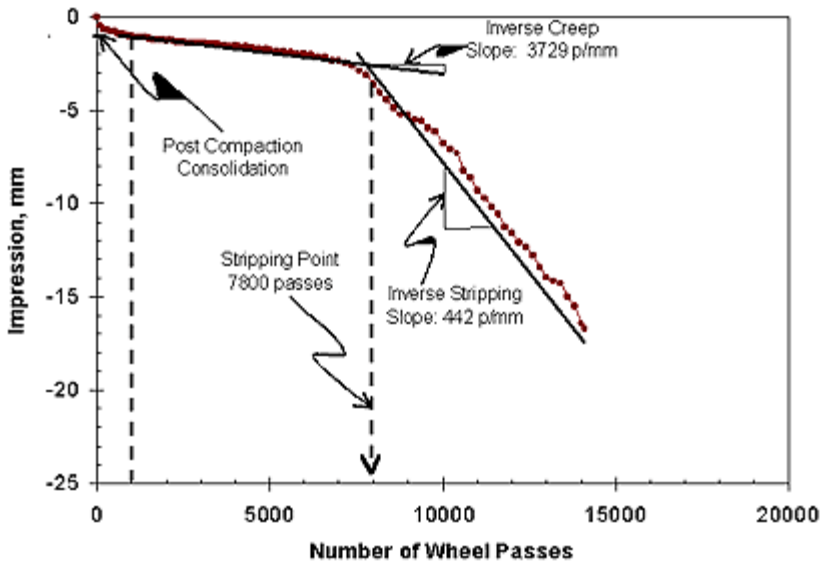

Figure 2.6 Rut Depth vs. Number of Wheel Passes

2.8.3 Georgia Loaded -Wheel Tester

The Georgia Loaded-Wheel Tester (GLWT) was developed during the mid 1980s through a cooperative research study between the Georgia Institute of Technology and the Georgia Department of Transportation (GaDOT). GaDOT later realized that some modifications to the wheel tracking device originally designed by C. R. Benedict of Benedict Slurry Seals, Inc. could meet their needs. The GLWT is shown in Figure 2.7.

Figure 2.7 Georgia Loaded Wheel Tester

The Georgia Loaded Wheel-Tester is capable of testing asphalt beam or cylindrical specimens. Beam dimensions are 7.62 x 7.62 x 38.1 cm (3 x 3 x 15 in) and can be compacted with a variety of methods. In this test, samples are preheated to the testing temperature, usually 35 to 60^0 C (95 to 140^0 F). The samples are then placed in the GLWT and are kept in position using concrete molds. Figure 2.8 shows a GLWT test specimen subjected to cycles. A 100-pound load is applied on a pneumatic linear hose, which is pressurized to 0.69 MPa (100 psi). This hose is usually 2.54 cm (1 in) diameter. Load is applied by an aluminum wheel, which rests on this linear hose, which rests on the specimen. This combination of weight and pressure produces a contact pressure of 100 psi. One cycle is one forward and one backward movement of the wheel over the specimen. Rut depths are measured at a predetermined number of cycles. The number of load cycles to be applied can be specified in the GLWT. After the specified number of cycles, the loaded-wheel stops automatically. Typically, samples are considered to pass in the GLWT if the rut depths are less than 0.762 cm (0.3 in) after 8,000 cycles. One sample can be tested in approximately 3 ½ hours.

Figure 2.8 GLWT Specimen Held Firm using Concrete Frame

2.9 Methods to Evaluate Field Performance of Asphalt Pavements

One major factor that determines a pavement's service life is the modulus values of its layers. These modulus values are used to determine the need for maintenance, rehabilitation, or reconstruction. One method of determining these modulus values is destructive testing, which involves extraction of core samples from the pavement. On the other hand, nondestructive testing does not require extraction of core samples. One such nondestructive testing device is the Falling Weight Deflectometer (FWD). The Falling Weight Deflectometer applies a load and measures the deflections in the pavement. The modulus values of the entire layer system can be backcalculated with the help of these surface deflections and the layer thickness values. Another way of determining the condition of in-service pavements is with the help of Pavement Condition Index (PCI) values. These values give an indication of the amount of distress and extent of repair needed for the pavement.

2.9.1 Surface Deflections

Measurement of surface deflection is one of the primary means of evaluating flexible and rigid pavement in-service conditions, as the magnitude of these deflections depends on the type of traffic and volume of traffic to which the pavement has been subjected. Deflection measurements can be used in backcalulation methods to determine pavement structural layer stiffness and the subgrade resilient modulus. Thus, many characteristics of a flexible pavement can be determined by measuring its deflection in response to the load. It has been found that the Falling Weight Deflectometer can be effectively used to determine the pavement characteristics.

2.9.1.1 Falling Weight Deflectometer

The Falling Weight Deflectometer measures the peaks of a deflection wave from an impulse load created by a falling weight that simulates a moving wheel load. The test load is distributed over a circular contact pressure area 300mm in diameter, and thus resembles in its duration, a passing heavy single-tire wheel load of a truck. An essential feature of the FWD test is that the peak deflections are measured at various distances from the load. The FWD can either be mounted in a vehicle or on a trailer that is equipped with a falling weight and several velocity transducer sensors. To perform a test, the vehicle is stopped and the loading plate is positioned over the desired location. The sensors are then lowered to the pavement surface, the weight is dropped, and the surrounding pavement vertical deflections are recorded. Figure 2.9 shows load plate and sensors used to measure deflections.

Figure 2.9 FWD Impulse Loading Mechanism

Some of the possible advantages of FWD include:

- FWD is a non-destructive testing device
- One-man operation
- Safe and convenient
- Accurate and fast (up to 60 test points/hr.)
- Can be used for multi-purpose pavement applications like unpaved roads and paved roads
- Wide loading range (7 – 120 kN) or (1,500 – 27,000 lb.)

2.9.1.2 Temperature Correction of FWD Deflections

Deflections measured in FWD testing must be corrected to a particular type of loading system and to a predefined environmental condition. The loading system factor is dependent on the type of nondestructive testing device, the frequency of loading, and the load level. It has been found that most critical environmental factor affecting the deflections in flexible pavements is the temperature of the asphalt concrete layer, because FWD measurements are collected at different temperatures [Murphy et al., 2000]. The 1993 AASHTO guide contains a temperature correction procedure for FWD deflections measured under the plate load. The curves in the AASHTO guide were originally developed by Southgate and Deen, and then were modified empirically by using AASHTO road test data. The reference temperature used in this procedure was 21^0 C (70^0 F). The effective temperature of the asphalt layer is determined by calculating the mean values of temperatures from the near surfaces, the mid layer and the bottom of asphalt layer. These temperatures are predicted from the sum of the measured surface temperatures and the average air temperature for the previous five days. The AASHTO procedure is inaccurate at temperatures over 38^0 C (100^0 F) [Kim et al., 1995].

Many other temperature correction procedures were developed in the past, but they were site specific. A universal equation was proposed by Kim, which allows users to use their own reference temperature. Since the temperature correction depends on the thickness of asphalt layer, Kim used an optimization technique to extract the thickness factor used in the equation. The equation proposed by Kim is:

$$D_{68} = D_T * [10^{(\alpha * (68 - Td))}] \quad \text{.....Equation 2.1}$$

Where,

$\alpha = 5.807 * 10\text{-}6 * (h_{AC})^{1.4635}$ *(For wheel paths)*

$\alpha = 6.560 * 10\text{-}6 * (h_{AC})^{1.4241}$ *(For Lane Center)*

h_{AC} *= Thickness of asphalt pavement in (mm)*

T_d *= Pavement mid-depth temperature.*

2.9.2 Backcalculation of Layer Moduli

Resilient modulus of pavement layers is an important factor in determining the pavement in-service life, allowable loads for existing pavement structures, rigidity, strength of pavement, and in assessing the need for rehabilitation. One way of determining these layer moduli is to drill cores from pavement section, but this will disturb the pavements structural integrity and is a destructive test. Another way of determining layer moduli is to backcalculate the layer moduli using the FWD deflection and layer thickness values.

Backcalculation is the ‘‘inverse’’ procedure of determining the material properties of pavement layers in response to the respective surface loading. The backcalculation procedure takes a measured surface deflection and attempts to match it with a calculated surface deflection generated from an identical pavement structure using assumed layer moduli with some tolerable error. The assumed layer moduli in the calculated model are adjusted until they produce a surface deflection that closely matches the measured one. The combination of assumed layer moduli that results in this match is then assumed to be near the actual in situ moduli for the various pavement layers. The backcalculation process is usually iterative and normally done with computer software.

Various computer programs are available to perform backcalculation of layer moduli, some of them include: EVERCALC 5.0, MODULUS, and MODCOMP3. Every program has its own advantages and shortcomings.

2.9.2.1 Description of Evercalc4.0

Joe Mahoney at the University of Washington developed EVERCALC4.0 for the Washington DOT. EVERCALC4.0 uses the WESLEA computer code developed by the Waterways Experimental Station, U.S. Army Corps of Engineers, as a forward calculation subroutine, and a modified augmented Gauss-Newton algorithm for solution optimization [Gergis, 1999]. The WESLEA computer code is based on the multilayer linear elasto-static theory that is traditionally used for purposes of flexible pavement analysis. This program can handle up to seven sensor measurements and eight drops per section. To initialize the backcalculation process, initial moduli, as well as moduli ranges need to be specified for all the layers. This feature prevents the program from producing out-of-range moduli for all the layers. At the end of each iteration, the deflections calculated by WESLEA are compared with the measured ones. The difference between the calculated and measured deflections is called Root Mean Square (RMS) error. The iterations are terminated when one of the following three conditions are satisfied: (1) RMS falls within the allowable tolerance, (2) the changes in modulus between two successive iterations fall within

the allowable tolerance, or (3) the number of iterations has reached the maximum limit. If the pavement section contains no more than three layers, the program can assign the seed moduli internally. One shortcoming of the EVERCALC4.0 program is that the output files are stored in binary format, which complicates the communication of EVERCALC4.0 with any other software. EVERCALC is user-friendly backcalculation software [Gergis, 1999].

2.9.3 Pavement Condition Index

Pavement Condition Index (PCI) values are obtained for pavements through a visual distress survey of the pavement. This method can be used both for asphalt surfaced as well as jointed Portland Cement Concrete (PCC) pavements. Nineteen distress types and measurement procedures are defined and used to come up with a single pavement condition index from 0 to 100, with 0 being the worst possible condition and 100 being the best possible condition. The Construction Engineering Research Laboratory of the U.S. Army Corps of Engineers developed this method. The PCI method has been adopted by the Federal Aviation Administration to determine the pavement condition of airport runways.

Pavement Condition Index values can be used to estimate the extent of repair works, likely cost, and gives an indication of when the pavement needs rehabilitation. The Pavement Condition Index values are determined based on the roughness, surface distress, and skid resistance of the pavement. The Pavement Condition Index (PCI) is calculated based on the methods described in ASTM D6433-99. Table 2.1 shows some standard ranges used to rate a pavement.

Table 2.1 Standard Pavement Rating Based on PCI

Pavement Condition Index	Rating
100 to 85	Excellent
85 to 70	Very good
70 to 55	Good
55 to 40	Fair
40 to 25	Poor
25 to 10	Very poor
10 to 0	Failed

2.10 Nitrogen Analysis

Asphalt is a unique material that readily coats and adheres to dry mineral aggregates. The asphalt-aggregate interfacial bond is a molecular phenomenon. Non-polar alkane and aromatic molecules readily adsorb on the surface hydroxyls and other material bonding sites such as silica and silica-alumina [Plancher and Petersen, 1998]. Aggregate bonding sites on model surfaces range from surface hydroxyls of varying acidities to hydrogen bonding sites having sufficient acidity to protonate pyridine, (pyridinium ions). Strong electropositive bonding sites can also be present. Metals present in the aggregates such as iron, magnesium, and calcium, often create these acid sites. Lewis acid sites formed at the aluminum atomic site in silica-alumina are typical. Oxide and hydroxyl functionalities in minerals provide adsorption sites for many chemical functionalities of the types found in asphalts (like carboxylic acids, pyridinics) , including water.

Water competes for aggregate bonding sites with many of the chemical functional groups in asphalts, and thus displaces asphalt already adsorbed on aggregate surfaces [Plancher and Petersen, 1998]. Moisture present on aggregates during the pavement mixing process interferes with effective bonding of the asphalt with the mineral. Model compounds containing polar chemical functional group types found in asphalts (like the pyridinics, carboxylic acids) can be used to simulate the adsorption-water displacement characteristics of asphalt molecules on mineral aggregate surfaces [Plancher and Petersen, 1998]. Carboxylic acids were confirmed as the functional type that strongly adsorbed on mineral aggregate surfaces, however they were most easily water displaced [Plancher and Petersen, 1998]. Pyridine mimics the actions of amine anti-stripping agents and basic nitrogen compounds in asphalts that might be beneficial in reducing pavement moisture damage.

2.11 Chapter Summary

Bottom ash accounts for 20% of the coal ash produced in the US. Most bottom ash is unused and is disposed of in landfills. Recent research has indicated that the use of bottom ash in asphalt mixes can improve the performance of pavements while providing an alternative to ash disposal. It is desirable to know if asphalt mixes containing bottom ash are more susceptible to stripping, low temperature cracking and rutting when bottom ash is added. All the three rut-testing devices can efficiently test for rutting but Georgia Loaded Wheel Tester was used because it is available here at University of Wyoming. The Thermal Stress Restrained Specimen Tester (TSRST) was used to evaluate for low temperature cracking because it simulates field conditions which the pavement is going to experience and the Modified Lottman Test was selected of all the other testing methods to evaluate stripping because this method was found to effectively evaluate stripping. FWD deflections and PCI values are some of the non-destructive test types used to evaluate field performance of asphalt pavements when bottom ash is added.

3. EXPERIMENTAL DESIGN

3.1 Introduction

The main objective of this study was to evaluate the performance of hot-mix asphalt pavements (HMA) when Wyoming bottom ash is added. This objective was accomplished by doing laboratory and field evaluation on the asphalt concrete mixes prepared with and without bottom ash. Laboratory evaluation was accomplished by preparing the samples with three types of bottom ash in the lab and testing them for low temperature cracking, rutting, and stripping. Nitrogen analyses on both the aggregate as well as the three bottom ashes were performed to determine the susceptibility of these aggregates and bottom ashes to moisture-induced damage.

Field evaluation was accomplished by construction of experimental pavement section in Gillette, Wyoming. Four test sections, each 800 feet in length, were constructed. One test section was a control section (without bottom ash) and the other three sections contained three bottom ashes from three power plants sources in Wyoming (one bottom ash for each section). The field performance of the test section was later evaluated using the Pavement Condition Index (PCI) and the layer modulii backcalculated from Falling Weight Deflectometer deflections.

3.2 Asphalt Mix Materials

The bottom ash used in this research project was obtained from three sources, the Jim Bridger, Laramie River, and Dave Johnston coal-fired power plants. The Jim Bridger power plant is located in the southwest corner of Wyoming near Point of Rocks. The Laramie River power plant is located in Wheatland, Wyoming. The Dave Johnston power plant is located in Glenrock, Wyoming. Each power plant burns coal from different mines located near their operations. All the three plants are considered "wet bottom" units, and thus produce wet bottom ash [Stephen, 1999].

Two types of aggregate were used in this study - granite and limestone - because those are the most commonly used aggregates in pavement construction. The limestone coarse aggregate was obtained from Pete Lien & Sons in Wyoming, and crushed limestone fines were obtained from Pete Lien & Sons in South Dakota. The granite aggregates were obtained from Lewis & Lewis in southwestern Wyoming.

Aggregate gradation can greatly affect the stability and durability of HMA mixes. Therefore, aggregate gradation is a primary concern in mix design. Gradation is normally determined by sieve analysis. It is a procedure in which a set of sieves with different sieve openings are stacked up. The top sieve has the largest opening size and sieves with progressive smaller openings are placed lower in of the stack. Aggregates retained on each sieve are weighed, and gradation is expressed as the percentage of materials passing each of the sieve sizes. Gradations of both the aggregates, with and without 15% bottom ash, are shown in Table 3.1 and 3.2.

Table 3.1 Limestone Aggregate Gradations for Control and with 15% Bottom Ash

	Control	Dave Johnston	Laramie River	Jim Bridger
Gradation	**% Passing**	**% Passing**	**% Passing**	**% Passing**
3/4”	100	99	100	99
1/2”	85	83	85	84
⅜”	78	75	77	76
#4	55	51	54	52
#8	31	29	33	31
#16	17	18	21	19
#30	10	11	14	13
#50	6	7	9	9
#100	5	4	5	5
#200	3.7	2.8	2.9	3.1

Table 3.2 Granite Aggregate Gradations for Control and with 15% Bottom Ash

	Control	Dave Johnston	Laramie River	Jim Bridger
Gradation	**% Passing**	**% Passing**	**% Passing**	**% Passing**
3/4“	100	99	99	100
1/2”	98	96	97	97
3/8”	83	80	82	81
#4	54	51	54	52
#8	31	30	33	31
#16	21	20	24	22
#30	15	15	18	18
#50	12	12	13	14
#100	8	7	8	8
#200	4.8	4.3	4.4	4.6

Asphalt cement with a performance grade of PG 64 - 22 was utilized in this study to prepare laboratory mixes and also for the experimental paving sections. The asphalt cement was obtained from Sinclair refinery in Casper, Wyoming. For the Nitrogen Analysis test, limestone, granite aggregates and three bottom ashes were sieved on a 60 – 80 mesh and the aggregate and bottom ash retained on the 80 mesh was used.

3.3 Laboratory Evaluation

This section describes the specimen preparation procedures needed to conduct the Indirect Tensile Strength Test, the Thermal Stress Restrained Specimen Test, the Georgia Loaded Wheel Test, and the Nitrogen Analysis Test.

3.3.1 Preparation of Samples for Indirect Tensile Strength Test, Georgia Loaded Wheel Test and Thermal Stress Restrained Specimen Test

Samples used for the three tests were of different dimensions. The Indirect Tensile Test requires cylindrical samples with a 2.5-inch (63.5 mm) height and 4-inch (100 mm) diameter. Samples used for the Georgia Loaded Wheel Test are 3 inches (76 mm) in height and 6 inches (150 mm) in diameter and the samples used for Thermal Stress Restrained Specimen Test are cylindrical with a 2-inch (51 mm) diameter and a height of 9.5 inches (241 mm).

Specimens used in this study for the Indirect Tensile Strength Test and Georgia Loaded Wheel Test were compacted using the Troxler Gyratory compactor. This compaction method resembles the method of compaction the asphalt would receive in the field. Proper compaction is very important because, if the loose mix were not properly compacted, the increase or decrease in the air void content would affect the moisture susceptibility of the asphalt mixes. The asphalt mixes were heated at 140^0 F for 16 hours. These mixes and the specimen molds were then heated to the 280^0 F compaction temperature for two hours. The asphalt mixes were then poured into a heated cylindrical mold having an inside diameter of 4 inches (100 mm) and a moveable lower puck. The amount of HMA mix needed to attain an air void of 6 to 8% was placed in the mold. The mold was then placed in the gyratory compactor, the ram was lowered, and compaction began. The gyratory compactor operates by compacting the loose HMA mix with a constant pressure of 87 psi (600kPa) while the specimen mold is gyrated at an angle of 1.25^0 from vertical. At this pressure and angle, the mold was gyrated at 30 rpm about its original central axis. Cores with 7 ± 1 air voids can also be prepared using the gyratory compactor by utilizing the gyrate-to-height feature.

Samples for the Georgia Loaded Wheel Test are prepared in the same way as for the Indirect Tensile Strength Test, except the mold size is different. The molds used for these test specimens have a 6-inch (150 mm) inside diameter, compared to the 4-inch (100 mm) for the Indirect Tensile Strength Test specimens. The HMA mix is then compacted to a height of 3 inches (76 mm).

Samples for the Tensile Stress Restrained Specimen Test are obtained by sawing a rectangular section from pavement or preparing rectangular sections in the lab. Then a cylindrical section with a 2-inch diameter and 9.5-inch length are drilled from the center of the rectangular section.

3.3.2 Preparation of Aggregate for Nitrogen Analysis Test

Limestone and granite aggregates and four bottom ashes sized to 60- 80 mesh were rinsed with tap water on an 80-mesh screen to remove mineral fines if any were sticking on the aggregate and bottom ashes and then rinsed several times with distilled water before removing the water by vacuum filtration. Moist aggregates and bottom ash were dried at 120^0 C for several days before treating the aggregates with a 90/10 mixture of benzene/pyridine solution in a small glass vial sealed with a Teflon cone-shaped stopper. The mixture was swirled numerous times during the adsorption/absorption treatment. After one hour, the treated materials were recovered and washed with 50ml benzene by vacuum filtration using a narrow glass-cintered tube. During the washing cycle, the aggregate was kept covered with solvent. The washed aggregate was then air dried for 48 hours. One gram of the treated aggregate was further treated for six

hours at 60^0 C in a capped vial with 15 ml of distilled water and 10 ml of benzene (to pick up displaced organics). Following the water treatment, the aggregate was recovered and washed with 2 5ml of benzene followed by 2 5ml of water; the treated aggregates were placed in a 60^0 C oven overnight prior to analysis.

3.3.3 Percent Air Voids

The AASHTO T-166 testing procedure is used to calculate the air voids for the specimens used in this study. Using this procedure, bulk specific gravity of each specimen was calculated. Prior to calculating the bulk specific gravity the percent-absorbed water by each specimen is calculated using Equation 3.1.

$$\% \text{ of Water Absorbed} = \frac{C - A}{C - B} * 100 \quad \text{.....Equation 3.1}$$

Where,
A = Mass of core in air,
B = Mass of core in water,
C = Saturated surface dry mass in air.

If the percentage of absorbed water is less than 2%, then the bulk specific gravity is calculated using Equation 3.2.

$$G_{SB} = \frac{A}{C - B} \quad \text{.....Equation 3.2}$$

Where,
A = Mass of core in air,
B = Mass of core in water,
C = Saturated surface dry mass in air.

The percentage of air void present in the specimen can be calculated using the following equation:

$$\% \text{ of Air voids} = 100 * \left(1 - \frac{A}{B}\right) \quad \text{..... Equations 3.3}$$

Where,
A = Bulk Specific Gravity (T-166)
B = Theoretical Maximum Specific Gravity (T-209).

3.3.4 Saturation and Conditioning

The Wyoming Modified AASHTO T-283 procedure was used to determine the resistance of asphalt mixes to moisture-induced damage. This was done mainly to check the indirect tensile strength.

Prior to subjecting the samples to freeze-thaw cycles, they are saturated so that air voids inside the specimens are filled to 55 to 80% of their capacity. This is done by placing the specimen in a vacuum container filled with water such that specimen is totally submerged in water and then applying vacuum pressure for a sufficient period to provide the specified saturation level. After the saturation, the cores were left in the vacuum vessel for an additional five minutes without the vacuum for the cores to reach an

equilibrium state. Then the cores were taken out and the bulk specific gravity was determined using the original dry weight of the cores. The saturation level is determined by multiplying the volume of the specimen by its original air voids.

3.4 Field Evaluation

In October 2002, a pavement test section was constructed in Gillette, Wyoming. The main purpose of this test section was to evaluate the field performance of the asphalt mixes containing the three bottom ashes. This section was a portion of the south lane of Warlow Drive, a street serving an industrial park and associated businesses and several residential subdivisions in Gillette, Wyoming.

3.4.1 Test Section Design and Construction

The test section is 3,200 feet long and 13.75 feet wide and consists of four 800-foot sections, each containing a different combination of the control mix and mixes containing bottom ashes from three power plant sources.

Prior to the construction of the test sections, the pavement and subgrade conditions were investigated and 3 to 8 inches of total existing pavement thickness was removed using a rotomill machine and trucks. Thermal cracks greater than 1.25 inches in width were repaired with additional milling over the cracks and placement of flexible, high-density asphaltic membrane laminated between layers of a non-woven and woven polygester geotextile fabric. The flexible membrane was then covered with a layer of compacted three-quarter-inch nominal maximum aggregate size hot mix asphalt. Smaller cracks received the same treatment but without the PavePrep fabric. Table 3.3 lists the four sections of the test area, the amount of material placed, and start and the end times of construction.

Table 3.3 Experimental Paving Section Data

Paving Mix	Start Station	End Station	Tons Placed	Start time	End Time
Control	34+15	27+00	168.92	9:50 AM	10:40 AM
Laramie River	27+00	19+00	200.67	11:00 AM	11:50 PM
Dave Johnston	19+00	11+00	200.46	12:00 PM	12:45 PM
Jim Bridger	11+00	2+65	200.63	1:00 PM	1:50 PM

Construction Engineers & Material Testing Labs (CE & MT) in Gillette, Wyoming, prepared the mix design for control and bottom ash asphalt mixes using the Marshall mix design method. Table 3.4 shows the volumetric mix design summary for both the aggregates with and without bottom ash.

Table 3.4 Mix Design Summary

MIX	Optimum Oil%	Bulk Density (pcf)	Rice Density (pcf)	Air Voids %	VMA %	VFA%
CAP (ICM) Limestone Aggregates						
CAP 3/4" Control	4.6	150.5	156.8	4	12.6	68.8
15% DJ Bottom Ash	6.1	146.4	152.4	4	15.6	73.9
15% JB Bottom Ash	5.2	144.8	150.8	4	15.3	83.3
15% LR Bottom Ash	5.7	147.8	154	4	14.6	72.9
Lewis & Lewis Granitic Aggregates						
L+L 1/2" Control	5.5	144.6	150.6	4	15.3	74
15% DJ Bottom Ash	6.2	142.8	148.9	4	15.3	73
15% JB Bottom Ash	6.2	139.5	145.8	4	16.1	75
15% LR Bottom Ash	6	142.9	149.4	4	15.2	72

The mix design summary shows that the control mixes required less asphalt when compared with the respective bottom ash mixes; this is because bottom ash absorbs asphalt. Granite control required more asphalt than the limestone control; this is because granite aggregate contains pores which absorb asphalt.

3.4.2 Test Section Evaluation

Test sections were evaluated using backcalculated layer moduli from FWD data, FWD deflections, and PCI values measured before and after overlay. The PCI values were measured in October 2002 (before overlay), April 2003 and October 2003 (after overlay). The FWD deflections were measured in May 2002 (before overlay) and July 2003 (after overlay). Although some of the conclusions made from this study are based on one-year field evaluations, the test sections will continue to be evaluated on an annual basis to check the long term performance of these asphalt mixes with bottom ash.

3.5 Chapter Summary

This chapter discussed the experimental design for both the laboratory and field evaluation. Laboratory evaluation involved preparing of specimens and testing them for rutting, low temperature cracking and stripping. Field evaluation involved constructing test sections and then evaluating the performance of the test sections using FWD deflections and PCI values. Data collected in the laboratory and in the field were then analyzed using standard statistical analysis procedures to obtain conclusions and recommendations.

4. LABORATORY EVALUATION

4.1 Introduction

This study involved preparation of specimens for the 16 HMA mixes using the gyratory compactor for the Indirect Tensile Strength Test, and then testing them with the Soiltest testing machine. Specimens were also prepared for the four HMA mixes with limestone as aggregate for the GLWT and TSRST. The tendency of the aggregates and bottom ash to resist moisture damage was evaluated by conducting nitrogen analysis tests. The overall purpose of these tests was to determine if the addition of bottom ash to asphalt mixes decreases resistance to moisture induced damage, low temperature cracking and rutting.

4.2 Materials

Limestone and granite were the two aggregates used in this study. Specimens were prepared using both of these aggregates. Consolidated Engineers & Materials Testers (CE & MT) in Gillette, Wyoming, provided the job mix design for both of the aggregates. The gradations of both the aggregates and the WYDOT specification limits are shown in Figures 4.1 and 4.2

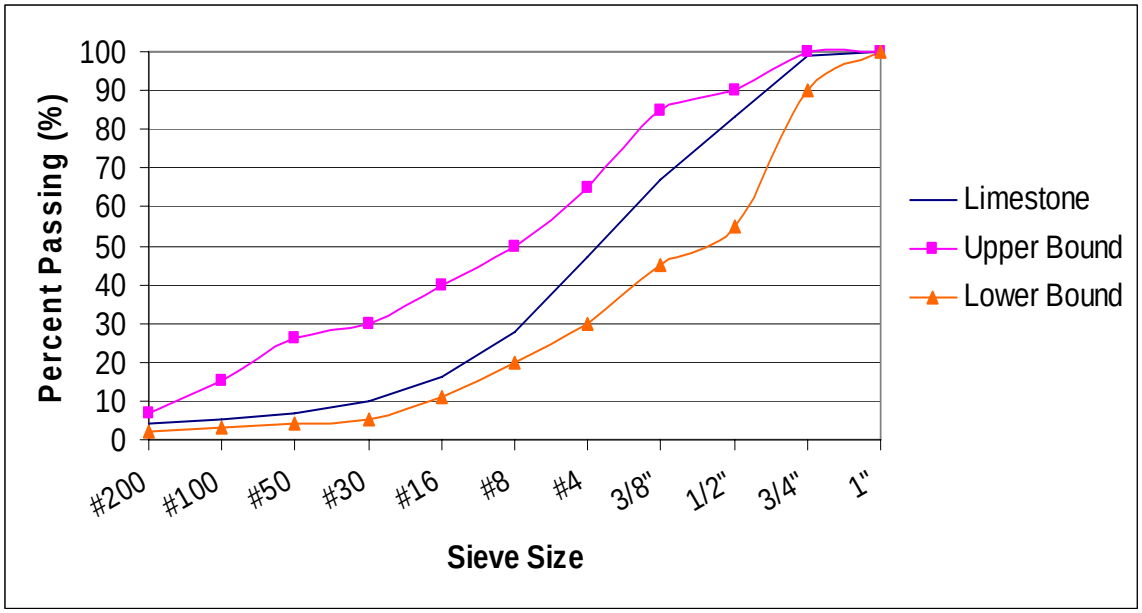

Figure 4.1 Limestone Gradation and Associated Specification Limits

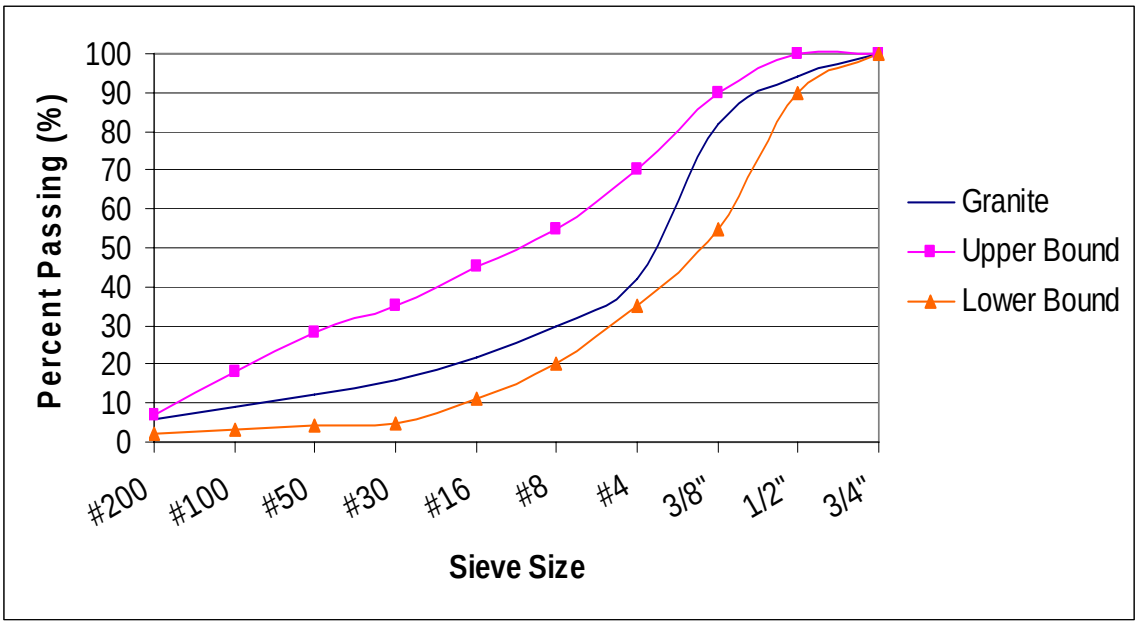

Figure 4.2 Granite Gradation and Associated Specification Limit

4.3 Indirect Tensile Strength Test

After the specified number of freeze-thaw cycles (see Section 3.3), the specimens were placed in a 77^0 F (25^0 C) water bath for two hours and then subjected to the Indirect Tensile Strength Test. The Soiltest machine was used for this test, and the specimens were compressed between two loading strips at a rate of 2 in/min (50.8 mm/min). These two loading plates are concave in shape so as to firmly hold the specimen. The Soiltest machine used for this test is shown in the Figure 4.3

Figure 4.3 Soiltest Machine

The maximum compressive load applied on the specimen is recorded from the dial gauge, and the tensile strength is calculated as follows:

$$\bullet \; Tensile\ Strength = \frac{2p}{\pi hD} \quad \text{.....Equation 4.1}$$

Where,

p = Maximum load, pounds,

h = Height of the specimen, inches,

D = Specimen diameter, inches.

The Tensile Strength Ratio indicates how resistant an asphalt mix is to moisture-induced damage. This Tensile Strength Ratio is calculated as the ratio of tensile strength of conditioned specimen to the tensile strength of unconditioned specimen.

$$\bullet \; Tensile\ Strength\ Ratio = \frac{TS_c}{TS_u} \quad \text{..... Equations 4.2}$$

Where,

TS_c = *Average tensile strength of conditioned specimens,*

TS_u = *Average tensile strength of unconditioned specimens.*

The minimum TSR allowable after one freeze-thaw cycle is 0.7.

The following equation evaluates the effect of multiple freeze-thaw cycles on the moisture susceptibility of asphalt mixes.

$$\bullet \; TSR = 1.0 - TSRR \times N \quad \text{.....Equation 4.3}$$

Where,

TSR = Tensile Strength Ratio,

TSRR = TSR rate,

N = Number of freeze-thaw cycles.

TSRR represents average loss of TSR per freeze-thaw cycle. A sample with TSRR value of zero is considered to be resistant to moisture-induced damage. A mix with higher TSRR value is considered to be susceptible to moisture-induced damage. Mix types are described in Table 4.1. Average TSR values and TSRR data are summarized in Table 4.2 and 4.3 [Conner, 2003].

Table 4.1 Mix Descriptions

Mix Number	Mix Type
1	Control W/o Lime
2	Dave Johnston W/o Lime
3	Jim Bridger W/o Lime
4	Laramie River W/o Lime
5	Control W Lime
6	Dave Johnston W Lime
7	Jim Bridger W Lime
8	Laramie River W Lime

Table 4.2 Tensile Strength, TSR, and TSRR for Granite Aggregate Mixes

Mix Number	1	2	3	4	5	6	7	8
	Unconditioned Tensile Strength (psi)							
	65.62	75	85.1	79.55	88.3	82.8	94.2	80.04
Number of Freeze-Thaw Cycles	Percent of Tensile Strength Retained							
0	100	100	100	100	100	100	100	100
1	96	76.2	84.7	89.8	90.07	92.2	94.1	82.6
2	-	74	82.8	82.4	85.29	98.4	88.3	72.5
4	43.8	65.8	46.6	86.5	86.03	67.84	77.9	84.2
6	49.8	45.9	58.8	74.7	77.21	74.12	86.2	88.3
8	49.8	56.3	37.4	66.1	90.81	81.2	80.7	85.7
10	31.8	32	47.7	80	72.8	62.36	77.6	70.2
15	16.9	21.2	31.7	62	62.3	55.5	74.5	48.7
	TSR Rate							
	0.0554	0.0525	0.455	0.0255	0.025	0.03	0.017	0.005

Table 4.3 Tensile Strength, TSR, and TSRR for Limestone Aggregate Mixes [Conner, 2003]

Mix Number	1	2	3	4	5	6	7	8
	Unconditioned Tensile Strength (psi)							
	71.4	59.1	98.1	96.8	67.6	52.6	75.3	66.9
Number of Freeze-Thaw Cycles	Percent of Tensile Strength Retained							
0	100	100	100	100	100	100	100	100
1	79	84	63	66	92	94	94	95
2	75	82	66	58	89	92	84	87
4	65	77	42	44	89	91	75	84
6	51	54	37	41	82	89	74	84
8	49	46	37	42	79	89	71	82
10	47	40	29	42	74	86	73	80
15	33	23	31	36	68	91	58	71
	TSR Rate							
	0.045	0.051	0.046	0.043	0.021	0.006	0.028	0.019

Appendix B contains the plots for all the eight HMA mixes and also the specimen data for the Indirect Tensile Strength tests.

4.4 Georgia Loaded Wheel Test

The Georgia Loaded Wheel Test was developed originally to test asphalt beams with dimensions of 7.62 x 7.62 x 38.1 cm (3 x 3 x 15 in). However, a set of testing procedures was developed at the University of Wyoming to test cylindrical specimens 15 cm (6 in) in diameter and 7.6 cm (3 in) tall. These samples require less material, are easier to compact in the lab, and cores of this size can be obtained in the field [Stephen, 1999].

Prior to testing of specimens in the GLWT, the specimens were compacted using the gyratory compactor, and were then preheated to a temperature of 46.1^0 C (115^0 F). The specimens were kept in position by specimen holding molds. Initial measurements were taken using three dial indicators attached to an aluminum dowel. The linear hose was pressurized to 689 kPa (100 psi.), and a wheel, loaded with a 45.4 kg (100 lb) was lowered on to the hose. Rut depths were measured after 1,000, 4,000 and 8,000 cycles of the wheel. Rut depths are summarized in the Table 4.4.

Table 4.4 GLWT Test Results for Lab Compacted, Lab Mixes [Conner, 2003]

Bottom Ash Source	Bottom Ash Percentage	Air Voids (%)	Rut Depth (inches)		
			1000 Cycles	4000 Cycles	8000 Cycles
Control	0	3.3	0.021	0.048	0.054
Control	0	4.1	0.025	0.027	0.048
Laramie River	15	3.1	0.021	0.026	0.037
Laramie River	15	3.4	0.019	0.039	0.047
Dave Johnston	15	4.0	0.035	0.061	0.071
Dave Johnston	15	5.3	0.033	0.052	0.063
Jim Bridger	15	3.1	0.050	0.056	0.074
Jim Bridger	15	4.0	0.038	0.066	0.087

4.5 Thermal Stress Restrained Specimen Test

In this test, the cabinet containing the test specimen is cooled, while the ends are restrained. As the specimen contracts, tensile stresses develop. When these stresses reach the tensile strength of specimen, the sample cracks. Temperature and tensile strength when the specimen cracks are noted, and are compared with other specimens to determine relative performance. The tensile strength and temperature at failure are summarized in Table 4.5.

Table 4.5 TSRST Results for Lab Compacted Specimens [Conner, 2003]

Mix Type	Failure		
	Temperature (^{o}C)	Load (lbs)	Tensile Stress (psi)
Control	-33.6	378	120
Control	-28.5	1304	415
(Average)	**-31.1**	**841**	**267**
Laramie River	-25	565	180
Laramie River	-25.2	1003	321
(Average)	**-25.1**	**784**	**250**
Dave Johnston	-28.8	1348	429
Dave Johnston	-27.3	671	213
(Average)	**-28.1**	**1009**	**321**
Jim Bridger	-26.1	932	296
Jim Bridger	-27.6	792	252
(Average)	**-26.9**	**862**	**274**

4.6 Nitrogen Analysis

Elemental Nitrogen Analysis was done on 0.25 g of treated and untreated aggregates using an Antek Model 772 computer controlled pyroreactor coupled to an Antek Model 720 digital nitrogen detector. The pyroreactor was programmed from 125 to 615^0 C at 25^0 C/ min with a 10 minute isothermal period shown in Figure 4.4.

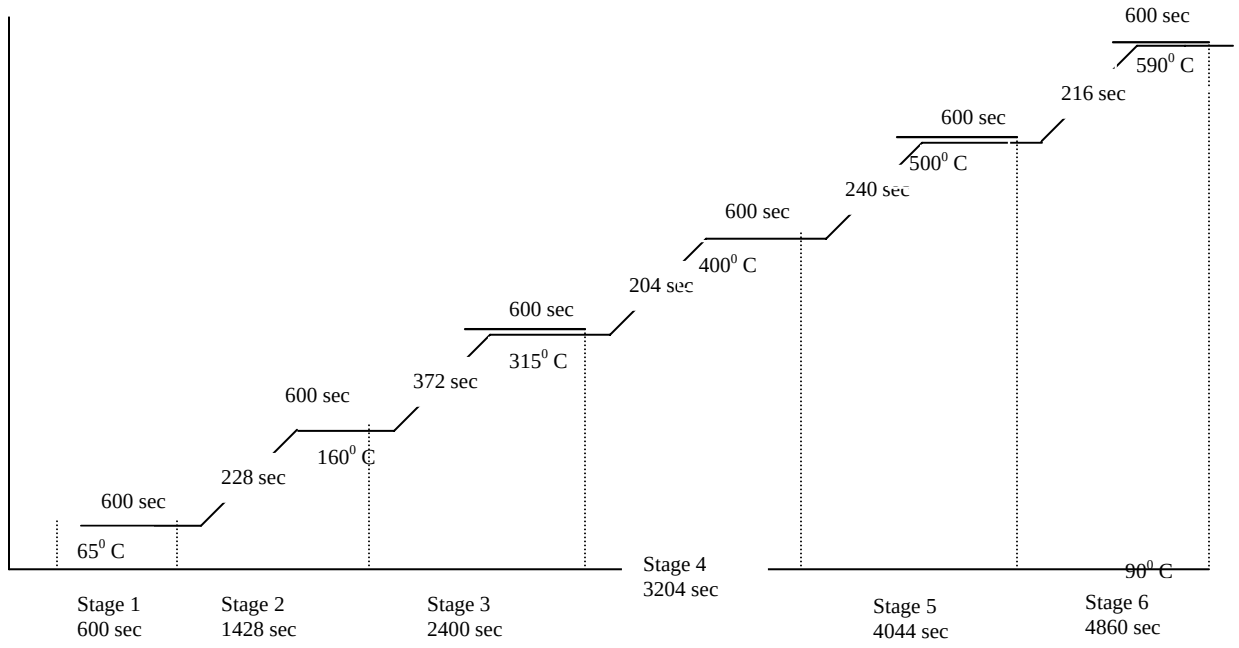

Figure 4.4 Temperature Programmed Stages

4.6.1 Discussion of Results

Nitrogen indigenous to the aggregates and/or strongly adsorbed on the aggregate and bottom ash surfaces was thermally desorbed during the six stage temperature ramps shown in Figure 4.4. Ten minute isothermal periods between each temperature ramp were sufficient to allow displacement of most of the nitrogen displaced at or below the isothermal temperatures. In this study, nitrogen desorbed during the 165 to 315^0 C and the 315 to 615^0 C ramps was of most interest because it is where the most strongly bound nitrogen occurs. Results of nitrogen analyses are summarized in Tables 4.6 to 4.15. Figures 4.5 to 4.14 show the resulting nitrogen thermograms obtained by the procedure described above.

Table 4.6 Pyridine-Treated Granite Aggregate

Inlet temp ^{0}C	Stage #	Time (sec)	Detector Area	Wt (%) = (Area/266.16)*100
125	1	0 – 600	0	0
160	2	601 - 1428	3.37	1.27
315	3	1429 - 2400	172.53	64.82
400	4	2401 - 3204	44.02	16.54
510	5	3205 - 4044	26.22	9.85
615	6	4045 - 4860	20.02	7.52
		Sum	266.16	

Table 4.7 Pyridine/Water-Treated Granite Aggregate

Inlet temp ^{0}C	Stage #	Time (sec)	Detector Area	Wt (%) = (Area/10.9)*100
125	1	0 – 600	0.00	0.00
160	2	601 – 1428	0.00	0.00
315	3	1429 – 2400	0.01	0.14
400	4	2401 – 3204	1.54	14.10
510	5	3205 – 4044	3.78	34.63
615	6	4045 – 4860	5.58	51.13
		Sum	10.90	

Table 4.6 and 4.7 show the nitrogen desorbed from granite aggregate and in the six stages before and after treatment with water. Detector area column in Table 4.6 indicates that large amounts of pyridine were initially retained by the aggregate, but could be desorbed in the temperature range of 165 to 615^0 C. Table 4.7 indicates that after the aggregate was treated with water, most of the pyridine which was initially retained was displaced by the water treatment, and such displacements are typical of an aggregate susceptible to moisture induced stripping in a bituminous pavement.

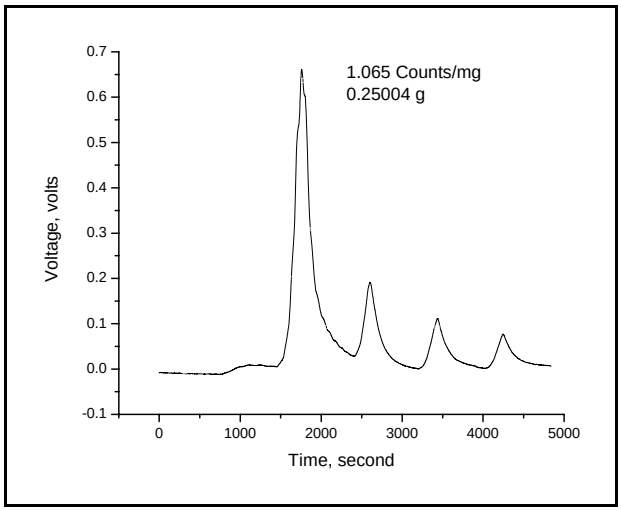

Figure 4.5 Pyridine-Treated Granite Aggregate

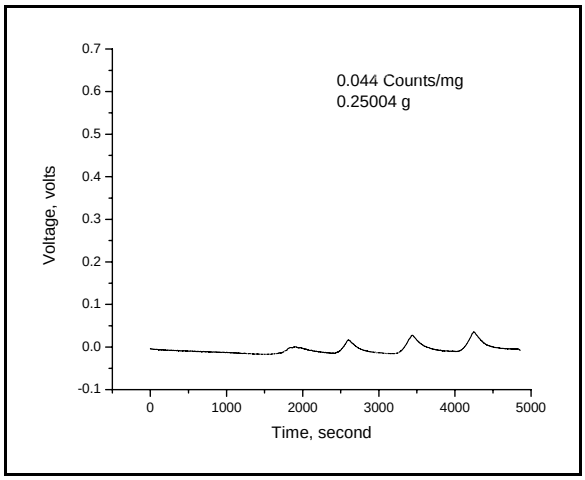

Figure 4.6 Pyridine/Water-Treated Granite Aggregate

Figures 4.5 and 4.6 are the nitrogen thermograms obtained for the two granite aggregates. The first plot indicates that significant amounts of pyridine were initially adsorbed by the aggregate. Five distinct nitrogen desorption peaks were observed in the temperature range of 160 to 615^0 C. The second figure indicates that significant amounts of pyridine were displaced from the granite aggregate by water treatment.

Table 4.8 Pyridine-Treated Limestone Aggregate

Inlet temp ^{0}C	Stage #	Time (sec)	Detector Area	Wt (%) = (Area/209.45)*100
125	1	0 – 600	0.00	0.00
160	2	601 – 1428	11.34	5.413
315	3	1429 – 2400	112.59	53.75
400	4	2401 – 3204	30.99	14.80
510	5	3205 – 4044	33.27	15.88
615	6	4045 – 4860	21.27	10.16
		Sum	209.45	

Table 4.9 Pyridine/Water-Treated Limestone Aggregate

Inlet temp ^{0}C	Stage #	Time (sec)	Detector Area	Wt (%) = (Area/16.83)*100
125	1	0 – 600	0.00	0.00
160	2	601 – 1428	0.00	0.00
315	3	1429 – 2400	3.90	23.16
400	4	2401 – 3204	4.13	24.51
510	5	3205 – 4044	6.50	38.64
615	6	4045 – 4860	2.30	13.69
		Sum	16.83	

Table 4.8 and 4.9 show the pyridine desorbed in the six stages before and after treatment with water from limestone aggregate. Detector area column in Tables 4.6 and 4.8 indicate that large amounts of pyridine were initially retained by the granite aggregate than limestone aggregate (266.16 vs 209.45), but after water treatment the limestone aggregate retained more pyridine (10.9 vs 16.8), which is obvious from Tables 4.7 and 4.9.

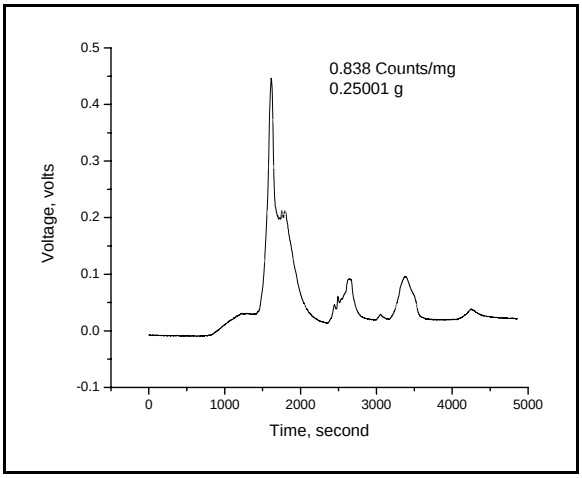

Figure 4.7 Pyridine-Treated Limestone Aggregate

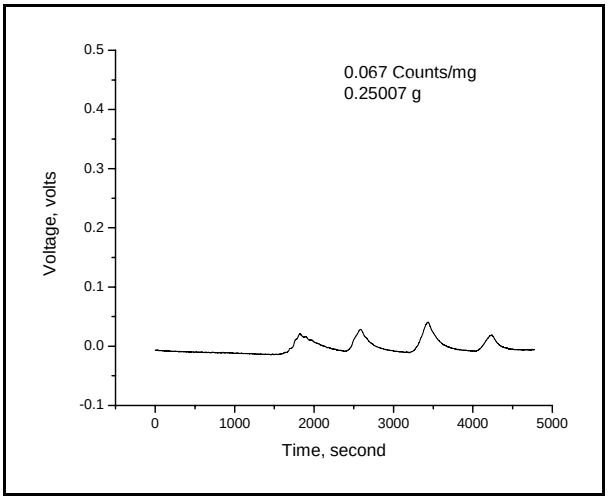

Figure 4.8 Pyridine/Water-Treated Limestone Aggregate

Figures 4.7 and 4.8 for the two limestone aggregates, although similar to those shown in Figures 4.5 and 4.6, are quite different in their relationship to detecting moisture susceptible aggregates used in paving applications. The first plot indicates that significant amounts of pyridine were initially adsorbed on aggregate. Five distinct nitrogen desorption peaks were observed in the temperature range of 160 to 615^0 C. The second figure indicates that nitrogen peak intensities in stages three to six were more intense. We can better compare this using the amount of nitrogen evolved; this can be obtained by dividing the total area under the curve and the weight of aggregate used. From the Figures 4.5 and 4.7 counts/mg after water treatment were 1.065 and 0.838 for the granite and limestone aggregate. These values indicate that

pyridine has strong interaction with limestone aggregate than with the granite aggregate. It was found that the more the interaction of aggregate with pyridine the less is it susceptible to moisture induce damage. This indicates that limestone aggregate is less susceptible to moisture-induced damage than the granite aggregate. These results are consistent with the Indirect Tensile Strength test which makes it clear that granite aggregate is more susceptible to moisture induced damage than the limestone aggregate.

Table 4.10 Pyridine-Treated Dave Johnston Bottom Ash

Inlet temp ^{0}C	Stage #	Time (sec)	Detector Area	Wt (%) = (Area/690)*100
125	1	0 – 600	0.00	0.00
160	2	601 – 1428	20.30	2.94
315	3	1429 – 2400	288.85	41.86
400	4	2401 – 3204	173.60	25.16
510	5	3205 – 4044	156.61	22.70
615	6	4045 – 4860	50.65	7.34
		Sum	690.00	

Table 4.11 Pyridine/Water-Treated Dave Johnston Bottom Ash

Inlet temp ^{0}C	Stage #	Time (sec)	Detector Area	Wt (%) = (Area/386.22)*100
125	1	0 - 600	0.00	0.00
160	2	601 - 1428	0.00	0.00
315	3	1429 - 2400	61.20	15.85
400	4	2401 - 3204	112.88	29.23
510	5	3205 - 4044	135.43	35.07
615	6	4045 - 4860	76.71	19.86
		Sum	386.22	

Table 4.10 and 4.11 show the pyridine desorbed from Dave Johnston bottom ash in the six stages before and after treatment with water. Detector area column in Table 4.10 indicates that large amounts of pyridine were initially retained by the aggregate but could be desorbed in the temperature range of 165 to 615^0 C. Table 4.11 indicates that after the aggregate was treated with water, pyridine was still adsorbed on the aggregate, which was desorbed in the temperature range of 165 to 615^0 C. This implies that water treatment did not desorb much of pyridine from the aggregate.

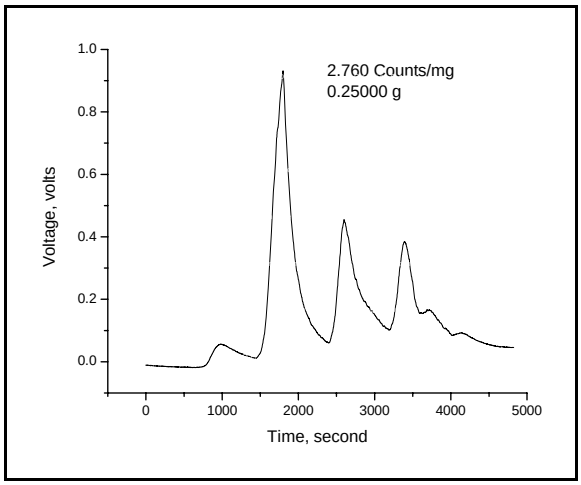

Figure 4.9 Pyridine-Treated Dave Johnston Bottom Ash

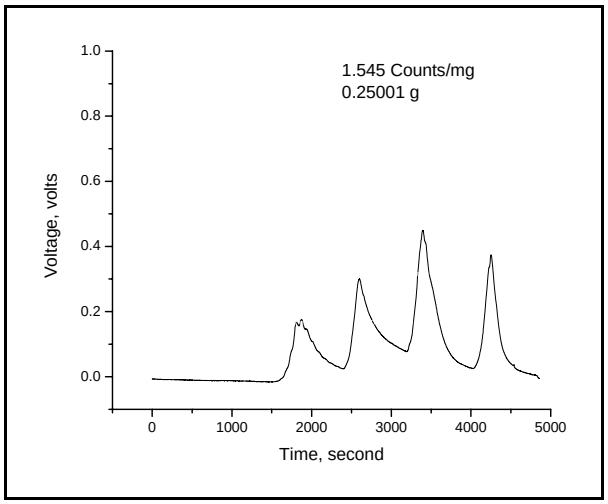

Figure 4.10 Pyridine/Water-Treated Dave Johnston Bottom Ash

Figures 4.9 and 4.10 are the nitrogen thermograms obtained for the two Dave Johnston bottom ashes. The first plot indicates that significant amounts of nitrogen were initially adsorbed by the aggregate. Five distinct nitrogen desorption peaks were observed in the temperature range of 160 to 615^0 C. The second figure indicates that significant amounts of pyridine was still adsorbed on to the material, which was desorbed in the temperature range of 160 to 615^0 C. This indicates that a significant amount of strongly adsorbed nitrogen was resistant to displacement by water.

Table 4.12 Pyridine-Treated Laramie River Bottom Ash

Inlet temp ^{0}C	Stage #	Time (sec)	Detector Area	Wt (%) = (Area/185.65)*100
125	1	0 – 600	0.00	0.00
160	2	601 – 1428	0.00	0.00
315	3	1429 - 2400	117.37	63.22
400	4	2401 - 3204	51.92	27.96
510	5	3205 - 4044	13.80	7.43
615	6	4045 - 4860	2.56	1.38
		Sum	185.65	

Table 4.13 Pyridine/Water-Treated Laramie River Bottom Ash

Inlet temp ^{0}C	Stage #	Time (sec)	Detector Area	Wt (%) = (Area/103.47)*100
125	1	0 – 600	0.00	0.00
160	2	601 – 1428	0.00	0.00
315	3	1429 – 2400	30.50	29.48
400	4	2401 – 3204	43.91	42.44
510	5	3205 – 4044	22.01	21.27
615	6	4045 – 4860	7.05	6.82
		Sum	103.47	

Table 4.12 and 4.13 show the nitrogen desorbed for Laramie River bottom ash before and after treatment with water. Detector area column in Table 4.12 indicates that significant amount of nitrogen were initially retained by the bottom ash, but could be desorbed in the temperature range of 165 to 615^0 C. Table 4.13 indicates that after the bottom ash was treated with water, a significant amount of nitrogen was still retained, which was desorbed in the above mentioned temperature range. This indicates that a significant amount of strongly adsorbed nitrogen was resistant to displacement by water.

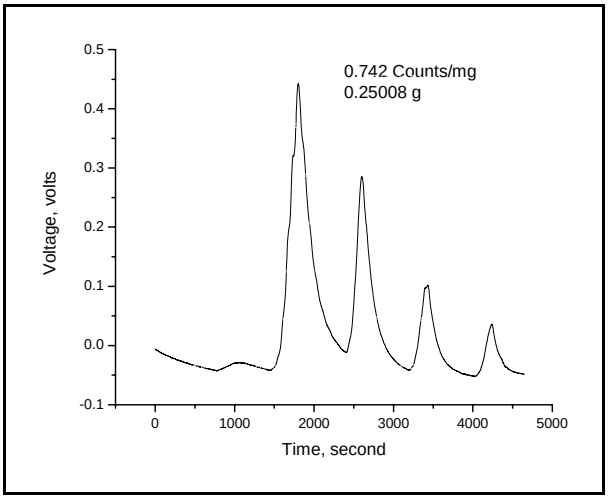

Figure 4.11 Pyridine-Treated Laramie River Bottom Ash

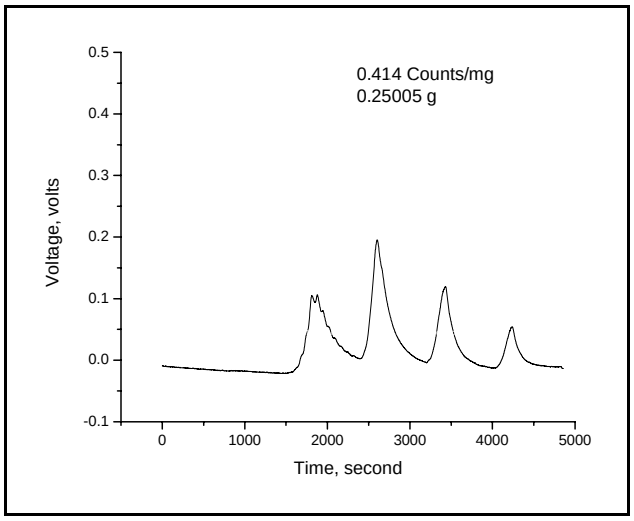

Figure 4.12 Pyridine/Water-Treated Laramie River Bottom Ash

Figures 4.11 and 4.12 are the nitrogen thermograms obtained for the two Laramie River bottom ashes. The first plot indicates that significant amounts of nitrogen were initially adsorbed by the aggregate. Five distinct nitrogen desorption peaks were observed in the temperature range of 160 to 615^0 C. The second figure indicates that significant amounts of nitrogen were still adsorbed on to the material, which was desorbed in the temperature range of 160 to 615^0 C. This indicates that a significant amount of strongly adsorbed nitrogen was resistant to displacement by water.

Table 4.14 Pyridine-Treated Jim Bridger Bottom Ash

Inlet temp ^{0}C	Stage #	Time (sec)	Detector Area	Wt (%) = (Area/247.9)*100
125	1	0 – 600	0.00	0.00
160	2	601 – 1428	0.00	0.00
315	3	1429 - 2400	34.37	13.86
400	4	2401 - 3204	52.47	21.17
510	5	3205 - 4044	120.17	48.47
615	6	4045 - 4860	40.90	16.50
		Sum	247.90	

Table 4.15 Pyridine/Water- Treated Jim Bridger Bottom Ash

Inlet temp ^{0}C	Stage #	Time (sec)	Detector Area	Wt (%) = (Area/172.74)*100
125	1	0 – 600	0.00	0.00
160	2	601 – 1428	0.00	0.00
315	3	1429 – 2400	7.21	4.17
400	4	2401 – 3204	38.35	22.20
510	5	3205 – 4044	91.34	52.88
615	6	4045 – 4860	35.84	20.75
		Sum	172.74	

Tables 4.14 and 4.15 show the nitrogen desorbed for Jim Bridger bottom ash before and after treatment with water. Detector area column in Table 4.14 indicates that significant amounts of nitrogen were initially retained by the bottom ash, but could be desorbed in the temperature range of 165 to 615^0 C. Table 4.13 indicates that after the bottom ash was treated with water, significant amounts of nitrogen were still retained, which were desorbed in the above mentioned temperature range. This indicates that a significant amount of strongly adsorbed nitrogen was resistant to displacement by water.

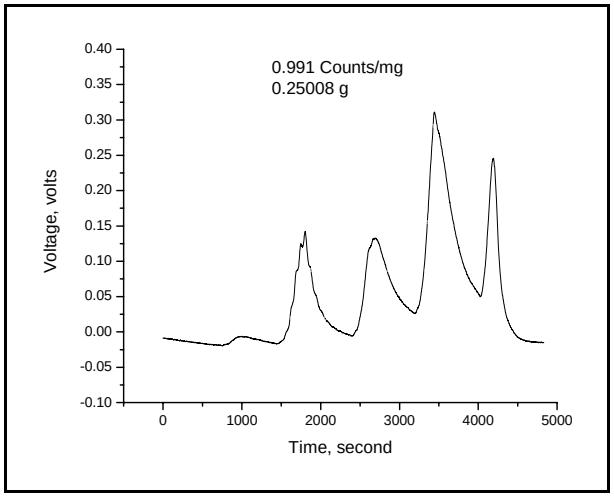

Figure 4.13 Pyridine-Treated Jim Bridger Bottom Ash

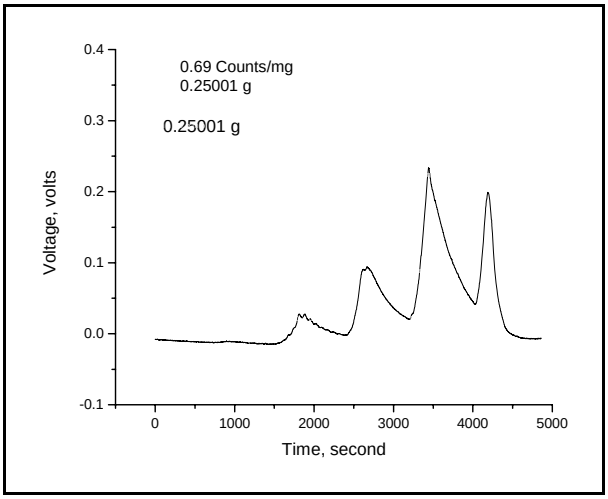

Figure 4.14 Pyridine/Water-Treated Jim Bridger Bottom Ash

Figures 4.13 and 4.14 are the nitrogen thermograms obtained for the two Jim Bridger bottom ashes. The first plot indicates that significant amounts of nitrogen were initially adsorbed by the material. Five distinct nitrogen desorption peaks were observed in the temperature range of 160 to 615^0 C. The second figure indicates that significant amounts of nitrogen were still adsorbed on to the material, which was desorbed in the temperature range of 160 to 615^0 C. This indicates that a significant amount of strongly adsorbed nitrogen was resistant to displacement by water. These above results coincide with the Indirect Tensile Strength test, which indicate that all the three bottom ashes may be more resistant to moisture induce damage than the granite and limestone aggregates.

Table 4.16 lists nitrogen peak intensities (counts/mg) and % nitrogen retained following water treatment.

Table 4.16 Amount of Nitrogen Detected

Sample Description	Nitrogen (Counts/mg)	Nitrogen (% Retained)
Pyridine Treated Granite	1.07	4.13
Pyridine Water Treated Granite	0.04	
Pyridine Treated Limestone	0.84	8.00
Pyridine Water Treated Limestone	0.07	
Pyridine Treated Dave Johnston	2.76	55.98
Pyridine Water Treated Dave Johnston	1.55	
Pyridine Treated Laramie River	0.74	55.80
Pyridine Water Treated Laramie River	0.41	
Pyridine Treated Jim Bridger	0.99	69.60
Pyridine Water Treated Jim Bridger	0.7	

Table above gives a detailed result of the amount of nitrogen retained after the aggregate was treated with water. The amount of nitrogen retained after pyridine treated aggregate was treated with water was 69.6% for Jim Bridger bottom ash, which indicates that Jim Bridger bottom ash may be more resistant to moisture-induced damage than any other aggregates and bottom ashes. The amount of nitrogen retained for Dave Johnston bottom ash was 55.98, which indicates that it is more resistant to moisture-induced damage than the Laramie River bottom ash, granite and limestone aggregate. The amount of nitrogen retained for granite aggregate is less than limestone aggregate, which indicates that granite aggregate may be more susceptible to moisture-induced damage.

4.7 Chapter Summary

This chapter discussed four test procedures. Indirect Tensile Strength test, GLWT, TSRST, and Nitrogen analysis, and presented the results obtained from these procedures. The TSR and nitrogen analysis values indicate the moisture susceptibility of an asphalt mix; GLWT values indicate the susceptibility of the different mixes to rutting, and TSRST values indicate the low temperature cracking behavior of asphalt mixes.

5. FIELD EVALUATION

5.1 Introduction

To evaluate the performance of the bottom ash mixes, an experimental test section in an actual roadway was constructed in Gillette, Wyoming, using the four HMA mixes with limestone as aggregate and lime additive. The performance of this test section was evaluated using FWD deflections, backcalculated layer moduli, and the Pavement Condition Index values. The purpose of this test section is to determine if the addition of bottom ash would degrade or enhance the performance of the pavements in-service conditions.

5.2 Falling Weight Deflectometer Deflections

Pavement surface deflection is an important means of evaluating the pavement in service conditions because the magnitude and shape of pavement deflection is a function of traffic (type and volume), pavement structural section, and temperature and moisture effects on the pavement structure.

The surface deflections of the pavement before and after the placement of the overlay were measured with a Falling Weight Deflectometer provided by the Wyoming Department of Transportation. Deflections were measured at various distances measured radially from load plate. Deflections measured by sensors at and near the load plate generally reflect the structural strength of the pavement near the top surface, while deflections further from the load plate reflect the strength of layers deeper in the pavement structure. Deflections were measured every 100 feet on the experimental pavement section and every 200 feet on the rest of project area. The measured deflections before and after overlay are summarized in Appendix A. These deflections were measured at different times of the day and thus had to be corrected to a reference temperature so as to be used in backcalculating subgrade and layer moduli.

5.2.1 Temperature Correction

The surface deflections measured using the FWD were corrected to a reference temperature of 20^0 C (68^0 F). Temperature correction was done using Equation 5.1.

$$D_{68} = D_T * [10^{(\alpha * (68 - Td))}] \quad \text{.....Equation 5.1}$$

Where,

D_{68} = *Adjusted deflection to the reference temperature of 20^0 C (68^0 F)(in.),*
T_d = *Pavement mid-depth temperature at depth d, ^{0}C,*
D_T = *Deflection measured at temperature T (^{0}F) (in.),*
$\alpha = 5.807 * 10\text{-}6 * (h_{AC})^{1.4635}$ *(For wheel paths)*
$\alpha = 6.560 * 10\text{-}6 * (h_{AC})^{1.4241}$ *(For Lane Center)*
h_{AC} = *Asphalt thickness in mm,*

Lukanen [2000] recently developed a set of equations for predicting pavement temperatures in a research project sponsored by the Federal Highway Administration (FHWA). These equations were referred to as Bell's equations and were developed using the temperature data from 41 Seasonal Monitoring Program (SMP) sites in North America. Independent variables used in the equation include surface temperature, time of test, and the previous five-day average air temperature. BELLS3 equation was intended for

routine testing and was developed to take into account the effects of shading on the infrared surface (IR) temperatures measured at the Seasonal Monitoring Program (SMP) sites. FWD tests on the Seasonal Monitoring Program (SMP) sites involve multiple drops with the result that each test point is shaded by the FWD for about six minutes. For routine FWD testing, deflection measurements on a given station will normally be completed in less than a minute. Thus, to allow for the effect of shading, the BELLS3 equation (Equation 5.2) adjusts measured IR temperatures [Lukanen et al., 2000].

$$T_d = 0.95 + 0.892 * IR + (\log(d) - 1.25) * (-0.448 * IR + 0.621 * (1 - day) + 1.83 * \sin(hr_{18} - 15.5)) + 0.042 * IR * \sin(hr_{18} - 15.5)) + 0.042 * IR * \sin(hr_{18} - 13.5)$$

…….Equation 5.2

Where,

IR = Infrared surface temperature, ^0C,

Log = Base 10 logarithm,

d = Depth at which temperature is to be predicted, mm,

1- Day = Average air temperature the day before testing, and

hr_{18} = Time of day, in 24-hr clock system, but calculated using an 18-hr asphalt concrete (AC) temperature rise-and fall-time cycle,

Figure 5.1 and 5.2 shows the measured deflections before and after overlay placement corrected for temperature. The test section overlays performed well, as demonstrated by reduced deflections after the overlay placement. All the mixes showed good structural improvement, and the Dave Johnston (D.J) and Jim Bridger (J.B) mixes showed the best performance of all the mixes.

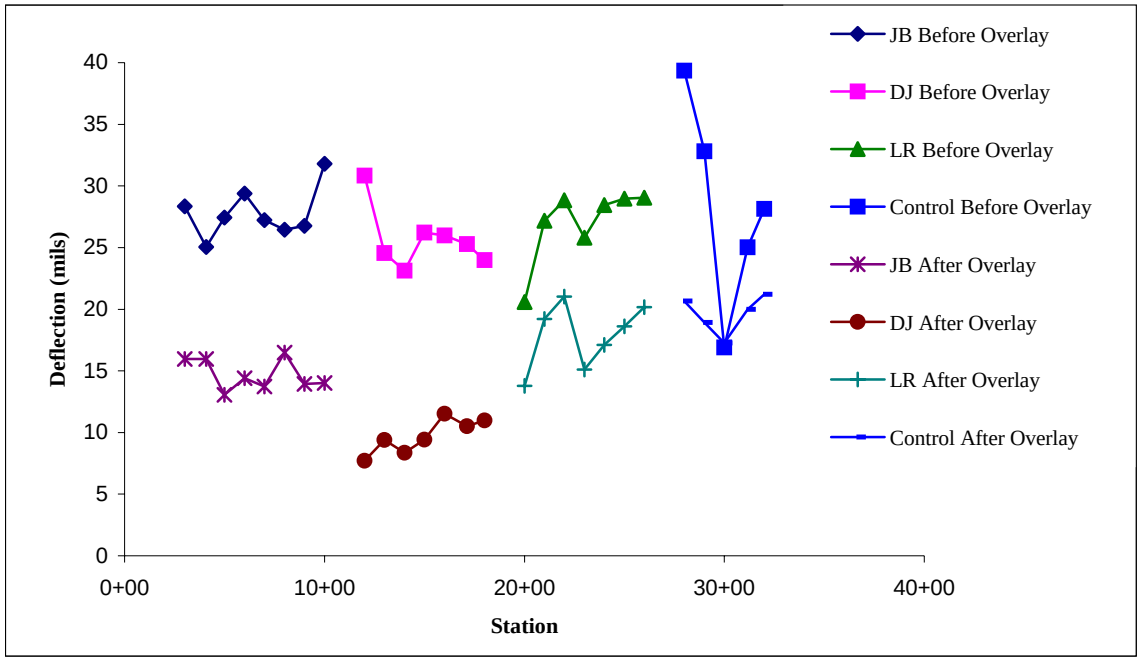

Figure 5.1 FWD Deflections under Load Plate Sensor

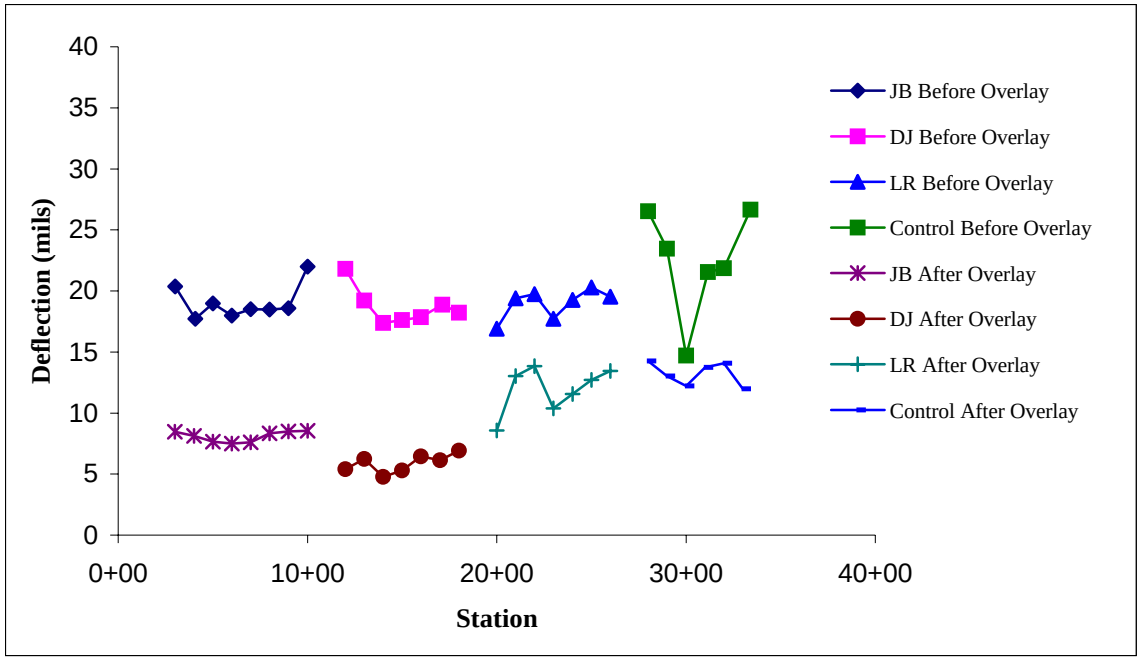

Figure 5.2 FWD Deflections at 12″ Radial Distance

5.3 Backcalculation of Layer Moduli

Modulus of elasticity is one of the pavement characteristics that has a major effect on how the pavement will perform under service conditions, how well it will carry load, and how long it will last. Modulus of elasticity is a measure of the pavement's ability to resist deformation under heavy load.

FWD deflections obtained from the experimental pavement section were analyzed using EVERCALC 5.0 because it is user friendly, readily available, and allows moduli ranges to be specified. The information required for backcalculating the layer moduli were the pavement's surface deflections, layer thickness, and layer type. The layer thickness and materials in the base and subbase were determined from the cores taken from the experimental pavement section. Some arbitrary layer moduli and poisson ratio were entered into this program and an initial trial run was made. The initial results were refined based on the Root Mean Square (RMS) error obtained. An RMS error of less than six suggests that the calculated moduli are reasonable, this value was set by Washington DOT who developed this software. Appendix A contains the backcalculated layer moduli before and after overlay placement. The rms error for these layer moduli values were well below 6. Figure 5.3 shows backcalculated layer moduli for the top layer, before and after overlay placement.

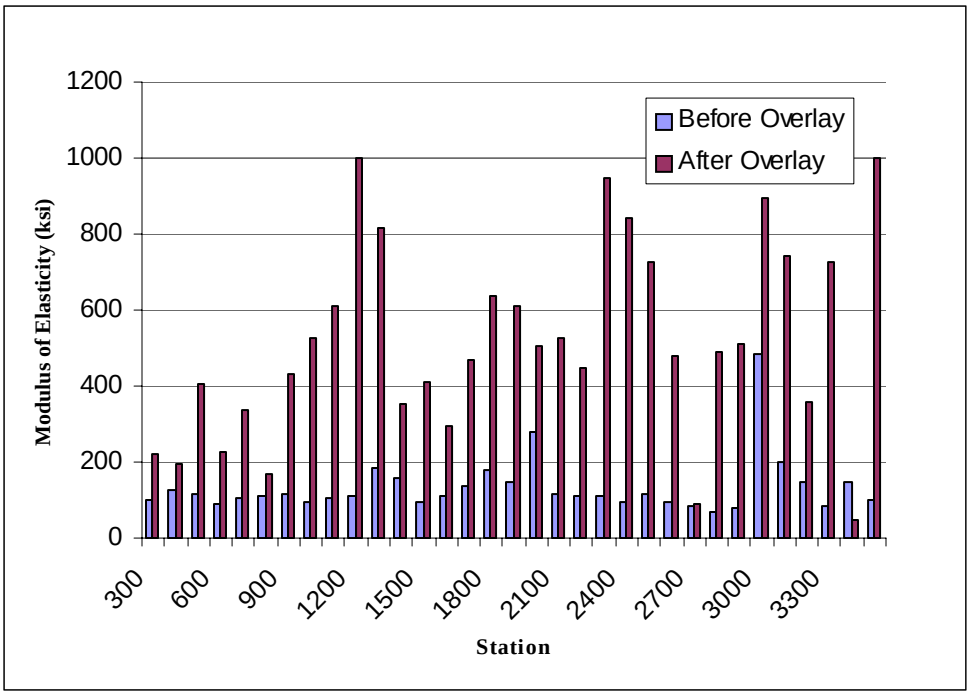

JB: Station 300 to 1100 **DJ:** Station 1100 to 1900
LR: Station 1900 to 2700 **Control:** Station 2700 to 3400

Figure 5.3 Modulus of Elasticity Before and After Overlay

The overlays in the test section performed well, as evidenced by increased moduli of elasticity after overlay placement for all the mixes (Figure 5.3). After overlay placement, all the mixes, except the Jim Bridger mix, had higher moduli of elasticity, but was comparable to the other mixes that was found from the Analysis of Variance conducted on these layer moduli values in data analysis chapter later in the data analysis chapter.

5.4 Pavement Condition Index

Prior to the placement of the overlay in the test section, all types of damages were recorded. After paving, condition surveys were done on the experimental pavement section at six months intervals. The Pavement Condition Index (PCI) calculations were based on the methods described in ASTM D6433-99 Standard Practice for Roads and Parking Lots Pavements.

The test section was rated before construction, six months after construction, and 12 months after construction. PCI results are summarized in the Table 5.1.

Table 5.1 ASTM D6433-99 Pavement Condition Index from Pre-Paving and Post-Paving Surveys

Survey	PCI Value	Pavement Rating
Pre-Paving October 2002	54	Fair
April 2003	99	Excellent
October 2003	90	Excellent

5.5 Chapter Summary

The methods used to evaluate the experimental pavement section are discussed in this chapter and the collected data is presented. Falling weight deflectometer values were used to evaluate the pavement's performance. The temperature correction procedure for the measured FWD deflections is also discussed. PCI values were also used to evaluate the performance of the pavement section.

6. DATA ANALYSIS

6.1 Introduction

Statistical analysis was done on the TSR data, the backcalculated layer moduli and after overlay placement on the experimental test section. The analysis was done using analysis of variance and non-linear regression methods. Calculations were done using SAS version 8.2 and Microsoft Excel.

This chapter discusses the statistical analyses used to evaluate the data gathered from both the laboratory and field evaluations and presents conclusions based on these results. Appendix C contains the details of the calculations performed in this study.

6.2 Statistical Analysis of the Elastic Moduli Data

These data were analyzed using Analysis of Variance (ANOVA). The purpose of AVOVA was to determine if the performance of bottom ash mixes is significantly different than that of control mixes (without bottom ash). An ANOVA is based on separation of the sums of squares and degrees of freedom associated with a response variable. ANOVA simplifies calculation of the F-test statistic and P-value so that significance of a difference in mean responses can be determined [Neter, 2004]. The p-value calculated by SAS is the probability of observing the calculated F-value or larger when the true mean responses are equal. Thus, if a p-value is greater than desired level of significance (α), then the hypothesis that the mean test results were equal is accepted. The level of significance used to compare the performance of asphalt mixes with and without bottom ashes was taken to be 0.05.

One-way analysis of variance was used for the Elastic Moduli in this project. This ANOVA is "one way" because only ash source was analyzed. All the mixes were plant mixes and only one type of aggregate (limestone) was used. It can be seen from the p-values reported in Table 6.1 that there is no significant difference between the three bottom ashes and control mixes. This indicates that an asphalt mix with bottom ash added as a portion of fine aggregate will not exhibit a significant reduction or increase in strength when compared with pavements prepared with no bottom ash.

Table 6.1 ANOVA-Based P-values

		JB	DJ	LR
JB	**P-value**	*	*	*
	Effect	*	*	*
DJ	**P-value**	0.0954	*	*
	Effect	Insignificant	*	*
LR	**P-value**	0.1007	0.9772	*
	Effect	Insignificant	Insignificant	*
C	**P-value**	0.1782	0.7760	0.7972
	Effect	Insignificant	Insignificant	Insignificant

The 95% confidence intervals were determined for the elastic moduli data for all four asphalt mixes to show schematically how the performances of all the asphalt mixes compared. The confidence intervals are presented in Figure 6.1. This figure indicates that there was no significant difference between the performance of all the bottom ash mixes and control mixes.

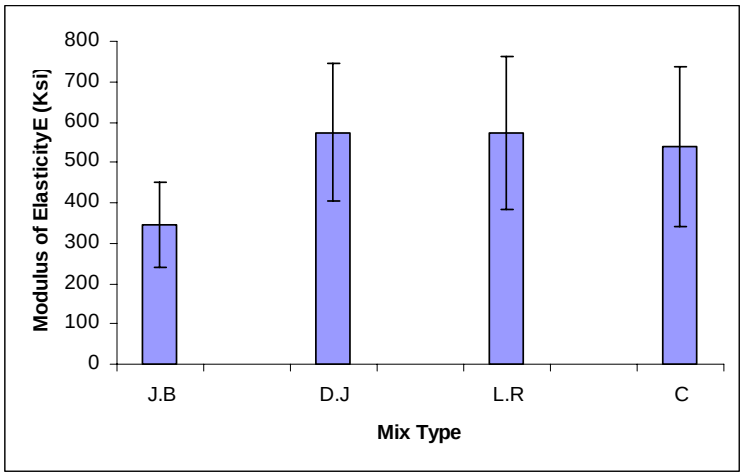

Figure 6.1 95% Confidence Intervals for Elastic Moduli

6.3 Statistical Modeling of TSR Results

The analysis of TSR results was based on the following simple non-linear regression model:

$$\text{Performance}(t) = t_0 * \exp(-\beta_1 t) + \text{Error} \quad \text{.....Equation 6.1}$$

Where,
β_1 = *Decay parameter,*
t_0 = *Performance at zero freeze thaw cycles (baseline performance),*
t = *Number of freeze thaw cycles the core was subjected to.*

This form of model was used for the TSR data analysis because there was no linear relationship found between the TSR and number of cycles to failure. The 95% confidence intervals for the slopes and intercepts for all eight of the HMA mixes were obtained from SAS output. Table 6.2 shows the confidence intervals for slopes and intercepts.

Table 6.2 95% Confidence Intervals

Mix Type	B_0 (Intercept)		β_1 (Slope)	
	Upper bound	Lower bound	Upper bound	Lower bound
Control, Mix w/Lime	100.0	85.26	-0.007	-0.036
Control, Mix w/o Lime	100.0	79.91	-0.067	-0.169
DJ, Mix w/Lime	100.0	83.93	-0.017	-0.065
DJ, Mix w/o Lime	100.0	79.65	-0.061	-0.128
JB, Mix w/Lime	100.0	86.95	-0.007	-0.029
JB, Mix w/o Lime	100.0	76.37	-0.046	-0.131
LR, Mix w/Lime	100.0	75.59	0.000	-0.056
LR, Mix w/o Lime	100.0	83.60	-0.011	-0.045

Using the criterion of asphalt failure when the core falls to 70% of the original performance, the number of cycles until failure was found to be:

$$N = \text{Log}(0.7)/(-\beta_1) \quad \text{.....Equation 6.2}$$

Where,

β_1 = *Slope of the regression model.*

Thus, a standard confidence interval (L, U) for β_1 can be used to obtain the confidence interval for the number of cycles until failure, [Log (0.7)/ Upper bound β_1, (Log (0.7)/Lower bound β_1)]. Table 6.3 summarizes the confidence intervals for the expected number of cycles to failure.

Table 6.3 95% Confidence Intervals for Cycles to Failure

Mix Type	Upper bound	Lower bound
Control, Mix w/Lime	22.00	4.28
Control, Mix w/o Lime	2.31	0.91
DJ, Mix w/Lime	9.17	2.4
DJ, Mix w/o Lime	2.50	1.21
JB, Mix w/Lime	22.16	5.34
JB, Mix w/o Lime	3.34	1.18
LR, Mix w/Lime	*	2.79
LR, Mix w/o Lime	13.59	3.48

(* Indicates that upper bound for LR mix prepared with lime was found to be more than 100)

This table here gives an indication of the lowest and the maximum possible number of cycles at which the mix would fail.

6.4 Moisture Susceptibility of Asphalt Mixes

Modeled tensile strength values are shown in Figure 6.2 and 6.3

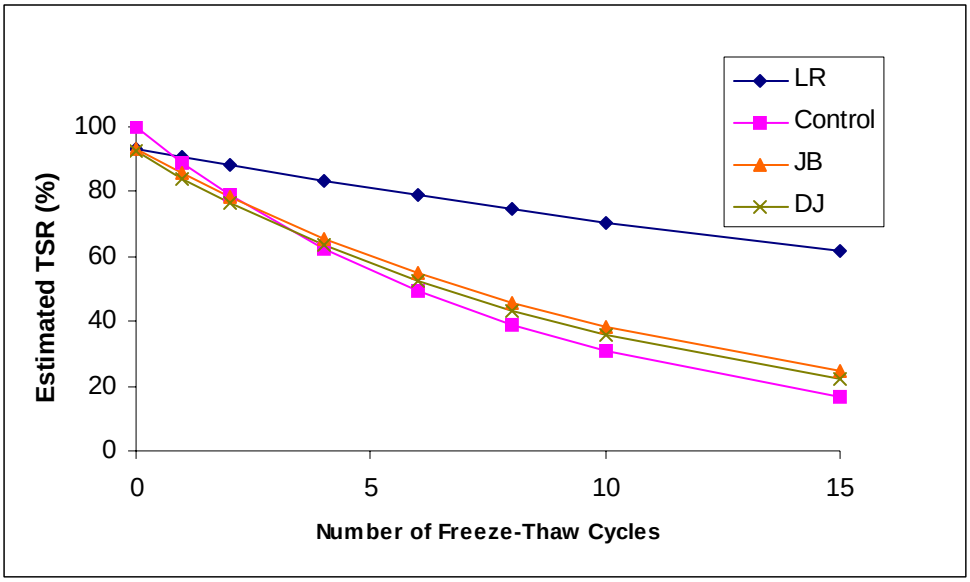

Figure 6.2 Modeled Tensile Strength Ratio for Lab Mixes without Lime

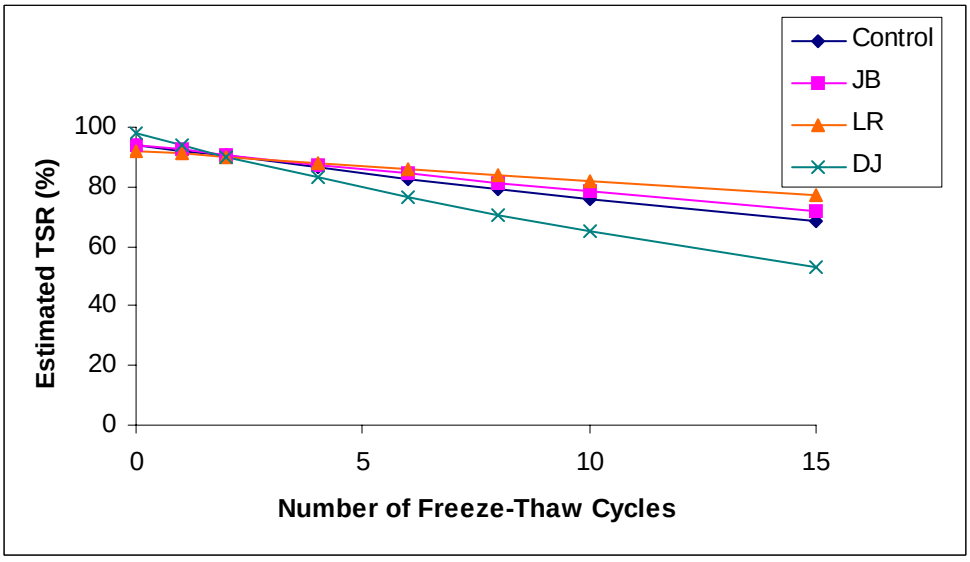

Figure 6.3 Modeled Tensile Strength Ratio for Lab Mixes with Lime

It is clear from the modeled TSR results shown in Figures 6.2 that in the asphalt mixes prepared without lime, the Laramie River bottom ash performed comparably better than the other bottom ashes and also the control mix. In Figure 6.3, the mixes containing lime as additive, all the mixes Laramie River, Jim Bridger and Dave Johnston performance were comparable to control mix performance and Laramie River, Jim Bridger performance exceeded the control mix performance.

6.5 Chapter Summary

This chapter discussed the statistical analysis done on the lab mixes and experimental pavement section data. The purpose of this analysis was to determine if the performance of asphalt mixes showed degradation in properties when bottom ash was added. The results of the analysis performed on TSR data showed that mix type had the most effect on the Tensile Strength. It was found the addition of bottom ash to asphalt mixes did not degrade properties when compared with control mix. In the mixes prepared without lime, Jim Bridger and Dave Johnston performance was poor when compared to Laramie River but comparably better than the control mix. In the mixes prepared with lime. all the bottom ash mix performances were comparably better than the control mix.

7. CONCLUSIONS AND RECOMMENDATIONS

7.1 Introduction

The main objective of this study was to evaluate the performance of bottom ash mixes. This objective was accomplished by performing laboratory and field evaluations of asphalt mixes with three bottom ashes. The laboratory evaluation was done using specimens prepared with limestone and granite aggregate. These specimens were tested for the most common distresses in asphalt pavements, which include: rutting, stripping, and low temperature cracking. The field evaluation was done on experimental pavement sections. FWD deflections, backcalculated layer moduli and PCI values were used to evaluate these experimental pavement sections.

7.2 Conclusions

The field and laboratory evaluations indicated that all the bottom ash mix performance was comparable or exceeded the control mix performance, which indicates that 15% addition of bottom ash will not degrade the performance of asphalt pavement. More specific conclusions are summarized in the following subsections.

7.2.1 Laboratory Evaluation

1. The indirect tensile strength tests performed on granite aggregate with no lime indicates that all the mixes except the Laramie River bottom ash mix showed degradation in tensile strength. Therefore, the Laramie River bottom ash may act as anti stripping agent.
2. When lime was added to all the granite mixes, the Laramie River and Jim Bridger bottom ash performance exceeded the performance of control mix. In addition the Dave Johnston mix performance was comparable to control mix performance.
3. The GLWT results indicate that limestone mixes with or without bottom ash have similar rut depth resistance.
4. TSRST results indicate that the performance of all bottom ash mixes was comparable to the control mix.
5. Nitrogen analysis results indicate that Dave Johnston, Jim Bridger and Laramie River bottom ash mixes may be more resistant to moisture-induced damage.
6. Nitrogen analysis results indicate that granite aggregate may be more susceptible to moisture-induced damage than limestone aggregate.

7.2.2 Field Evaluation

1. Backcalculated layer moduli of experimental pavement sections before and after the overlay indicates that bottom ash did not degrade the performance of asphalt mixes and the performance of test sections with 15% bottom ash was comparable to the control test section performance.
2. FWD deflections indicate that the Jim Bridger and Dave Johnston test sections' performance was comparably better than the control and Laramie River test sections.
3. PCI values indicate that 15% addition of bottom ash into asphalt pavement did not degrade the pavement;s performance and the condition of the pavement is still excellent even after one year of construction.

7.3 Recommendations

1. Laramie River bottom ash mix showed good tensile strength after 15 freeze-thaw cycles when no lime additive was added, which indicates that it is resistant to moisture-induced damage. Lime is found to be a good anti-stripping additive, but it increases the overall cost of asphalt mixes. Therefore, further research needs to be initiated to field test bottom ash paving materials with and without lime. This way, bottom ash could be tested as an anti-stripping agent to eliminate the addition of lime into mixes which are susceptible to stripping.
2. Lime additive acts as a good anti-stripping agent, and thus should be added to asphalt mixes that are more susceptible to moisture-induced damage.
3. When no lime was added, mixes prepared with limestone aggregate showed better performance than that prepared with granite aggregate. Therefore, limestone aggregate should be used for better performance.
4. Nitrogen analysis was performed on individual aggregates and bottom ashes, so further analysis has to be done on a mixture of bottom ash and aggregate to find the interaction of pyridine when bottom ash is mixed with granite and limestone aggregate.

REFERENCES

- "American Coal Ash Association." *ACAA Releases 2002 Coal Combustion Products Production and Use Figures.* http://fp.acaa-usa.org/PDF/acaa_2002_ccp_svy(11-25-03).pdf. Accessed June 17, 2004.
- "American Coal Ash Association." *ACAA Frequently Asked Questions.* http://fp.acaa-usa.org/FAQ.htm. Accessed June 17, 2004.
- Anderson D. E. Dukatz (1982). "The Effect of Anti-stripping Additives on the Properties of Asphalt Cement." *Association of Asphalt Paving Technologies, Vol. 51, pp 298-317.*
- Anderson David A, Usmen Mumtaz, Lyle K. Moulton. "Utilization of Ash from Coal Burning Power Plants in Highway Construction." *Transportation Research Record No. 430*, Transportation Research Board, Washington, DC, 1973.
- Aschenbrener, Timothy and Kevin Stuart (1992). "Description of the Demonstration of European Testing Equipment for Hot Mix Asphalt Pavement." *CDOT-DTD-R-92-10*.
- Brown E Ray, Prithvi S Khandal, Jingna Zhang (2001). "Performance Testing for Hot Mix Asphalt." *NCAT Report No 01-05*.
- Conner L. Gary (2003). "Moisture Susceptibility of Bottom Ash Asphalt Mixes." M.S. Laramie, Wyoming: University of Wyoming Department of Civil Engineering.
- Department of Energy (DOE) (2003). "U.S. Coal Supply and Demand: 2003 Review." "Table ES1. U.S. Coal Supply, Disposition, and Prices, 2002-2003." DOE Web Site: http://www.eia.doe.gov/cneaf/coal/page/acr/acr_sum.html#tes1
- Erickson, Ryan (1997). "Evaluation of Low Temperature Cracking in Asphalt Pavement Mixes." M.S. Laramie, Wyoming: University of Wyoming Department of Civil Engineering.
- Evans, Larry D (1995). "State Solid Waste Regulations Governing the Use of Coal Combustion By-Products (CCBs)." Prepared for: American Coal Ash Association, Alexandria, Virginia.
- Gergis W. William (1999). "Backcalculation of Pavement Layer Moduli Using 3D Nonlinear Explicit Finite Element Analysis." M.S. Morgantown, West Virginia: West Virginia University Department of Civil Engineering.
- Haas, R.C.G. and K.O. Anderson (1969). "A Design Subsystem for the Response of Flexible Pavements at Low Temperatures." *Proceedings of the Association of Asphalt Paving Technologies.*
- Huang, Wei-Hsing (1990). "Use of Bottom Ash in Highway Embankments, Subgrades, and Subbases." West Lafayette, Indiana. Purdue University School of Civil Engineering.
- http://www.tfhrc.gov/hnr20/recycle/waste/cbabs1.htm.
- Kennedy T., F. Roberts, K. Lee. "Evaluation of Moisture Effects on Asphalt Concrete Mixtures." *Transportation Research Record No.911*, Transportation Research Board, Washington, DC, 1983.
- Khandal, Prithvi S. "Moisture Susceptibility of HMA Mixes: Identification of Problem and Recommended Solutions." *National Asphalt Pavement Association Quality Improvement Publication (QIP)* 119, December 1992.
- Kim Y. Richard, Bradley O. Hibbs, Yung-Chen Lee. "Temperature Correction of Deflections and Backcalculated Asphalt Concrete Moduli." *Transportation Research Record No.1473*, Transportation Research Board, Washington, DC, 1995.
- Ksaibati, Khaled and Zeng, Menglan. "Evaluation of Moisture Susceptibility of Asphalt Mixtures Containing Bottom Ash." *Transportation Research Record No.1832*, Transportation Research Board, Washington, DC, 2003.

- Lottman, R.P., L. White, and D. Frith. "Methods of Predicting and Controlling Moisture Damage in Asphalt Concrete." *Transportation Research Record No. 1171*, Transportation Research Board, Washington, DC, 1988.
- Lukanen E.O, Stubstad R.N, Briggs, R (2000). "Temperature Predictions and Adjustment Factors for Asphalt Pavements." *Report No. FHWA-RD-98-085*. Federal Highway Administration.
- Murphy Mike, Dar-Hao Chen, John Bilyeu, Huang-Hsiung Lin. "Temperature Correction on Falling Weight Deflectometer Measurements." *Transportation Research Record No.1716*, Transportation Research Board, Washington, DC, 2000.
- Neter John, Christopher J. Nachtsheim, Michael H. Kutner (2004). "Applied Linear Regression Models." Fourth Edition.
- Parker, F. and F. Gharaybeh. "Evaluation of Indirect Tensile Tests for Assessing Stripping." *Transportation Research Record No.1115*, Transportation Research Board, Washington, DC, 1987.
- Plancher Henry and Petersen J. Claine (1998). "Model Studies and Interpretative Review of the Competitive Adsorption and Water Displacement of Petroleum Asphalt Chemical Functionalities on Mineral Aggregate Surfaces." Western Research Institute, Laramie, Wyoming.
- Roberts, F., P. Khandal, E. Brown, D. Lee, and T.Kennedy (1996). "Hot Mix Asphalt Materials, Mixture Design, and Construction." 2nd Edition: NAPA Education Foundation.
- Stephen, Jason (1999). "Utilization of Bottom Ash in Asphalt Mixes." M.S. Laramie, Wyoming: University of Wyoming Department of Civil Engineering.
- Tunnicliff, D. and R. Root. "Use of Antistipping Additives in Asphalt Concrete Mixtures." *NCHRP Report 274*, Washington, DC, 1984.
- Vinson, T.S., V.C. Janoo, and R. Haas. "Test Methods to Characterize Low Temperature Cracking." *Proceedings of the Fourth Workshop in Paving in Cold Areas*, Sapporo, Japan, 1990.

APPENDIX A

FALLING WEIGHT DEFLECTOMETER (FWD) DATA

- **D = Deflection**
- **D0 = Deflection at radial distance**
- **Air = Air Temperature**
- **Pave = Pavement Temperature**
- **E = Modulus of Elasticity**
- **E1 = Modulus of Elasticity of top layer**
- **E2 = Modulus of Elasticity of second layer**

Deflections Before Overlay

Station	Load(lbf)	D0(mils)	D1(mils)	D2(mils)	D3(mils)	D4(mils)	D5(mils)	D6(mils)	Air(0F)	Pave(0F)
106	9624	25.26	17.75	13.27	8.81	6.15	3.49	1.95	54	70
106	9615	25.21	17.82	13.33	8.85	6.24	3.56	1.95	54	70
106	9631	25.04	17.77	13.27	8.85	6.19	3.56	1.93	54	70
200	9615	26.51	18.66	13.97	9.33	6.4	3.48	1.73	51	70
200	9609	26.3	18.58	13.98	9.27	6.43	3.48	1.74	51	70
200	9612	26.18	18.52	13.91	9.33	6.37	3.48	1.72	51	70
301	9440	30.68	21.9	16.18	10.77	7.56	4.03	2.06	50	70
301	9393	30.44	21.9	16.16	10.84	7.59	4.06	2.05	50	70
301	9393	30.27	21.84	16.16	10.8	7.53	4	2.05	50	70
408	9506	25.98	18.35	13.72	9.52	6.77	3.8	1.87	50	68
408	9540	25.81	18.29	13.68	9.51	6.82	3.83	1.87	50	68
408	9493	25.69	18.23	13.66	9.49	6.77	3.77	1.86	50	68
500	9462	29.62	20.41	15.26	10.26	7.21	3.85	1.75	52	70
500	9462	29.45	20.39	15.29	10.39	7.23	3.87	1.77	52	70
500	9462	29.33	20.36	15.23	10.32	7.25	3.9	1.78	52	70
600	9400	31.16	18.89	13.7	8.98	6.28	3.41	1.66	51	69
600	9400	30.92	18.99	13.8	9.06	6.31	3.45	1.71	51	69
600	9456	30.68	18.88	13.78	9.04	6.37	3.48	1.68	51	69
700	9434	27.74	18.68	13.56	8.79	5.93	3.05	1.42	51	67
700	9462	27.52	18.77	13.64	8.85	6.02	3.05	1.46	51	67
700	9418	27.28	18.68	13.56	8.85	5.99	3.05	1.44	51	67
800	9458	27.4	19.01	14	9.38	6.5	3.51	1.69	51	68
800	9368	27.16	18.99	13.89	9.41	6.5	3.5	1.69	51	68
800	9446	27.28	19.13	14.03	9.41	6.56	3.53	1.67	51	68
900	9400	27.69	19.08	14.2	9.89	7.04	3.91	1.88	51	68
900	9473	27.62	19.22	14.28	9.97	7.1	3.98	1.92	51	68
900	9466	27.45	19.16	14.31	9.96	7.07	3.92	1.9	51	68
1000	9363	31.11	21.36	15.97	10.78	7.55	4.16	2.02	53	65
1000	9371	30.82	21.37	15.97	10.74	7.5	4.1	2.02	53	65
1000	9347	30.56	21.25	15.9	10.71	7.52	4.1	1.99	53	65
1100	9412	30.05	21.51	16.26	11.59	8.42	5.01	2.59	53	67
1100	9396	29.62	21.25	16.13	11.44	8.33	4.97	2.5	53	67
1100	9371	29.4	21.2	16.07	11.42	8.27	4.91	2.48	53	67
1200	9290	32.03	22.51	17.58	13.09	9.76	5.96	2.88	55	68
1200	9290	31.69	22.48	17.62	12.97	9.74	5.95	2.9	55	68
1200	9340	31.62	22.4	17.6	12.95	9.7	5.91	2.9	55	68
1300	9388	26.99	21	17	13.24	10.29	6.58	3.18	52	71
1300	9440	26.92	21.12	17.08	13.24	10.3	6.61	3.25	52	71
1300	9440	26.75	20.98	17.06	13.2	10.29	6.6	3.21	52	71
1400	9444	24.85	18.57	14.82	11.08	8.33	5.33	2.63	56	70
1400	9456	24.92	18.8	14.98	11.16	8.48	5.41	2.73	56	70
1400	9456	24.71	18.6	14.87	11.05	8.39	5.37	2.69	56	70

Station	Load(lbf)	D0(mils)	D1(mils)	D2(mils)	D3(mils)	D4(mils)	D5(mils)	D6(mils)	Air(0F)	Pave(0F)
1500	9412	28.51	18.96	13.81	9.58	6.93	4.26	2.31	55	70
1500	9453	28.1	18.91	13.79	9.46	6.93	4.22	2.24	55	70
1500	9440	27.79	18.85	13.72	9.49	6.88	4.21	2.23	55	70
1600	9438	27.5	18.76	13.52	8.94	6.18	3.29	1.54	56	69
1600	9440	27.28	18.74	13.5	8.87	6.11	3.25	1.55	56	69
1600	9484	27.16	18.8	13.52	8.96	6.18	3.26	1.6	56	69
1713	9412	26.63	19.71	15.29	11.19	8.54	5.33	2.64	57	69
1713	9416	26.44	19.86	15.37	11.19	8.54	5.33	2.66	57	69
1713	9451	26.46	19.77	15.29	11.19	8.52	5.36	2.68	57	69
1800	9424	25.24	19.1	15.46	11.81	9.04	5.62	2.72	63	69
1800	9375	25.09	19.1	15.45	11.72	9.01	5.62	2.73	63	69
1800	9396	25.16	19.08	15.52	11.69	9	5.63	2.68	63	69
1900	9318	30.44	23.49	18.85	14.2	10.65	6.38	2.97	60	69
1900	9318	30.39	23.63	18.96	14.12	10.7	6.42	2.97	60	69
1900	9309	30.29	23.46	18.82	14.07	10.6	6.38	2.91	60	69
2000	9403	21.24	17.38	14.82	11.86	9.44	6.13	3.04	60	68
2000	9456	21.17	17.4	14.84	11.77	9.44	6.17	3.07	60	68
2000	9456	21.05	17.32	14.67	11.75	9.33	6.05	3.02	60	68
2100	9294	28.7	20.35	15.65	10.96	8.07	4.82	2.37	56	69
2100	9363	28.51	20.31	15.56	10.94	8.06	4.8	2.4	56	69
2100	9340	28.27	20.36	15.56	10.94	8.04	4.77	2.38	56	69
2200	9300	27.93	18.99	14.09	9.41	6.64	3.59	1.61	57	65
2200	9371	27.86	19.13	14.2	9.49	6.68	3.66	1.66	57	65
2200	9355	27.81	19.07	14.22	9.46	6.67	3.69	1.66	57	65
2300	9397	22.59	15.48	11.4	7.62	5.4	2.99	1.5	55	60
2300	9456	22.52	15.44	11.42	7.65	5.46	3.07	1.48	55	60
2300	9425	22.4	15.44	11.4	7.67	5.45	3.02	1.53	55	60
2400	9278	27.04	18.26	13.58	9.16	6.49	3.66	1.87	54	64
2400	9335	26.92	18.23	13.66	9.16	6.46	3.64	1.88	54	64
2400	9245	26.8	18.2	13.6	9.1	6.45	3.64	1.86	54	64
2500	9381	28.1	19.55	14.62	10.02	7.33	4.1	1.9	52	65
2500	9449	27.91	19.58	14.64	10.05	7.31	4.12	1.9	52	65
2500	9462	27.93	19.63	14.7	10.13	7.37	4.14	1.9	52	65
2600	9344	26.51	17.79	12.77	8.46	5.72	2.94	1.47	51	62
2600	9359	26.39	17.71	12.71	8.34	5.67	2.9	1.45	51	62
2600	9412	26.22	17.69	12.69	8.38	5.71	2.91	1.43	51	62
2700	9416	30.34	21.04	15.23	10.13	6.97	3.68	1.71	50	60
2700	9440	30.1	20.95	15.06	10.02	6.9	3.6	1.73	50	60
2700	9424	30.03	20.85	15.12	10.05	6.93	3.6	1.67	50	60
2800	9243	36.1	24.21	17.3	10.88	7.22	3.49	1.73	50	62
2800	9233	35.64	24.05	17.19	10.86	7.19	3.49	1.76	50	62
2800	9215	35.45	23.95	17.19	10.84	7.16	3.52	1.73	50	62
2900	9377	31.33	22.23	16.44	11.14	7.69	4.39	2.39	51	64
2900	9456	31.09	22.26	16.44	11.02	7.69	4.38	2.39	51	64
2900	9465	30.68	22.06	16.1	10.96	7.65	4.38	2.37	51	64

Station	Load(lbf)	D0(mils)	D1(mils)	D2(mils)	D3(mils)	D4(mils)	D5(mils)	D6(mils)	Air(0F)	Pave(0F)
3000	9300	15.34	13.32	11.84	9.97	8.25	5.72	2.97	49	62
3000	9478	15.34	13.35	11.89	10.01	8.26	5.75	2.97	49	62
3000	9531	15.34	13.35	12.01	9.96	8.29	5.79	2.99	49	62
3116	9534	22.71	19.49	15.76	12.08	9.42	6.01	2.94	50	62
3116	9550	22.68	19.55	15.84	12.05	9.42	6.02	2.97	50	62
3116	9522	22.71	19.61	15.87	12.12	9.48	6.05	2.96	50	62
3200	9497	24.1	18.69	15.31	11.53	8.97	5.73	2.91	49	59
3200	9477	24.1	18.68	15.31	11.53	9.01	5.77	2.95	49	59
3200	9493	23.86	18.62	15.29	11.52	8.97	5.74	2.9	49	59
3341	9431	29.4	23.29	16.24	11.38	8.55	5.32	2.78	49	60
3341	9418	29.23	23.26	16.18	11.36	8.55	5.33	2.78	49	60
3341	9396	28.82	23.06	16.02	11.22	8.45	5.29	2.76	49	60
3412	9550	26.32	20.02	16.49	12.05	8.96	5.05	2.35	49	61
3412	9544	26.1	20	16.44	12	8.94	5.01	2.36	49	61
3412	9607	26.18	19.96	16.3	12.02	8.97	5.04	2.35	49	61
3528	9440	33.28	25.83	20.34	14.29	9.99	4.98	2	48	58
3528	9453	33.04	25.78	20.24	14.29	9.94	4.96	2	48	58
3528	9431	32.92	25.69	20.27	14.29	9.98	5	1.98	48	58
3600	9659	21.74	18.1	14.19	10.52	8.01	4.65	2.06	48	59
3600	9607	21.58	18.06	14.09	10.49	7.9	4.64	2.02	48	59
3600	9581	21.46	18.07	14.09	10.49	7.91	4.62	2.04	48	59
3700	9591	18.59	14.3	11.4	8.07	5.82	3.04	1.36	48	60
3700	9655	18.45	14.38	11.42	8.12	5.83	3.09	1.33	48	60
3700	9615	18.47	14.3	11.4	8.04	5.78	3.07	1.32	48	60

Deflections After Overlay

Station	Load(lbf)	D0(mils)	D1(mils)	D2(mils)	D3(mils)	D4(mils)	D5(mils)	D6(mils)	Air(0F)	Pave(0F)
300	8514	50.37	26.33	15.53	8.37	5.61	3.21	2.24	86	115
300	8603	49.08	26.09	15.47	8.4	5.6	3.2	2.21	86	115
300	8640	48.52	26	15.53	8.48	5.65	3.24	2.24	86	115
400	8646	48.91	24.63	13.68	7.27	4.99	2.93	2.07	89	114
400	8663	47.61	24.35	13.68	7.27	4.99	2.94	2.07	89	114
400	8688	46.94	24.19	13.68	7.32	5.04	2.98	2.09	89	114
500	8685	44.97	26.11	15.8	8.48	5.61	2.99	2.03	86	118
500	8703	43.9	25.84	15.77	8.51	5.62	3.01	2.03	86	118
500	8723	43.56	25.78	15.83	8.59	5.68	3.02	2.04	86	118
600	8615	48.35	24.74	14.04	7.07	4.51	2.44	1.71	87	117
600	8666	47.11	24.57	14.09	7.16	4.55	2.46	1.73	87	117
600	8681	46.38	24.41	14.09	7.16	4.58	2.46	1.75	87	117
700	8662	47.5	25.95	15.44	7.49	4.78	2.49	1.72	87	118
700	8685	46.26	25.67	15.39	7.54	4.81	2.48	1.72	87	118
700	8688	45.64	25.48	15.33	7.57	4.82	2.52	1.75	87	118
800	8590	57.69	28.62	15.53	7.98	5.37	3.01	2.16	86	118
800	8600	55.33	28.12	15.5	8.04	5.41	3.01	2.14	86	118
800	8680	54.37	27.9	15.55	8.12	5.42	3.04	2.16	86	118
900	8661	48.18	29.09	18.28	10.41	6.83	3.55	2.33	87	118
900	8657	47	28.78	18.17	10.38	6.81	3.58	2.33	87	118
900	8639	46.21	28.48	18.11	10.38	6.83	3.58	2.34	87	118
1000	8574	48.35	29.22	17.98	9.74	6.27	3.43	2.38	88	118
1000	8657	47.39	28.89	17.98	9.74	6.3	3.43	2.4	88	118
1000	8636	46.49	28.59	17.98	9.77	6.34	3.47	2.44	88	118
1100	8580	47.9	30.32	19.6	11.67	8.26	4.83	3.34	87	119
1100	8613	47.05	30.05	19.63	11.78	8.31	4.89	3.38	87	119
1100	8597	45.98	29.58	19.41	11.64	8.23	4.83	3.33	87	119
1200	8776	27.75	19.4	15.44	11.45	8.61	5.14	3.4	85	120
1200	8848	27.63	19.43	15.47	11.45	8.67	5.17	3.44	85	120
1200	8917	27.69	19.48	15.55	11.51	8.7	5.20	3.46	85	120
1300	8694	34.22	22.59	16.43	11.84	9.02	5.57	3.82	89	120
1300	8722	33.66	22.45	16.43	11.86	8.99	5.58	3.82	89	120
1300	8672	33.43	22.23	16.38	11.81	8.97	5.54	3.8	89	120
1400	8730	32.42	18.27	12.47	8.48	6.5	4.08	2.96	87	122
1400	8784	31.86	18.22	12.47	8.48	6.48	4.08	2.94	87	122
1400	8708	31.46	18.05	12.39	8.45	6.47	4.07	2.93	87	122
1500	8643	39.12	21.71	13.08	7.96	5.61	3.33	2.32	87	124
1500	8665	38.16	21.52	13.02	7.98	5.62	3.35	2.34	87	124
1500	8611	37.54	21.3	13.02	7.98	5.62	3.33	2.36	87	124
1600	8506	44.91	24.79	15.22	8.7	5.85	3.14	2.07	88	122
1600	8528	43.79	24.57	15.22	8.75	5.88	3.17	2.07	88	122
1600	8578	43.34	24.46	15.3	8.81	5.94	3.20	2.07	88	122
1700	8564	39.51	22.78	14.64	9.22	6.8	4.14	2.9	88	121

Station	Load(lbf)	D0(mils)	D1(mils)	D2(mils)	D3(mils)	D4(mils)	D5(mils)	D6(mils)	Air(0F)	Pave(0F)
1700	8644	38.89	22.76	14.73	9.3	6.83	4.21	2.96	88	121
1700	8622	38.38	22.56	14.67	9.28	6.84	4.19	2.94	88	121
1800	8623	40.07	25.07	17.07	10.79	7.9	4.64	3.09	87	120
1800	8656	39.4	24.88	17.12	10.87	7.96	4.67	3.12	87	120
1800	8623	39	24.74	17.09	10.93	7.98	4.65	3.12	87	120
1900	8533	49.92	31.73	21.25	13.08	9.19	5.38	3.56	86	120
1900	8500	48.63	31.26	21.09	13.02	9.16	5.34	3.52	86	120
1900	8536	48.18	31.09	21.11	13.08	9.2	5.38	3.57	86	120
2000	8478	50.43	31.12	19.82	11.84	8.43	5.05	3.44	88	120
2000	8518	49.53	30.85	19.9	11.97	8.53	5.1	3.46	88	120
2000	8500	48.68	30.57	19.82	11.92	8.5	5.09	3.46	88	120
2100	9104	31.8	21.46	15.19	9.61	6.7	3.85	2.56	75	94
2100	9153	31.24	21.22	15.11	9.58	6.67	3.85	2.56	75	94
2100	9166	31.12	21.16	15.11	9.58	6.67	3.84	2.56	75	94
2200	9090	33.77	22.04	15.55	9.41	6.33	3.35	2.12	77	93
2200	9147	33.32	21.96	15.53	9.41	6.33	3.35	2.08	77	93
2200	9155	32.93	21.85	15.47	9.44	6.34	3.36	2.09	77	93
2300	9158	23.47	16.04	11.56	7.43	5.25	2.95	1.93	79	92
2300	9226	23.13	15.93	11.53	7.4	5.25	2.95	1.96	79	92
2300	9223	23.08	15.91	11.53	7.4	5.27	2.97	1.95	79	92
2400	9127	28.31	19.01	14.2	9.36	6.57	3.63	2.44	80	94
2400	9125	27.92	18.85	14.09	9.28	6.53	3.63	2.4	80	94
2400	9147	27.69	18.85	14.09	9.33	6.57	3.63	2.4	80	94
2500	9077	29.89	20.28	15.42	10.1	7.15	4.07	2.6	80	93
2500	9041	29.38	20.14	15.33	10.07	7.13	4.08	2.58	80	93
2500	9090	29.32	20.09	15.28	10.07	7.13	4.08	2.6	80	93
2600	9002	32.31	21.44	15.44	9.5	6.51	3.57	2.33	79	93
2600	9035	31.91	21.3	15.39	9.5	6.51	3.55	2.34	79	93
2600	9015	31.69	21.27	15.42	9.5	6.51	3.61	2.36	79	93
2700	8921	44.35	26.03	16.54	9.22	6	3.2	2.1	81	93
2700	8927	43.45	25.76	16.46	9.19	5.98	3.18	2.09	81	93
2700	8947	43.17	25.67	16.49	9.28	6.04	3.23	2.1	81	93
2800	9049	34.28	23.53	16.96	10.3	6.7	3.48	2.25	81	94
2800	8995	33.66	23.25	16.85	10.24	6.68	3.46	2.26	81	94
2800	8940	33.38	23.09	16.74	10.18	6.65	3.44	2.24	81	94
2900	9001	31.29	21.44	15.58	9.69	6.75	4.04	2.88	81	94
2900	8984	30.9	21.3	15.53	9.69	6.74	4.03	2.86	81	94
2900	9023	30.62	21.19	15.44	9.66	6.71	4.03	2.85	81	94
3000	8937	29.04	20.53	16.13	11.48	8.56	5.23	3.54	81	95
3000	9065	29.15	20.61	16.21	11.59	8.61	5.27	3.6	81	95
3000	9059	29.1	20.58	16.21	11.59	8.61	5.25	3.58	81	95
3100	8949	33.88	23.14	18.33	13.05	9.57	5.61	3.66	81	95
3100	8974	33.71	23.17	18.33	13.08	9.62	5.62	3.68	81	95
3100	9013	33.43	23.09	18.28	13.02	9.59	5.61	3.68	81	95
3200	8949	36.19	23.89	17.15	11.26	8.1	4.95	3.42	82	95
3200	8982	35.63	23.66	17.01	11.18	8.06	4.94	3.41	82	95

Station	Load(lbf)	D0(mils)	D1(mils)	D2(mils)	D3(mils)	D4(mils)	D5(mils)	D6(mils)	Air(0F)	Pave(0F)
3200	8970	35.35	23.55	16.98	11.15	8.06	4.93	3.41	82	95
3300	8988	29.55	20.89	15.42	9.96	7.33	4.42	3.02	83	96
3300	9016	29.15	20.78	15.36	9.99	7.33	4.42	3.02	83	96
3300	9047	28.99	20.75	15.33	9.91	7.31	4.4	3.04	83	96
3400	8581	62.92	38.3	23.65	12.41	7.58	3.91	2.62	80	97
3400	8622	61.4	37.86	23.62	12.44	7.67	3.97	2.69	80	97
3400	8680	60.28	37.42	23.54	12.44	7.61	3.91	2.65	80	97
3500	9084	23.47	19.01	16.1	11.89	8.74	4.83	2.7	83	95
3500	9113	23.36	18.99	16.13	11.86	8.74	4.82	2.72	83	95
3500	9117	23.3	18.82	16.02	11.78	8.69	4.83	2.7	83	95

Backcalculation Summary After Overlay

Backcalculation by Evercalc 5.0 – Summary Output						
Route: WITH OVERLAY						
Plate Radius (in): 5.9				No of Layers: 4		
No of Sensors: 7		Stiff Layer: No		P-Ratio: .350 .350 .400 .450		
Offsets (in): .0 7.9 11.8 17.7 23.6 35.4 59.1						
Station	Load (lbf)	E(1)(ksi)	E(2)(ksi)	E(3)(ksi)	E(4)(ksi)	RMS Error
300	Thickness (in)	3	8.2	3.55	-	-
300	8514	208.5	33.5	17.1	53.7	3.73
300	8603	221.1	34.8	17.8	55	3.29
300	8640	236.4	35	18.5	54.6	3.33
300	Norm.	0	0	0	0	3.45
400	Thickness (in)	3	8.2	3.55	-	-
400	8646	176.2	32.4	25.3	58.5	4.03
400	8663	196.7	32.7	26.3	58.6	4.01
400	8688	206.7	33.1	27.7	58.2	3.92
400	Norm.	0	0	0	0	3.99
500	Thickness (in)	3	8.2	3.55	-	-
500	8685	375.4	40.7	14.9	64.4	3.14
500	8703	416.5	40.9	15.4	64.4	2.97
500	8723	431.2	41.6	15.1	64.3	3.08
500	Norm.	0	0	0	0	3.06
600	Thickness (in)	3	8.2	3.55	-	-
600	8615	201.6	39	14.4	74.2	3.16
600	8666	229.6	39.5	14.7	74.1	3.24
600	8681	246.4	39.7	15	73.9	3.58
600	Norm.	0	0	0	0	3.33
700	Thickness (in)	3	8.2	3.55	-	-
700	8662	307.1	38	13	75.1	3
700	8685	339.2	38.8	13	75.4	3.08
700	8688	361.4	38.4	13.8	74.5	3.07
700	Norm.	0	0	0	0	3.05
800	Thickness (in)	3	8.2	3.55	-	-
800	8590	149.3	32.5	17.8	62.2	4.24
800	8600	168.4	34	17.4	62.5	4.07
800	8680	183.7	34.6	17.9	62.6	3.99
800	Norm.	0	0	0	0	4.1
900	Thickness (in)	3	8.2	3.55	-	-
900	8661	387.6	41.3	10.8	55.1	2.71
900	8657	434.2	40.9	11.4	54.9	2.5
900	8639	465.4	40.9	11.7	54.7	2.57
900	Norm.	0	0	0	0	2.59
1000	Thickness (in)	3	8.2	3.55	-	-
1000	8574	477.7	31.5	16.7	55.2	3.3
1000	8657	529.5	31.4	17.9	55.6	3.51
1000	8636	577.3	30.5	19.9	54.9	3.67
1000	Norm.	0	0	0	0	3.49
1100	Thickness (in)	3	8.2	3.55	-	-

Station	Load (lbf)	E(1)(ksi)	E(2)(ksi)	E(3)(ksi)	E(4)(ksi)	RMS Error
1100	8580	557.6	31.5	39.6	42.2	4.13
1100	8613	624.8	30	51.4	42.1	4.08
1100	8597	644.5	31.3	46.8	42.4	4.08
1100	Norm.	0	0	0	0	4.09
1200	Thickness (in)	3	8.2	3.55	-	-
1200	8776	1500	95.8	51.2	43.8	4.22
1200	8848	1500	97.7	53.6	43.8	4.27
1200	8917	1500	99.4	52.1	44	4.26
1200	Norm.	0	0	0	0	4.25
1300	Thickness (in)	3	8.2	3.55	-	-
1300	8694	758.5	66.8	100	39.8	4.49
1300	8722	832.9	67.4	100	40	4.43
1300	8672	851.9	67.1	100	39.9	4.51
1300	Norm.	0	0	0	0	4.47
1400	Thickness (in)	3	8.2	3.55	-	-
1400	8730	325.1	86.9	100	58.3	6.31
1400	8784	360	88.1	100	58.8	6.13
1400	8708	365.7	89	100	58.4	6.22
1400	Norm.	0	0	0	0	6.22
1500	Thickness (in)	3	8.2	3.55	-	-
1500	8643	378.3	57.7	51	71.7	4.4
1500	8665	417.8	58.3	54.8	71.5	4.53
1500	8611	441.8	58.7	54.3	71.2	4.83
1500	Norm.	0	0	0	0	4.58
1600	Thickness (in)	3	8.2	3.55	-	-
1600	8506	282.1	54.2	15.5	69.3	2.88
1600	8528	296.8	57	15.2	69.7	2.8
1600	8578	308.3	58.3	15.4	69.4	2.3
1600	Norm.	0	0	0	0	2.66
1700	Thickness (in)	3	8.2	3.55	-	-
1700	8564	440.2	47.6	95.5	53.1	4.75
1700	8644	477.2	48.4	100	53	4.85
1700	8622	493.6	48.9	100	53	4.79
1700	Norm.	0	0	0	0	4.79
1800	Thickness (in)	3	8.2	3.55	-	-
1800	8623	592.1	49.3	39.9	46.5	3.44
1800	8656	652.5	49.4	41.9	46.3	3.56
1800	8623	670	50.4	39.5	46.2	3.76
1800	Norm.	0	0	0	0	3.58
1900	Thickness (in)	3	8.2	3.55	-	-
1900	8533	575.1	34	29.2	39.4	3.03
1900	8500	615.4	34.8	28.4	39.6	2.96
1900	8536	648.4	34.4	31	39.5	3.1
1900	Norm.	0	0	0	0	3.03
2000	Thickness (in)	3	8.2	3.55	-	-
2000	8478	463.9	31.6	44.6	41.6	3.81
2000	8518	507.1	32	45.6	41.4	3.7
2000	8500	547.1	31.3	52.2	41.4	3.74
2000	Norm.	0	0	0	0	3.75
2100	Thickness (in)	3	8.2	3.55	-	-

Station	Load (lbf)	E(1)(ksi)	E(2)(ksi)	E(3)(ksi)	E(4)(ksi)	RMS Error
2100	9104	497.8	30	13.2	26.9	3.47
2100	9153	535.9	30	14	27	3.46
2100	9166	547.1	30	14.1	27.1	3.51
2100	Norm.	0	0	0	0	3.48
2200	Thickness (in)	3	8.2	3.55	-	-
2200	9090	412.2	30	6.5	29.9	2.41
2200	9147	450.5	30	6.4	30.4	1.99
2200	9155	473.5	30	6.6	30.3	2.05
2200	Norm.	0	0	0	0	2.15
2300	Thickness (in)	3	8.2	3.55	-	-
2300	9158	920.2	30	23.6	33.1	2.99
2300	9226	955.1	30	26.2	33.2	3.35
2300	9223	972.9	30	26.2	33.2	3.13
2300	Norm.	0	0	0	0	3.16
2400	Thickness (in)	3	8.2	3.55	-	-
2400	9127	802.3	30	16.2	28.3	4.02
2400	9125	845.3	30	16.4	28.4	3.74
2400	9147	874.3	30	16.4	28.5	3.68
2400	Norm.	0	0	0	0	3.81
2500	Thickness (in)	3	8.2	3.55	-	-
2500	9077	699.5	30	13.2	25	2.82
2500	9041	740.3	30	13.3	25	2.65
2500	9090	745.5	30	13.9	25	2.76
2500	Norm.	0	0	0	0	2.74
2600	Thickness (in)	3	8.2	3.55	-	-
2600	9002	459.7	30	8.5	27.7	3.14
2600	9035	489.1	30	8.7	27.8	3.39
2600	9015	494.3	30	9	27.5	3.19
2600	Norm.	0	0	0	0	3.24
2700	Thickness (in)	3	8.2	3.55	-	-
2700	8921	80.2	30	5	29.9	4.18
2700	8927	91.2	30	5	30.2	4.12
2700	8947	98.3	30	5	30	3.71
2700	Norm.	0	0	0	0	4.01
2800	Thickness (in)	3	8.2	3.55	-	-
2800	9049	474.5	30	5.5	29.4	3.48
2800	8995	497.2	30	5.6	29.3	3.72
2800	8940	502.8	30	5.6	29.3	3.75
2800	Norm.	495.1	30	5.6	29.3	3.65
2900	Thickness (in)	3	8.2	3.55	-	-
2900	9001	485.4	30	17.2	25.1	5.64
2900	8984	511.2	30	17.2	25.2	5.51
2900	9023	528.2	30	18	25.3	5.42
2900	Norm.	486.9	30	17.2	25.1	5.52
3000	Thickness (in)	3	8.2	3.55	-	-
3000	8937	879.2	30	53.9	20.4	4.14
3000	9065	894	30	58.6	20.5	4.43
3000	9059	906	30	56.8	20.5	4.36
3000	Norm.	893	30	55.4	20.5	4.31
3100	Thickness (in)	3	8.2	3.55	-	-

Station	Load (lbf)	E(1)(ksi)	E(2)(ksi)	E(3)(ksi)	E(4)(ksi)	RMS Error
3100	8949	720.1	30	19.3	19.1	3.9
3100	8974	742.7	30	19.5	19.1	3.97
3100	9013	765.5	30	20.2	19.2	3.95
3100	Norm.	757.9	30	20	19.2	3.94
3200	Thickness (in)	3	8.2	3.55	-	-
3200	8949	341.2	30	19.9	21.4	4.71
3200	8982	362.6	30	21.7	21.5	4.67
3200	8970	373	30	21.8	21.5	4.68
3200	Norm.	0	0	0	0	4.69
3300	Thickness (in)	3	8.2	3.55	-	-
3300	8988	695.7	30	33.1	24.8	4.37
3300	9016	738	30	34.5	24.9	4.35
3300	9047	744.4	30	36	25	4.66
3300	Norm.	713.9	30	33.7	24.8	4.46
3400	Thickness (in)	3	8.2	3.55	-	-
3400	8581	50	30	5	24.7	13.91
3400	8622	50	30	5	24.2	12.83
3400	8680	50	30	5	25	12.67
3400	Norm.	0	0	0	0	13.13
3500	Thickness (in)	3	8.2	3.55	-	-
3500	9084	1500	60.6	5	25	3.61
3500	9113	1500	61.6	5	25	3.81
3500	9117	1500	62.7	5	25.1	3.54
3500	Norm.	0	0	0	0	3.65

Backcalculation Summary Before Overlay

Backcalculation by Evercalc 5.0 - Summary Output					
Route: Without Overlay					
Plate Radius (in): 5.9			P-Ratio: .350 .400 .450		
No of Sensors: 7		Stiff Layer: No		No of Layers: 3	
Offsets (in): .0 8.0 12.0 18.0 24.0 36.0 60.0					
Station	Load (lbf)	E(1)(ksi)	E(2)(ksi)	E(3)(ksi)	RMS Error
301	Thickness (in)	8.2	3.55	-	-
301	9440	99.9	2.3	19.8	2.06
301	9393	102	2.2	19.8	2.14
301	9393	101.5	2.2	19.9	1.92
301	Norm.	0	0	0	2.04
408	Thickness (in)	8.2	3.55	-	-
408	9506	122.7	2.8	21	2.55
408	9540	126.2	2.7	21.1	2.71
408	9493	125.3	2.7	21.1	2.39
408	Norm.	0	0	0	2.55
500	Thickness (in)	8.2	3.55	-	-
500	9462	116.4	1.9	22.6	3.59
500	9462	117.4	1.9	22.4	3.23
500	9462	118.4	1.9	22.3	3.45
500	Norm.	0	0	0	3.42
600	Thickness (in)	8.2	3.55	-	-
600	9400	87.5	2.7	23	5
600	9400	86.9	2.8	22.5	4.38
600	9456	91.5	2.7	22.9	4.95
600	Norm.	0	0	0	4.78
700	Thickness (in)	8.2	3.55	-	-
700	9434	105	1.9	25.9	3.7
700	9462	105.2	2	25.5	3.07
700	9418	107.1	1.9	25.7	3.2
700	Norm.	0	0	0	3.32
800	Thickness (in)	8.2	3.55	-	-
800	9458	111.2	2.3	22.7	2.97
800	9368	111.8	2.2	22.6	2.9
800	9446	114.2	2.2	22.9	3.24
800	Norm.	0	0	0	3.04
900	Thickness (in)	8.2	3.55	-	-
900	9400	115.7	2.4	20.4	3.19
900	9473	116.6	2.5	20.2	3.11
900	9466	117.6	2.4	20.4	2.79
900	Norm.	0	0	0	3.03
1000	Thickness (in)	8.2	3.55	-	-
1000	9363	91.7	2	17.8	2.87
1000	9371	91.7	2	17.9	2.48
1000	9347	94.4	2	18.1	2.69

Station	Load (lbf)	E(1)(ksi)	E(2)(ksi)	E(3)(ksi)	RMS Error
1000	Norm.	0	0	0	2.68
1100	Thickness (in)	8.2	3.55	-	-
1100	9412	99.5	3.5	15	2.01
1100	9396	104.3	3.2	15.4	2.44
1100	9371	105.4	3.1	15.5	2.26
1100	Norm.	0	0	0	2.24
1200	Thickness (in)	8.2	3.55	-	-
1200	9290	112.4	2.9	13.4	3.29
1200	9290	112.5	3	13.4	2.99
1200	9340	112.5	3	13.5	2.84
1200	Norm.	0	0	0	3.04
1300	Thickness (in)	8.2	3.55	-	-
1300	9388	186.5	3.2	13.5	2.33
1300	9440	182.3	3.6	13.3	2.09
1300	9440	188.3	3.3	13.5	2.13
1300	Norm.	0	0	0	2.18
1400	Thickness (in)	8.2	3.55	-	-
1400	9444	160.6	4.6	15.9	2.46
1400	9456	156.5	5.3	15.4	2.09
1400	9456	161.8	5	15.6	2.15
1400	Norm.	0	0	0	2.23
1500	Thickness (in)	8.2	3.55	-	-
1500	9412	84.3	7.1	18	2.01
1500	9453	89.4	6.3	18.4	2.46
1500	9440	114.3	2.2	25.1	3.72
1500	Norm.	0	0	0	2.73
1600	Thickness (in)	8.2	3.55	-	-
1600	9438	111.4	2.2	25	3.95
1600	9440	109.8	2.3	25	3.61
1600	9484	109.5	2.4	24.6	3.05
1600	Norm.	0	0	0	3.54
1713	Thickness (in)	8.2	3.55	-	-
1713	9412	135.5	4.3	15.3	2.73
1713	9416	135.6	4.4	15.2	2.71
1713	9451	134.3	4.7	15.2	2.73
1713	Norm.	0	0	0	2.72
1800	Thickness (in)	8.2	3.55	-	-
1800	9424	177.9	3.1	15	2.13
1800	9375	176.3	3.3	14.9	2.12
1800	9396	179.7	3	15.2	2.41
1800	Norm.	0	0	0	2.22
1900	Thickness (in)	8.2	3.55	-	-
1900	9318	148.1	1.8	13.5	1.89
1900	9318	148.8	1.8	13.5	2.09
1900	9309	150.9	1.7	13.8	2.23
1900	Norm.	0	0	0	2.07
2000	Thickness (in)	8.2	3.55	-	-

Station	Load (lbf)	E(1)(ksi)	E(2)(ksi)	E(3)(ksi)	RMS Error
2000	9403	277.9	3	13.8	0.9
2000	9456	278	3.3	13.7	1.08
2000	9456	276.8	3.3	13.9	0.92
2000	Norm.	0	0	0	0.97
2100	Thickness (in)	8.2	3.55	-	-
2100	9294	113.3	3.1	16.5	2.84
2100	9363	113.3	3.4	16.6	2.54
2100	9340	115.3	3.2	16.7	2.5
2100	Norm.	0	0	0	2.63
2200	Thickness (in)	8.2	3.55	-	-
2200	9300	108.1	1.8	21.6	4.39
2200	9371	108	1.9	21.2	4.12
2200	9355	108.3	1.9	21.1	4.32
2200	Norm.	0	0	0	4.28
2300	Thickness (in)	8.2	3.55	-	-
2300	9397	107.2	2.9	21.8	2.82
2300	9456	112.9	2.8	22	3.58
2300	9425	108.9	3	21.5	2.56
2300	Norm.	0	0	0	2.98
2400	Thickness (in)	8.2	3.55	-	-
2400	9278	93.9	2.9	18.8	2.5
2400	9335	95.3	2.9	19.1	2.31
2400	9245	94.5	2.9	18.9	2.41
2400	Norm.	0	0	0	2.41
2500	Thickness (in)	8.2	3.55	-	-
2500	9381	114.3	2.1	18.6	5.05
2500	9449	113.2	2.1	18.9	3.92
2500	9462	114.9	2	18.9	3.88
2500	Norm.	0	0	0	4.28
2600	Thickness (in)	8.2	3.55	-	-
2600	9344	92.8	2.1	22.7	2.71
2600	9359	92.8	2.1	23.1	2.79
2600	9412	96.5	2	23.4	3
2600	Norm.	0	0	0	2.84
2700	Thickness (in)	8.2	3.55	-	-
2700	9416	85.7	1.6	18.6	3.66
2700	9440	84	1.6	18.6	3.12
2700	9424	87.3	1.5	19.1	3.48
2700	Norm.	0	0	0	3.42
2800	Thickness (in)	8.2	3.55	-	-
2800	9243	65.4	1.3	18.9	2.77
2800	9233	65.5	1.4	18.7	2.44
2800	9215	66.8	1.4	18.8	2.8
2800	Norm.	0	0	0	2.67
2900	Thickness (in)	8.2	3.55	-	-
2900	9377	78.1	2.8	15.3	1.62
2900	9456	79.1	2.8	15.5	1.85

Station	Load (lbf)	E(1)(ksi)	E(2)(ksi)	E(3)(ksi)	RMS Error
2900	9465	81.1	2.9	15.6	2.01
2900	Norm.	0	0	0	1.83
3000	Thickness (in)	8.2	3.55	-	-
3000	9300	460.9	3.5	12.9	0.69
3000	9478	493.1	2.8	13.4	0.54
3000	9531	493.1	2.8	13.4	0.8
3000	Norm.	0	0	0	0.68
3116	Thickness (in)	8.2	3.55	-	-
3116	9534	200.3	2.4	12.6	2.45
3116	9550	197.4	2.6	12.5	2.52
3116	9522	201.5	2.5	12.5	2.64
3116	Norm.	0	0	0	2.54
3200	Thickness (in)	8.2	3.55	-	-
3200	9497	145.7	4.1	11.7	1.63
3200	9477	143.6	4.5	11.5	1.58
3200	9493	150.5	3.9	11.7	1.67
3200	Norm.	0	0	0	1.63
3341	Thickness (in)	8.2	3.55	-	-
3341	9431	80.7	4.1	12.2	4.54
3341	9418	81.8	4	12.2	4.64
3341	9396	82.5	4.2	12.2	4.76
3341	Norm.	0	0	0	4.65
3412	Thickness (in)	8.2	3.55	-	-
3412	9550	144.2	1.5	14.8	0.83
3412	9544	144.2	1.5	14.8	0.78
3412	9607	146.6	1.6	14.9	0.89
3412	Norm.	0	0	0	0.83
3528	Thickness (in)	8.2	3.55	-	-
3528	9440	98.4	0.8	15.3	1.44
3528	9453	99	0.8	15.4	1.47
3528	9431	100.8	0.7	15.4	1.58
3528	Norm.	0	0	0	1.5

APPENDIX B

TENSILE STRENGTH RATIO GRAPHS & SPECIMEN DATA FOR INDIRECT TENSILE TEST

TSR Graphs for Granite Aggregate Mixes

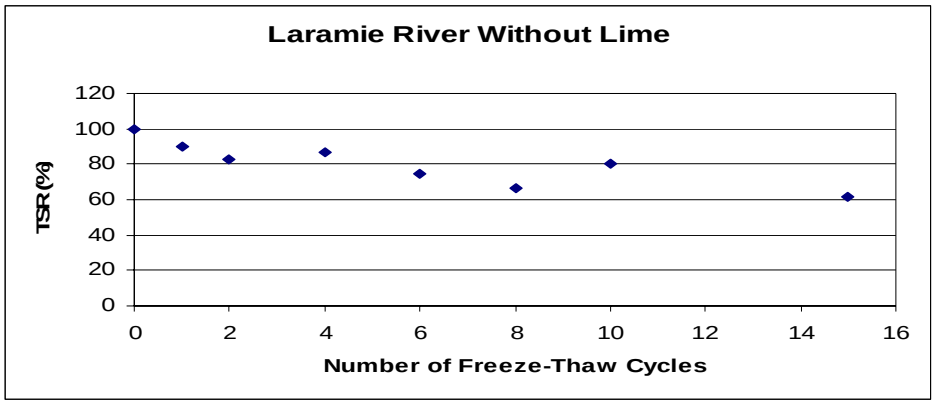

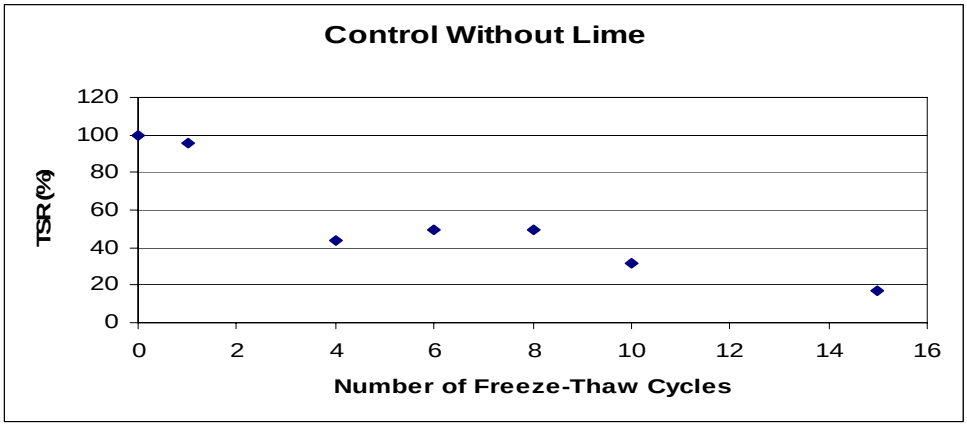

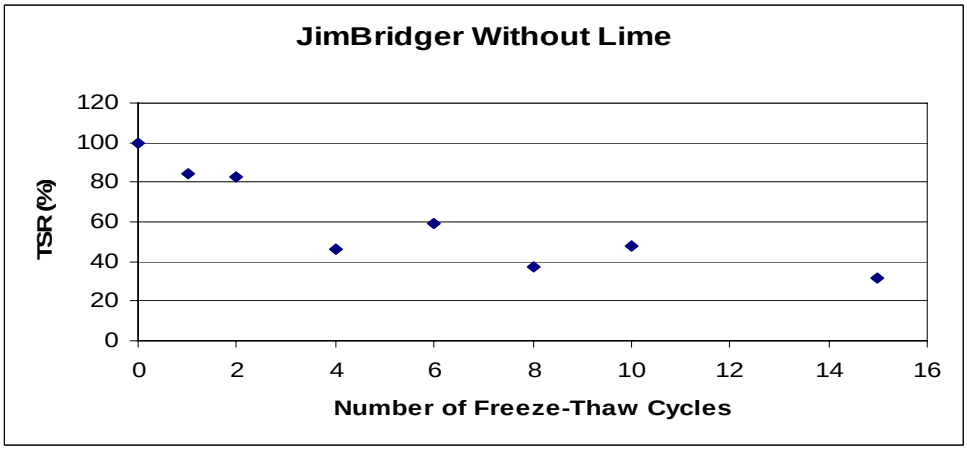

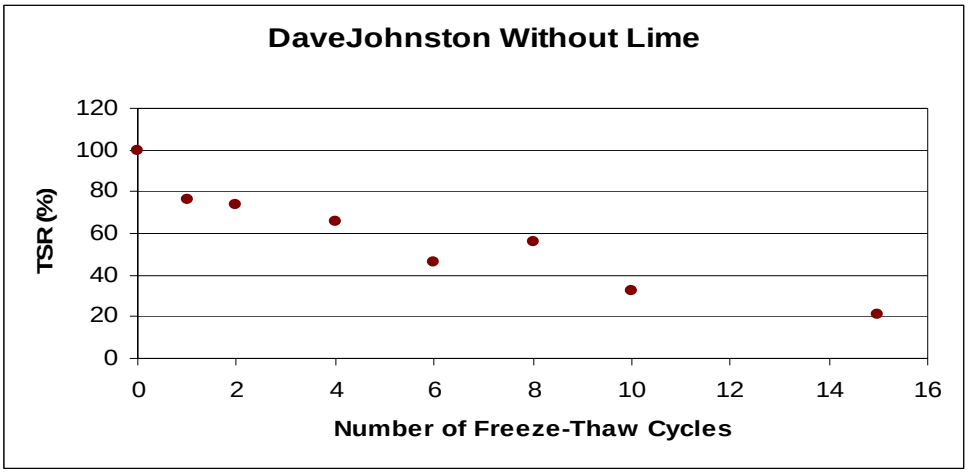
DaveJohnston Without Lime
TSR (%)
120
100
80
60
40
20
0
0
2
4
6
8
10
12
14
16
Number of Freeze-Thaw Cycles

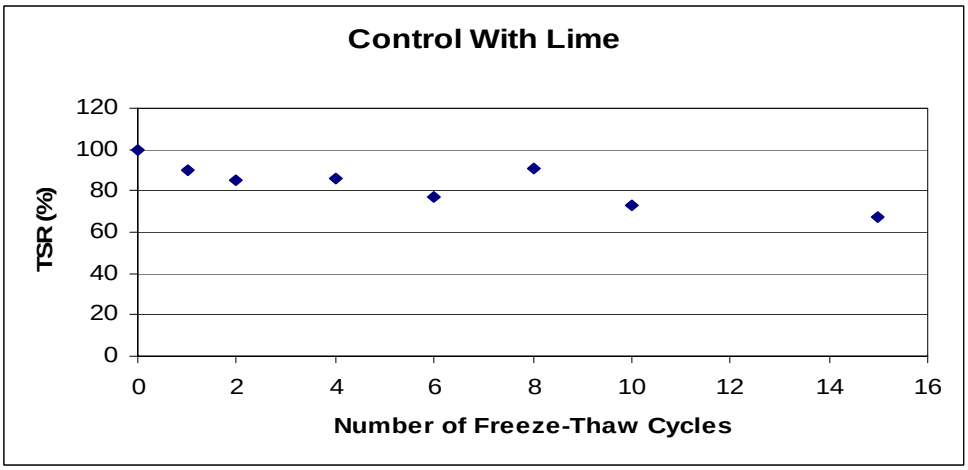
Control With Lime
TSR (%)
120
100
80
60
40
20
0
0
2
4
6
8
10
12
14
16
Number of Freeze-Thaw Cycles

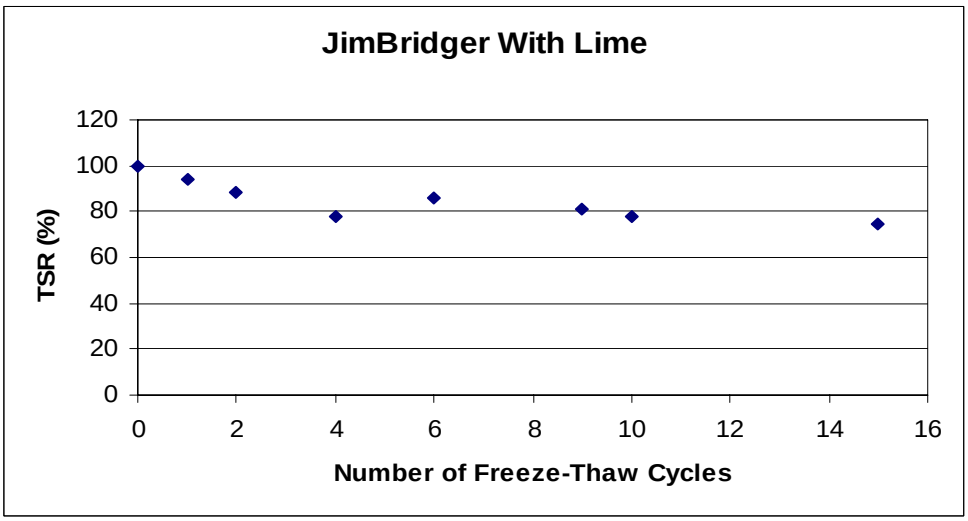
JimBridger With Lime
TSR (%)
120
100
80
60
40
20
0
0
2
4
6
8
10
12
14
16
Number of Freeze-Thaw Cycles

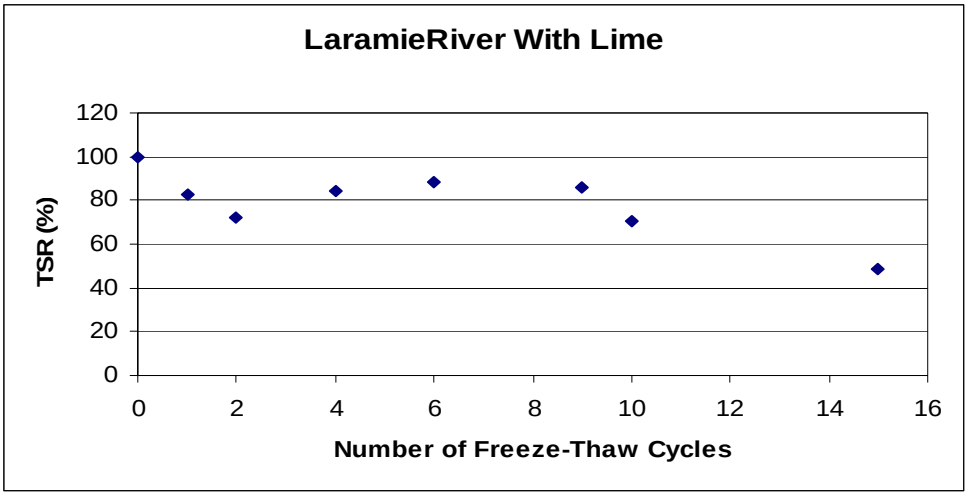
LaramieRiver With Lime
TSR (%)
120
100
80
60
40
20
0
0
2
4
6
8
10
12
14
16
Number of Freeze-Thaw Cycles

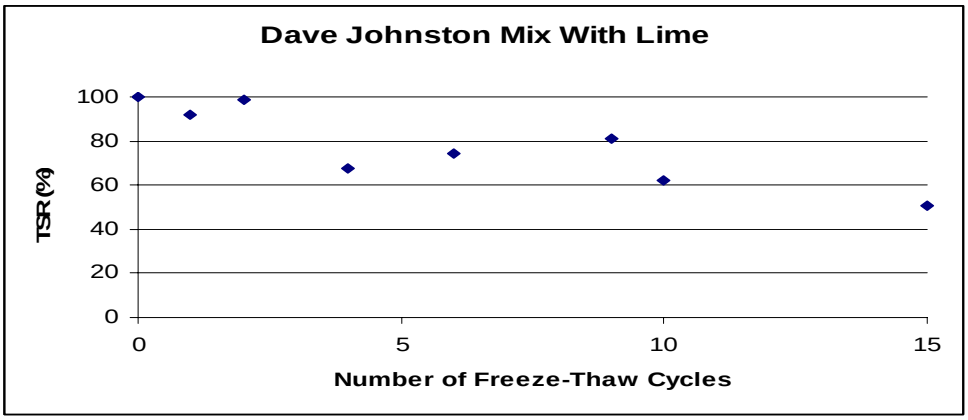
Dave Johnston Mix With Lime
TSR (%)
100
80
60
40
20
0
0
5
10
15
Number of Freeze-Thaw Cycles

TSR Graphs for Limestone Aggregate

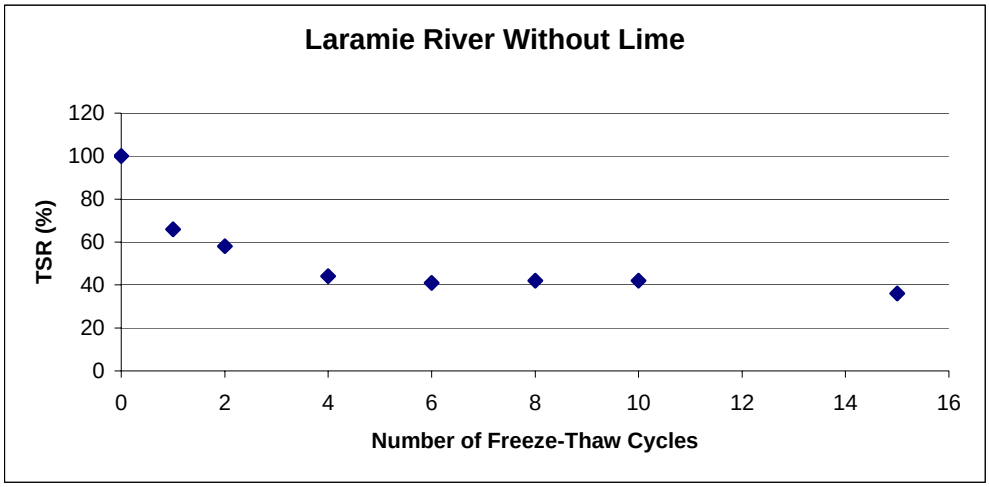

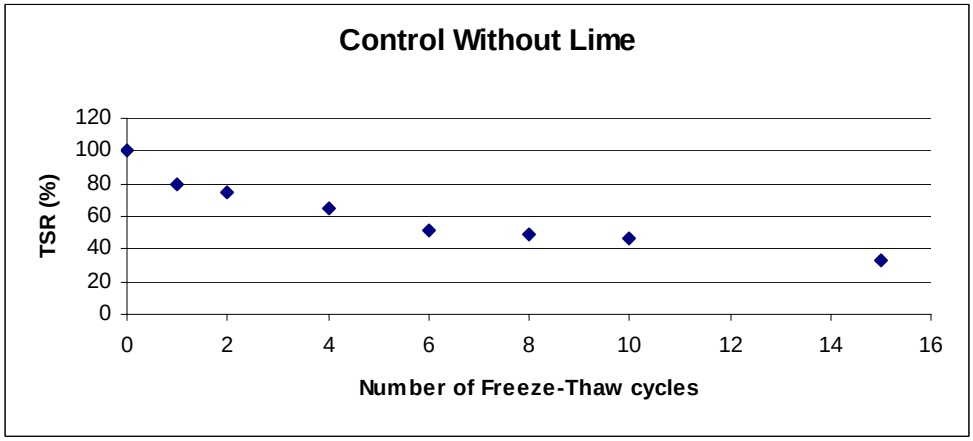

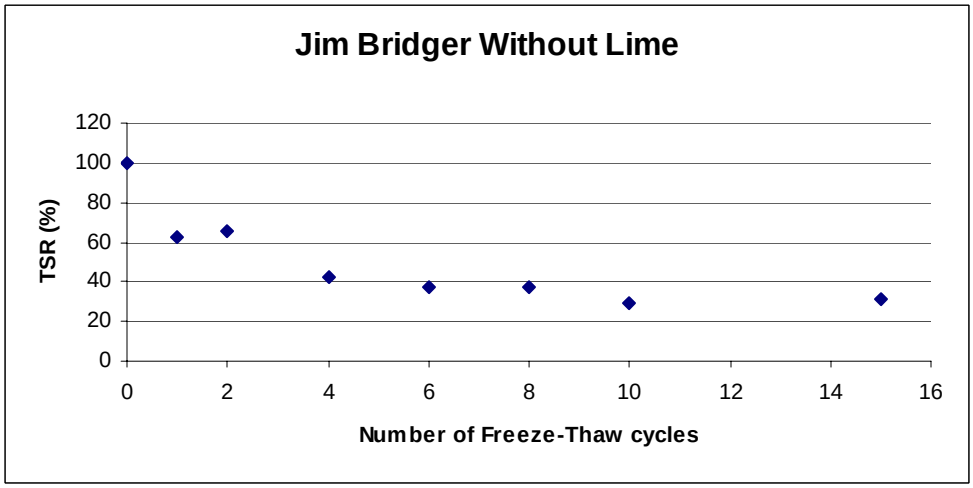

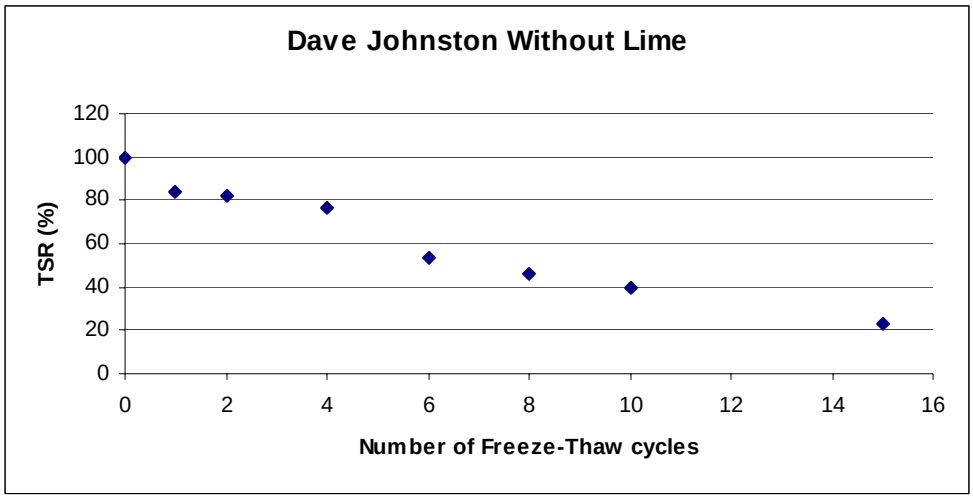
Dave Johnston Without Lime
TSR (%)
120
100
80
60
40
20
0
0
2
4
6
8
10
12
14
16
Number of Freeze-Thaw cycles

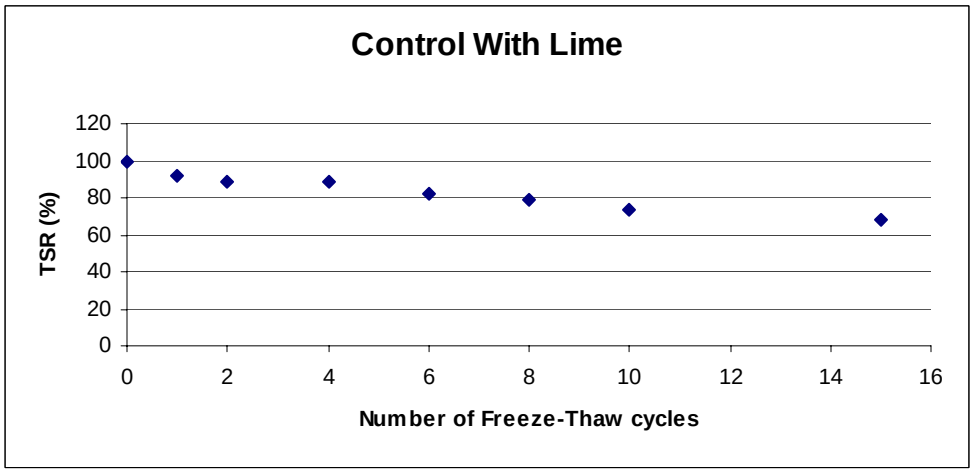
Control With Lime
TSR (%)
120
100
80
60
40
20
0
0
2
4
6
8
10
12
14
16
Number of Freeze-Thaw cycles

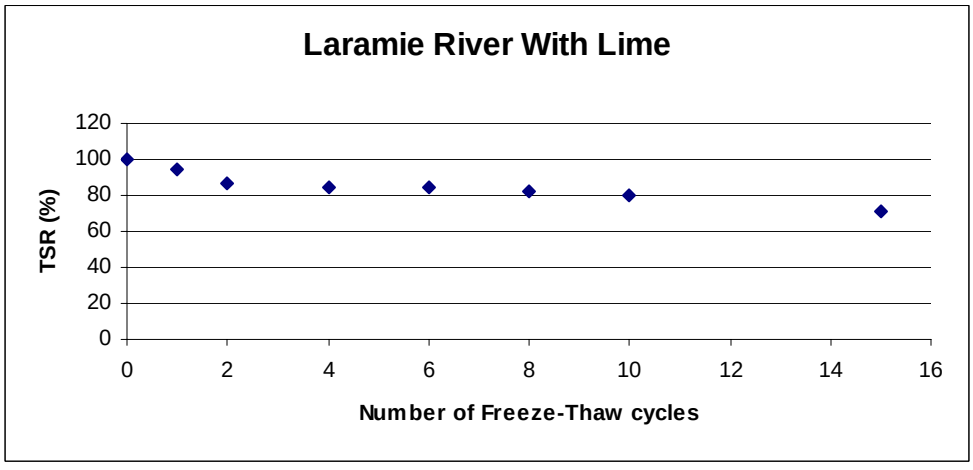
Laramie River With Lime
TSR (%)
120
100
80
60
40
20
0
0
2
4
6
8
10
12
14
16
Number of Freeze-Thaw cycles

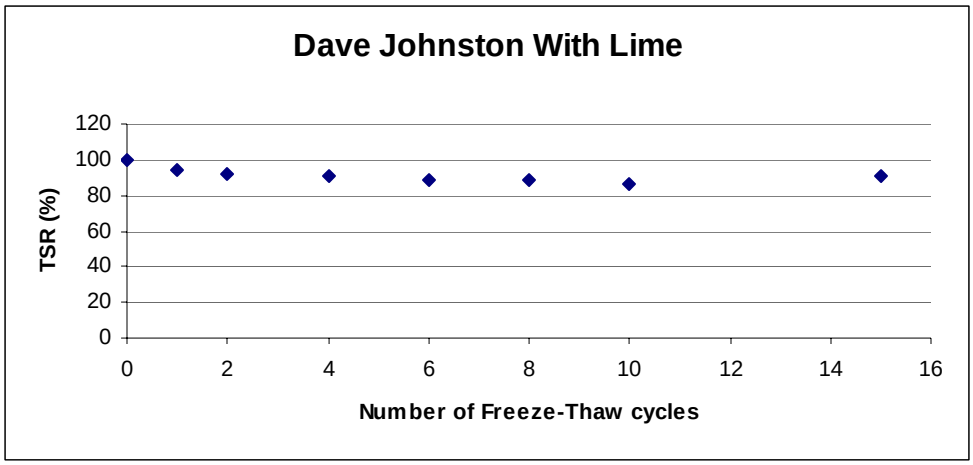
Dave Johnston With Lime
TSR (%)
120
100
80
60
40
20
0
0
2
4
6
8
10
12
14
16
Number of Freeze-Thaw cycles

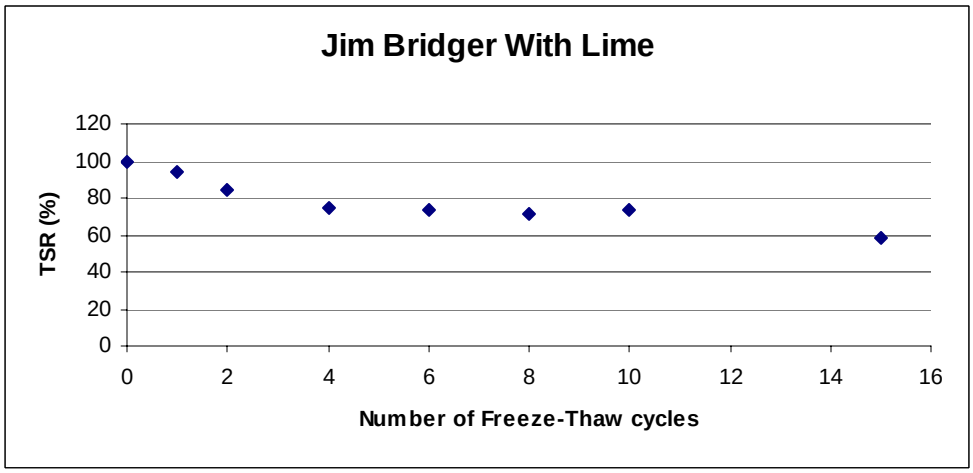
Jim Bridger With Lime
TSR (%)
120
100
80
60
40
20
0
0
2
4
6
8
10
12
14
16
Number of Freeze-Thaw cycles

Core Designation	Ash	Bulk Specific Gravity	% Air Voids	# of Freeze-thaw Cycles	Tensile Strength (lbs)
L01	LR	2.23	6.29	0	1234.2
L02	LR	2.20	7.51	0	1264.8
L03	LR	2.21	7.12	1	1040.4
L04	LR	2.20	7.53	1	1203.6
L05	LR	2.19	7.70	2	979.2
L06	LR	2.21	7.14	2	1081.2
L07	LR	2.21	7.08	4	1071.0
L08	LR	2.24	6.00	4	1091.4
L09	LR	2.22	6.88	6	867.0
L10	LR	2.20	7.32	6	999.6
L11	LR	2.20	7.48	8	734.4
L12	LR	2.21	6.98	8	918.0
L13	LR	2.22	6.67	10	958.8
L14	LR	2.21	6.90	10	1040.4
L15	LR	2.23	6.23	15	765.0
L16	LR	2.21	6.94	15	785.0
C01	C	2.24	7.14	0	1009.8
C02	C	2.25	6.79	0	1040.4
C03	C	2.24	7.01	1	999.6
C04	C	2.24	7.19	1	969.0
C05	C	2.24	7.07	2	979.2
C06	C	2.23	7.70	2	1081.2
C07	C	2.25	6.70	4	459.0
C08	C	2.23	7.64	4	438.6
C09	C	2.25	6.74	6	459.0
C10	C	2.24	7.34	6	561.0
C11	C	2.23	7.43	8	561.0
C12	C	2.24	7.34	8	459.0
C13	C	2.25	6.77	10	346.8
C14	C	2.24	7.13	10	306.0
C15	C	2.24	7.01	15	153.0
C16	C	2.24	7.24	15	193.8
JB 01	JB	2.17	7.20	0	1326.0
JB 02	JB	2.17	7.06	0	1346.4
JB 03	JB	2.17	6.92	1	1091.4
JB 04	JB	2.18	6.84	1	1173.0
JB 05	JB	2.19	6.07	2	1224.0
JB 06	JB	2.18	6.57	2	989.4
JB 09	JB	2.18	6.63	4	540.6
JB 10	JB	2.18	6.66	4	703.8
JB 11	JB	2.18	6.50	6	765.0
JB 12	JB	2.18	6.89	6	805.8
JB 13	JB	2.18	6.80	8	530.4

Core Designation	Ash	Bulk Specific Gravity	% Air Voids	# of Freeze-thaw Cycles	Tensile Strength (lbs)
JB 07	JB	2.18	6.75	10	601.8
JB16	JB	2.16	7.75	15	367.2
JB17	JB	2.14	8.00	15	479.4
DJ01	DJ	2.20	7.65	0	1213.8
DJ02	DJ	2.19	8.00	0	1142.4
DJ03	DJ	2.21	7.53	1	836.4
DJ04	DJ	2.22	7.01	1	958.8
DJ05	DJ	2.21	7.60	2	785.4
DJ06	DJ	2.21	7.33	2	958.8
DJ07	DJ	2.22	6.96	4	775.2
DJ08	DJ	2.21	7.53	4	0.0
DJ09	DJ	2.21	7.30	6	612.0
DJ10	DJ	2.21	7.35	6	469.2
DJ11	DJ	2.21	7.38	8	591.6
DJ12	DJ	2.21	7.45	8	734.4
DJ13	DJ	2.22	7.10	10	377.4
DJ14	DJ	2.23	6.56	10	0.0
DJ15	DJ	2.21	7.53	15	193.8
DJ16	DJ	2.19	8.00	15	306.0
LL01	LR	2.23	6.14	0	1428.0
LL02	LR	2.23	6.40	0	1275.0
LL03	LR	2.23	6.26	1	1142.4
LL04	LR	2.23	6.32	1	1091.4
LL06	LR	2.23	6.34	2	1009.8
LL07	LR	2.22	6.72	2	948.6
LL09	LR	2.23	6.34	4	1132.2
LL10	LR	2.20	7.35	4	1142.4
LL12	LR	2.22	6.60	6	1264.8
LL13	LR	2.21	7.06	6	1122.0
LL14	LR	2.20	7.30	8	1264.8
LL15	LR	2.21	7.00	8	1050.6
LL16	LR	2.20	7.40	10	999.6
LL17	LR	2.20	7.68	10	897.6
LL18	LR	2.20	7.35	15	632.4
LL19	LR	2.20	7.29	15	683.4
CL15	C	2.26	6.16	0	1387.2
CL16	C	2.26	6.36	0	1387.2
CL01	C	2.25	6.96	1	1071.0
CL02	C	2.26	6.52	1	1428.0
CL03	C	2.26	6.34	2	1142.4
CL04	C	2.26	6.36	2	1224.0
CL05	C	2.25	6.69	4	1183.2
CL06	C	2.25	6.86	4	1203.6
CL07	C	2.27	6.00	6	999.6
CL08	C	2.25	6.63	6	1142.4

Core Designation	Ash	Bulk Specific Gravity	% Air Voids	# of Freeze-thaw Cycles	Tensile Strength (lbs)
CL10	C	2.27	6.02	8	1224.0
CL13	C	2.26	6.36	10	-
CL14	C	2.26	6.47	15	979.2
CL17	C	2.23	7.65	15	887.4
JBL01	JB	2.19	6.46	0	1530.0
JBL04	JB	2.19	6.45	0	1428.0
JBL02	JB	2.19	6.08	1	1254.6
JBL03	JB	2.19	6.39	1	1530.0
JBL05	JB	2.18	6.80	2	1387.2
JBL06	JB	2.18	6.66	2	1224.0
JBL07	JB	2.18	6.81	4	979.2
JBL08	JB	2.20	6.00	4	1326.0
JBL09	JB	2.18	6.54	6	1224.0
JBL10	JB	2.19	6.12	6	1326.0
JBL11	JB	2.19	6.13	8	1224.0
JBL12	JB	2.19	6.45	8	1162.8
JBL13	JB	2.19	6.19	10	1132.2
JBL14	JB	2.19	6.31	10	1162.8
JBL15	JB	2.20	6.00	15	1203.6
JBL16	JB	2.19	6.09	15	999.6
DJL03	DJ	2.22	7.17	0	1275.0
DJL04	DJ	2.22	7.10	0	1326.0
DJL01	DJ	2.20	7.91	1	1132.2
DJL02	DJ	2.21	7.33	1	1264.8
DJL05	DJ	2.22	6.91	2	1213.8
DJL06	DJ	2.24	6.35	2	1346.4
DJL07	DJ	2.21	7.31	4	765.0
DJL08	DJ	2.21	7.32	4	999.6
DJL09	DJ	2.23	6.66	6	836.4
DJL10	DJ	2.23	6.66	6	1091.4
DJL11	DJ	2.25	6.00	8	1152.6
DJL12	DJ	2.24	6.27	8	958.8
DJL13	DJ	2.25	6.00	10	724.2
DJL14	DJ	2.23	6.50	10	897.6
DJL15	DJ	2.23	6.76	15	612.0
DJL16	DJ	2.24	6.11	15	714.0

APPENDIX C

SAS ANALYSIS

Analysis of Variance for Modulus of Elasticity

The SAS System
The GLM Procedure

Class Level Information

Class	Levels	Values
TRT	4	1 2 3 4

Number of observations 31

The SAS System
The GLM Procedure

Coefficients for Contrast 1 v. 2

		Row 1
Intercept		0
TRT	1	1
TRT	2	-1
TRT	3	0
TRT	4	0

The SAS System
The GLM Procedure

Coefficients for Contrast 1 v. 3

		Row 1
Intercept		0
TRT	1	1
TRT	2	0
TRT	3	-1
TRT	4	0

The SAS System
The GLM Procedure

Coefficients for Contrast 1 v. 4

		Row 1
Intercept		0
TRT	1	1
TRT	2	0
TRT	3	0
TRT	4	-1

The SAS System
The GLM Procedure

Coefficients for Contrast 2 v. 3

		Row 1
Intercept		0
TRT	1	0
TRT	2	1
TRT	3	-1
TRT	4	0

The SAS System
The GLM Procedure

Coefficients for Contrast 2 v. 4

		Row 1

Intercept		0
TRT	1	0
TRT	2	1
TRT	3	0
TRT	4	-1

The SAS System
The GLM Procedure

Coefficients for Contrast 3 v. 4

		Row 1
Intercept		0
TRT	1	0
TRT	2	0
TRT	3	1
TRT	4	-1

The SAS System
The GLM Procedure

Dependent Variable: TSR

Source	DF	Sum of Squares	Mean Square	F Value	Pr > F
Model	3	232232.190	77410.730	1.34	0.2811
Error	27	1555874.775	57624.992		
Corrected Total	30	1788106.965			

R-Square	Coeff Var	Root MSE	TSR Mean
0.129876	46.89610	240.0521	511.8806

Source	DF	Type I SS	Mean Square	F Value	Pr > F
TRT	3	232232.1899	77410.7300	1.34	0.2811

Source	DF	Type III SS	Mean Square	F Value	Pr > F
TRT	3	232232.1899	77410.7300	1.34	0.2811

Contrast	DF	Contrast SS	Mean Square	F Value	Pr > F
1 v. 2	1	172133.7121	172133.7121	2.99	0.0954
1 v. 3	1	166439.5209	166439.5209	2.89	0.1007
1 v. 4	1	110107.0938	110107.0938	1.91	0.1782
2 v. 3	1	47.8864	47.8864	0.00	0.9772
2 v. 4	1	4760.7144	4760.7144	0.08	0.7760
3 v. 4	1	3882.8570	3882.8570	0.07	0.7972

Regression Analysis for TSR Data

Regression for LR Mix without Lime

The NLIN Procedure
Dependent Variable y
Method: Gauss-Newton

Iterative Phase

Iter	g0	g1	Sum of Squares

0	100.0	-0.00001	4222.4
1	92.2682	-0.0210	340.3
2	93.2296	-0.0275	268.5
3	93.3440	-0.0279	268.3
4	93.3482	-0.0279	268.3
5	93.3483	-0.0279	268.3

Source	DF	Sum of Squares	Mean Square	F Value	Approx Pr > F
Regression	2	52274.7	26137.3	584.50	<.0001
Residual	6	268.3	44.7171		
Uncorrected Total	8	52543.0			
Corrected Total	7	1088.3			

Parameter	Estimate	Approx Std Error	Approximate 95% Confidence Limits	
b0	93.3483	3.9842	83.5994	103.1
b1	-0.0279	0.00677	-0.0445	-0.0114

Y^ = (93.3483)* Exp (-0.0279*t)

Regression for Control Mix without Lime

The NLIN Procedure
Dependent Variable y
Method: Gauss-Newton

Iterative Phase

Iter	g0	g1	Sum of Squares
0	100.0	-0.00001	19772.0
1	89.6171	-0.0544	2248.5
2	97.1330	-0.1023	588.5
3	99.5960	-0.1167	516.5
4	99.8699	-0.1182	515.9
5	99.8895	-0.1183	515.9
6	99.8906	-0.1183	515.9

Source	DF	Sum of Squares	Mean Square	F Value	Approx Pr > F
Regression	2	26870.4	13435.2	130.21	<.0001
Residual	5	515.9	103.2		
Uncorrected Total	7	27386.3			
Corrected Total	6	5875.3			

Parameter	Estimate	Approx Std Error	Approximate 95% Confidence Limits	
b0	99.8906	7.7714	79.9139	119.9
b1	-0.1183	0.0199	-0.1694	-0.0672

Y^ = (99.8906)*Exp(-0.1183*t)

Regression for JB Mix without Lime

The NLIN Procedure
Dependent Variable y
Method: Gauss-Newton

Iterative Phase

Iter	g0	g1	Sum of Squares
0	100.0	-0.00001	16392.8
1	85.7530	-0.0427	1748.5
2	90.9575	-0.0773	692.4
3	93.1120	-0.0873	646.0
4	93.4666	-0.0887	645.2
5	93.5086	-0.0889	645.2
6	93.5132	-0.0889	645.2
7	93.5137	-0.0889	645.2

Source	DF	Sum of Squares	Mean Square	F Value	Approx Pr > F
Regression	2	33692.6	16846.3	156.65	<.0001
Residual	6	645.2	107.5		
Uncorrected Total	8	34337.9			

Corrected Total	7	4362.1		

Parameter	Estimate	Approx Std Error	Approximate 95% Confidence Limits	
b0	93.5137	7.0068	76.3686	110.7
b1	-0.0889	0.0173	-0.1313	-0.0464

Y^ = (93.5137)*Exp (-0.0889*t)

Regression for DJ Mix without Lime

The NLIN Procedure
Dependent Variable y
Method: Gauss-Newton

Iterative Phase

Iter	g0	g1	Sum of Squares
0	100.0	-0.00001	18072.4
1	86.1497	-0.0473	1557.4
2	91.1269	-0.0855	386.0
3	92.4699	-0.0940	357.2
4	92.5280	-0.0943	357.1
5	92.5289	-0.0943	357.1

Source	DF	Sum of Squares	Mean Square	F Value	Approx Pr > F
Regression	2	32006.3	16003.1	268.87	<.0001
Residual	6	357.1	59.5191		
Uncorrected Total	8	32363.4			
Corrected Total	7	4582.9			

Parameter	Estimate	Approx Std Error	Approximate 95% Confidence Limits	
g0	92.5289	5.2622	79.6528	105.4
g1	-0.0943	0.0136	-0.1276	-0.0610

Y^ = (92.5289)*Exp(-0.0943*t)

Regression for Control Mix with Lime

The NLIN Procedure
Dependent Variable y
Method: Gauss-Newton

Iterative Phase

Iter	g0	g1	Sum of Squares
0	100.0	-0.00001	2922.7
1	93.7581	-0.0175	268.9
2	94.2642	-0.0215	237.2
3	94.2851	-0.0216	237.1
4	94.2852	-0.0216	237.1

Source	DF	Sum of Squares	Mean Square	F Value	Approx Pr > F
Regression	2	56584.7	28292.4	715.83	<.0001
Residual	6	237.1	39.5239		
Uncorrected Total	8	56821.9			
Corrected Total	7	795.6			

Parameter	Estimate	Approx Std Error	Approximate 95% Confidence Limits	
g0	94.2852	3.6885	85.2597	103.3
g1	-0.0216	0.00597	-0.0362	-0.00704

Y^ = (94.2852)*Exp(-0.216*t)

Regression for JB Mix with Lime

The NLIN Procedure
Dependent Variable y
Method: Gauss-Newton

Iterative Phase

Iter	g0	g1	Sum of Squares
0	100.0	-0.00001	2373.5
1	93.4649	-0.0146	170.9
2	93.9782	-0.0179	148.3
3	94.0325	-0.0180	148.2
4	94.0344	-0.0180	148.2

Source	DF	Sum of Squares	Mean Square	F Value	Approx Pr > F
Regression	2	58089.3	29044.7	1175.60	<.0001
Residual	6	148.2	24.7063		
Uncorrected Total	8	58237.6			
Corrected Total	7	554.8			

Parameter	Estimate	Approx Std Error	Approximate 95% Confidence Limits	
g0	94.0344	2.8953	86.9499	101.1
g1	-0.0180	0.00450	-0.0290	-0.00699

Y^ = (94.0344)*Exp(-0.018*t)

Regression for LR Mix with Lime

The NLIN Procedure
Dependent Variable y
Method: Gauss-Newton

Iterative Phase

Iter	g0	g1	Sum of Squares
0	100.0	-0.00001	5173.6
1	92.1026	-0.0223	837.7
2	92.2666	-0.0277	774.7
3	92.1495	-0.0276	774.7
4	92.1532	-0.0276	774.7
5	92.1530	-0.0276	774.7

Source	DF	Sum of Squares	Mean Square	F Value	Approx Pr > F
Regression	2	50816.8	25408.4	196.79	<.0001
Residual	6	774.7	129.1		
Uncorrected Total	8	51591.5			
Corrected Total	7	1651.5			

Parameter	Estimate	Approx Std Error	Approximate 95% Confidence Limits	
g0	92.1530	6.7697	75.5883	108.7
g1	-0.0276	0.0114	-0.0555	0.000313

Y^ = (92.153)*Exp (-0.0276*t)

Regression for DJ Mix with Lime

The NLIN Procedure
Dependent Variable y
Method: Gauss-Newton

Iterative Phase

Iter	g0	g1	Sum of Squares
0	100.0	-0.00001	5939.4
1	95.9902	-0.0300	661.9
2	97.5806	-0.0401	506.8
3	97.7165	-0.0407	506.4
4	97.7189	-0.0407	506.4

Source	DF	Sum of Squares	Mean Square	F Value	Approx Pr > F
Regression	2	50847.8	25423.9	301.21	<.0001
Residual	6	506.4	84.4064		
Uncorrected Total	8	51354.2			
Corrected Total	7	2203.9			

Parameter	Estimate	Approx Std Error	Approximate 95% Confidence Limits	
g0	97.7189	5.6360	83.9281	111.5
g1	-0.0407	0.00972	-0.0645	-0.0169

Y^ = (97.7189)*Exp (-0.0407*t)